DETAILED INVESTIGATION ON POLYCARBONATE SYNTHESIS AND

MOLECULAR DESIGN OF NOVEL LIQUID CRYSTALLINE

POLYCARBONATES IN scCO$_2$ MEDIA

by

YEŞİM MÜGE ÇALIK (ŞAHİN)

Submitted to the Graduate School of Engineering and Natural Sciences

in partial fulfillment of

the requirements for the degree of

Doctor of Philosophy

Sabancı University

June 2006

DETAILED INVESTIGATION ON POLYCARBONATE SYNTHESIS AND
MOLECULAR DESIGN OF NOVEL LIQUID CRYSTALLINE
POLYCARBONATES IN scCO$_2$ MEDIA

APPROVED BY:

Assoc. Prof. Yusuf Ziya Menceloğlu   ………………………….
(Thesis Supervisor)

Prof. İbrahim Ersin Serhatlı   ………………………….
(Thesis Cosupervisor)

Prof. Yuda Yurum   ………………………….

Prof. Ayşen Önen   ………………………….

Ass. Prof. Melih Papila   …………………….........

DATE OF APPROVAL: ……16.06.2006………

DETAILED INVESTIGATION ON POLYCARBONATE SYNTHESIS AND MOLECULAR DESIGN OF NOVEL LIQUID CRYSTALLINE POLYCARBONATES IN scCO$_2$ MEDIA

YEŞİM MÜGE ÇALIK (ŞAHİN)

MAT, PhD Thesis, 2006

Thesis Supervisor: Assoc.Prof. Yusuf Ziya Menceloğlu
Thesis Cosupervisor: Prof. Dr. İbrahim Ersin Serhatlı

Keywords: Liquid Crystals, Polycarbonate, Supercritical Carbon Dioxide, Chiral, Structural Analysis

ABSTRACT

In the first part of this study, the experimental demonstration of a novel and environmentally benign supercritical carbon dioxide (scCO$_2$) technique that yields polycarbonates in a single-step reaction, have been reported. Different chiral and racemic epoxy monomers have been copolymerized and some detailed micro and macro structure investigations have been conducted. By these examinations, it is aimed to say more about the modes of the ring opening of epoxides in scCO$_2$ media in coordination with the utilized catalyst as well as the tacticity and the microstructure of the resultant polymers.

In the second part, optically active side chain liquid crystalline polycarbonates having no spacer unit and its homologue with six spacer unit have been synthesized under scCO$_2$ conditions. The obtained polymers are worthwhile since they are highly stereoregular and can find applications in an enlarged mesomorphic temperature range compared to their acrylic analogues. The synthesized materials were characterized by IR, ^{1}H-NMR and ^{13}C-NMR while the thermal properties were measured by DSC. Polarized optical micrograph and wide angle X-ray diffraction were used for the mesogenic property characterization of the copolymers. The DSC analyses of the copolymers indicate that the Ti values do not change dramatically, whereas a pronounced decrease in Tg values are observed from that of their acrylic analogues. Hence, the obtained polymers exhibit another practical benefit by widening the mesomorphic temperature range. This study is the insightful combination of material processing and chemical design that elucidates the advantages of scCO$_2$ application in terms of liquid crystallinity and the tacticity of the obtained polymers.

SÜPERKRİTİK KARBON DİOKSİT ORTAMINDA YENİ SIVI KRİSTAL
POLİKARBONATLARIN MOLEKÜLER TASARIMI VE POLİKARBONAT
ÜZERİNE DETAYLI İNCELEME

YEŞİM MÜGE ÇALIK (ŞAHİN)

MAT, PhD Thesis, 2006

Tez Danışmanı: Doç. Dr. Yusuf Ziya Menceloğlu
Yardımcı Tez Danışmanı: Prof. Dr. İbrahim Ersin Serhatlı

Anahtarkelimeler: Likit kristaller, Polikarbonat, Süperkritik Karbon
Dioksit, Kiral, Yapısal Analiz

ÖZET

Bu calışmanın ilk bölümünde, polikarbonatların tek reaksyon adımda eldelerini mümkün kılan, yeni ve cevreyle uyumlu olan süperkritik karbon dioksit tekniğinin deneysel gösterimi rapor edilmiştir. Farklı çiral ve rasemik epoksi monomerlerin kopolimerizasyonu gerçekleştirilmiş olup bunların küçük ve büyük ölçekte yapısal araştırmaları yapılmıştır. Bu araştırmalarla, epoksi halkalarının süperkritik karbondiosit ortamında ve kullanılan katalizör eşliğinde halka açılımları ile elde edilen polimerin taktisite ve küçük ölçekli yapılanması hakkında daha fazla bilgilenmek amaçlanmıştır.

İkinci bölümde ise, optikçe aktif yan zincirli likit kristal polikarbonatlardan tekli ve altılı zincir uzunluğuna sahip eşlenikleri süperkritik karbon dioksit ortamda sentezlendi. Elde edilen polimerler, yüksek stereo-düzenli olmaları ve akrilik eşleniklerine oranla geniş mezomorfik sıcaklık aralıklarında kullanılabilmeleri açısından dikkate değer bulunmuştur. Sentezlenen malzemeler IR, ^{1}H-NMR and ^{13}C-NMR altında karakterize edilirken DSC kullanılarak da termal özellikleri ölçülmüştür. Kopolimerlerin mezojenik özelliklerinin karakterize edilmesinde polarize edilmiş optik mikrograf ve geniş açılı X-ışını kırınım tekniği kullanılmıştır. Akrilik benzerlerine kıyasla, kopolimerlerin DSC analizleri, Ti değerlerinin çarpıcı biçimde değişmemekle birlikte Tg değerlerinde hatırı sayılır bir düşüş olduğunu göstermiştir. Böylece, elde edilen polimerin bir başka pratik yararı da mezomorfik sıcaklık aralıklarını genişletmesi olmuştur. Bu çalışma, süperkritik karbon dioksit kullanımının likit kristallik ve polimer taktisitesi üzerindeki avantajlarını aydınlatan ve malzeme işlemiyle kimyasal dizaynın faydalı şekilde birleşmesinin bir ürünüdür.

to my Mother and Father,

ACKNOWLEDGEMENTS

TABLE OF CONTENTS

LIST OF FIGURES

xv

LIST OF SCHEMES

LIST OF TABLES

LIST OF ABBREVIATIONS

(CO_2)	: Carbon Dioxide
(DMF)	: Dimethylformamide
(DSC)	: Differensial Scanning Calorimetry
(FTIR-ATR)	: Fourier Transform Infrared – Attenuated Total Reflectance
(LC)	: Liquid Crystal
(LCD)	: Liquid Crystalline Display
(LCP)	: Liquid Crystalline Polymer
(MCLCP)	: Main Chain Liquid Crystalline Polymer
(N)	: Nematic
(N*)	: Cholesteric (Chiral Nematic)
(NMR)	: Nuclear Magnetic Resonance
($scCO_2$)	: Supercritical Carbon Dioxide
(SCLCP)	: Side Chain Liquid Crystalline Polymer
(Sm)	: Smectic
(Sm*)	: Chiral Smectic
(ΔT)	: Mesomorphic Temperature Range
(TBAOH)	: Tetrabuthyl ammonium hydroxide
(Tg)	: Glass Transition Temperature
(Ti)	: Isotropization Temperature
(XRD)	: X-Ray Difraction

1   CHAPTER 1

GENERAL INTRODUCTION

1.1   Green Chemistry and Green Engineering

The "Green Chemistry" is the universally accepted term to describe the movement towards more environmentally acceptable chemical processes and products and it can be achieved by applying environmentally friendly technologies [1] .

Green Chemistry focuses on the design of chemical products and processes that reduce or eliminate the use and generation of hazardous substances. It provides the foundation on which to design the green engineering technologies needed to implement sustainable products, processes, and systems. This green route enhances the safety of a process by employing inherently safer substances throughout the design process, including the selection of feedstocks, reagents, and solvents, and designing the final product [1].

In these days, much better understanding is obtained for the interaction between functional groups in a molecule and biological organisms as a consequence of the advances in toxicology and mechanistic chemistry. More accurate measurements can be done for substances released into the environment with developed instruments and methods capable of detecting pollutants at very small concentrations [2]. Armed with this information, chemists can design syntheses to eliminate the use of volatile organic solvents, transforming functional groups using less toxic reagents, and developing products that do not persist in the environment. In the below figure the representation of an "ideal synthesis", on which the Green Chemistry is directing, is given.
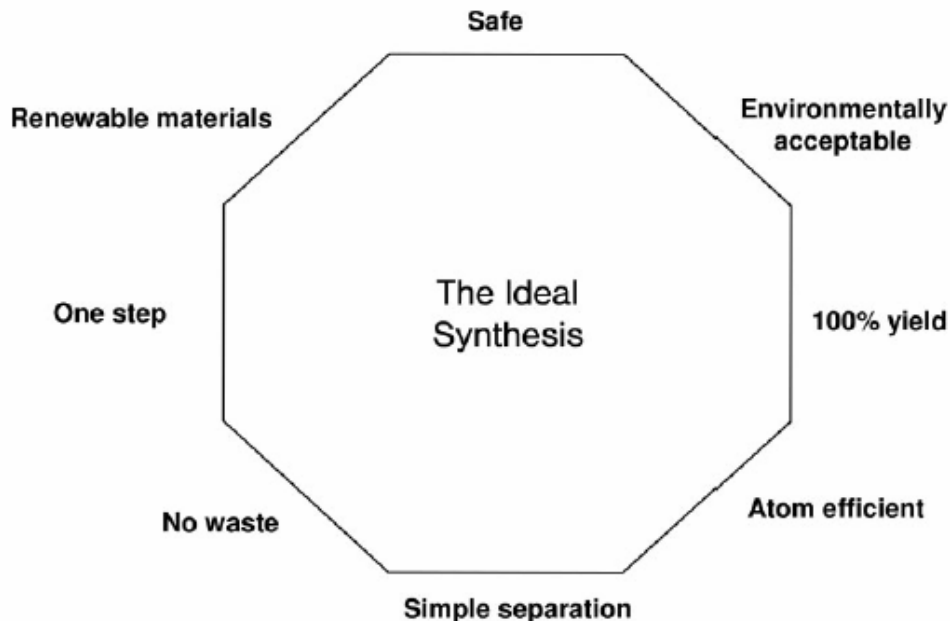
Figure 1.1 Features of the "ideal synthesis" [3].

To sum up, Green Chemistry has been heavily focused on developing new, cleaner, chemical processes using the technologies. Increasing legislation is forcing an increasing emphasis on products but it is important that these in turn are manufactured by green chemical methods. So as the Green Chemistry in this thesis, not only mention the consumption method of the greenhouse gas CO_2 as a feedstock will be mentioned, but also a green chemical method of polycarbonate synthesis will be pointed out.

1.2   The Greenhouse Gas CO_2, as Feedstock

Many chemical compounds found in the Earth's atmosphere act as "greenhouse gases." These gases allow sunlight to enter the atmosphere freely. When sunlight strikes the Earth's surface, some of it is reflected back towards space as infrared radiation (heat). Greenhouse gases absorb this infrared radiation and trap the heat in the atmosphere. Over time, the amount of energy sent from the sun to the Earth's surface should be about the same as the amount of energy radiated back into space, leaving the temperature of the Earth's surface roughly constant. For thousands of years, the Earth's atmosphere has changed very little. In other words, the temperature and the careful

balance of greenhouse gases have stayed just right for humans, animals and plants to survive. But today, we are having problems keeping this balance. Because we burn fossil fuels to heat our homes, run our cars, produce electricity, and manufacture all sorts of products, we are adding more greenhouse gases to the atmosphere. These activities are changing the atmosphere at a greater rate than humans have ever experienced. Rising temperatures may, in turn, produce changes in weather, sea levels, and land use patterns, commonly referred to as "climate change".

Many gases exhibit these "greenhouse" properties. Some of them occur in nature (water vapor, carbon dioxide, methane, and nitrous oxide), while others are exclusively human-made (like gases used for aerosols). Levels of several important greenhouse gases have increased by about 25 percent since large-scale industrialization began around 150 years ago. Since 1896 it has been known that the gases carbon dioxide, methane and nitrous oxide (dinitrogen oxide) help to stop the Sun's infrared radiation [4]. By letting most of the Sun's light radiation through, and only letting a smaller amount of the resultant infrared radiation out again, these gases help to maintain the relatively warm temperatures that allow the oceans to exist and life to flourish on Earth. Because they act in a similar way to the glass panes of a greenhouse (*i.e.* letting in more light radiation from the Sun than they let infrared radiation out), they have been called as 'greenhouse gases'. But more importantly the amount of these gases should be balanced.

Carbon dioxide is the most important of the greenhouse gases released by human activities. It is the main contributor to climate change because of the quantities released, especially through the burning of fossil fuels. When fossil fuels are burned, the carbon content is oxidized and released as carbon dioxide; every tone of carbon burned produces 3.7 tones of carbon dioxide. The global consumption of fossil fuels is estimated to release 22 billion tones of carbon dioxide into the atmosphere every year and the amounts are still climbing. This can lead to major climatic changes such as a change in rainfall patterns, changes in ocean circulation patterns, warming in some areas, dramatic cooling in others, rising sea levels and coastal flooding, due to melting ice sheets and thermal expansion of seawater. All of these will have serious implications for agricultural productivity.

The use of carbon dioxide as a solvent or raw material has been investigated somewhat continuously in academia and/or industry since 1950. The interest in the use of CO_2 in these roles has intensified during the past 20 years as large scale plants using CO_2 have been brought on line. In the literature, many of the studies on the consumption of CO_2 is related with its chemical utilization in organic sythesis. On the other hand, in the search for new polymerization solvents, scientists have turned to supercritical fluids. The supercritical fluids in general exhibit interesting physical properties [2], specific interest in CO_2 as a supercritical fluid, is magnified by its perceived 'green' properties that carbon dioxide is non flammable, relatively non-toxic, and relatively inert.

As the literature reveals, the use of CO_2, has permeated almost all parts of the chemical industry, and that careful application of CO_2 technology can result in products that are cleaner, less expensive and of purity [5]. Prominent among the current efforts which aim the chemical utilization of carbon dioxide, is the copolymerization of epoxides and CO_2 to yield polycarbonates. In comparison to the alternative route involving the use of highly toxic phosgene, polycarbonate synthesis in $scCO_2$ media, presents a single-step reaction and an environmentally benign approach [6, 7]. The work presented in this thesis, utilizes supercritical CO_2 as monomer, and solvent that is viable and promising alternative to the traditional solvents used in polymer synthesis. So, in this thesis we will not only mention the consumption method of the greenhouse gas CO_2 as a feedstock, but also will point out a synthesis method for polycarbonates with an environmentally benign supercritical carbon dioxide method in comparison to its alternative synthesis route containing a highly toxic phosgene.

1.3   The Supercritical Fluid CO_2, as Processing Media

1.3.1   Brief Background on Supercritical Fluids (SCFs)

The supercritical state was first discovered by the French scientist, Baron Charles Cagniard de la Tour, in 1821. However, intensive research in the area actually belongs to the last few decades. Initially SCFs were utilized in the chromatographic separation

and extraction separation processes. One important example to SCF extraction process is the caffeine extraction from coffee with $scCO_2$. Similarly the process has been expanded to different extraction applications with products such as tea, and spices. Recently, SCFs have been used as reaction media due to discovered benefits of their special properties [8]. SCFs have also found great interest in the area of polymer synthesis and processing [9, 10].

1.3.2 Definition and Properties

The supercritical phase of a compound is a phase in which the compound is above the critical points (critical pressure P_c, and critical temperature T_c) and below the solid state. In this phase, a compound bears both the properties of a gas and a liquid. The most important property of a supercritical fluid is its tunability in the temperature range since a small change in temperature will cause drastic changes in the pressure, followed by changes in other physical variables related to pressure and temperature.

The main variables that are affected by such changes and that play important roles in supercritical applications are the density (d) and the dielectric constant (ε). The density is a variable known to be directly proportional to the solvency power, and this is the basis for supercritical fluid extraction processes. The tunability of the dielectric constant also gives power to tune the solvency power, since it relates to the solvent polarity and other important solvent effects.

Supercritical fluids have many important properties that increase their attractiveness for use. Their high diffusivity, low viscosity and high density make them suitable for continuous-flow processes. Another advantage of supercritical fluids is that they have tunable solvating power. In this way, different conditions may be set for a wide range of applications concerning different compounds. Also, supercritical fluids are volatile compounds, which can be easily removed after usage, avoiding any solvent wastes and costly separations. Even though the costs of the equipment needed to run a supercritical process are high, they are generally outweighed by the economic benefits brought by SCF applied processes [11]. Figure 1.2 illustrates a general pressure-

5

temperature phase diagram for a pure compound. The supercritical phase and the pressure-temperature range defining this phase are shown on the figure.
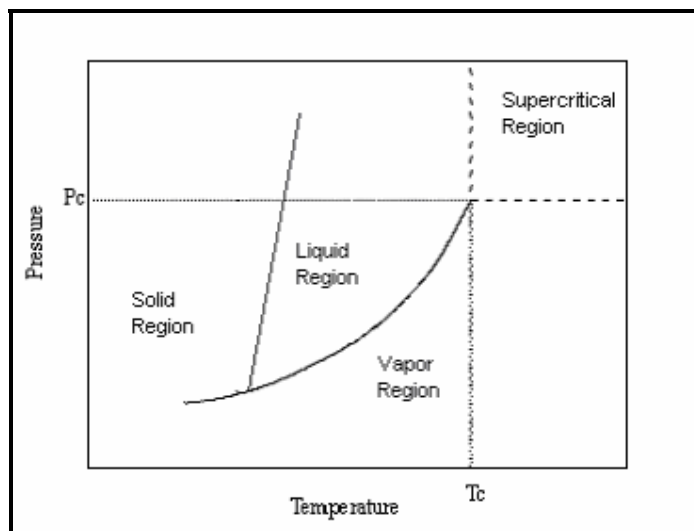
Figure 1.2 A basic temperature-pressure phase diagram for a pure substance [12].

Important supercritical properties can be summarized under the following items:

i.   A SCF is a substance under pressure above its critical temperature.

ii.   Under these conditions the division between gas and liquid does not apply and substance can only be described as a fluid.

iii.   SCFs have physical intermediate properties to those of gases and liquids, and these properties are controlled by the pressure.

iv.   SCFs do not condense or evaporate to form a liquid or a gas. Compounds like supercritical xenon, ethane and carbon dioxide afford a wide range of uncommon chemical opportunities in both synthetic and analytical chemistry.

v.   As the density increases, solubility increases too (i.e. with increasing pressure). Fast expansion of supercritical solutions leads to precipitation of a finely divided solid.

vi.   The fluids are completely miscible with permanent gases (e.g. N_2 or H_2) and this leads to much higher concentrations of dissolved gases than can be achieved in conventional solvents. This effect adds benefit in the applications with organometallic reactions and hydrogenation.

1.3.3　Temperature and Pressure Effect on Solubility in SCF

Basically, solubility is directly proportional to pressure; that is to say, the higher the pressure, the higher the dissolving power of the supercritical fluid. Figure 1.3 shows the solubility of naphthalene in $scCO_2$. Solubility increases initially and gets almost constant after approximately 250 atm. This behavior represents the density changes occurring in the solvent.

The effect of temperature on solubility is more complex, though. The solubility of a certain solute depends both on its vapor pressure and on the density of the solvent. The temperature dependence of both variables causes the crossover effect on the solubility of the solute. The intersection of the isotherms of a given solute at a pressure-solubility diagram gives the crossover pressure as represented in Figure1.4. The region below the crossover pressure is the retrograde region. In this zone, any increase in temperature causes the density to fall, in turn decreasing the solubility. At any pressure greater than the crossover value, the effect of temperature on density is not very high and the dominant effect is caused by the vapor pressure of the solute. Temperature increase in this region increases the vapor pressure, which in turn results in enhanced solubility [13]. For this reason an appropriate temperature pressure couple should be chosen for the application used.
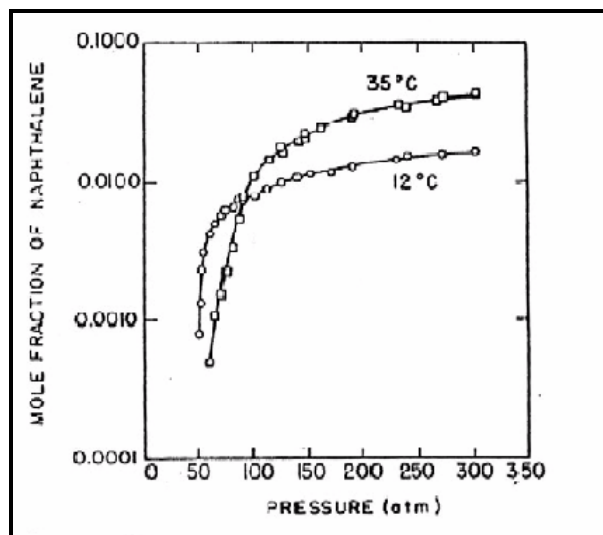
Figure 1.3　The solubility of naphthalene in supercritical ethylene, showing the crossover effect [14].

1.3.4   Supercritical carbon dioxide (scCO$_2$)

Having several important environmental, chemical, process, health and safety advantages, the scCO$_2$ is the most widely exploited SCF fluid. Most important properties of scCO$_2$ are summarized in Table 1.1. [15].

Table 1.1 Benefits of scCO$_2$ as an industrial solvent

Environmental Benefits	Health and Safety Benefits	Chemical Benefits	Process Benefits
Does not contribute to smog	Non-carcinogenic	High miscibility with gases	No solvent residues
Does not damage ozone layer	Non-toxic	Altered cage strength	Facile separation of products
No acute ecotoxicity	Non-flammable	Variable dielectric constant	High diffusion rates
No liquid waste		High compressibility	Low viscosity
		Local density augmentation	Adjustable solvent power
		High diffusion rate	Adjustable density
			Inexpensive

Table 1.2 describes the variations between some basic parameters defining physical phase properties [15]. The density of scCO$_2$ is approximately 0.4 g/cm^3. Due to the liquid-like density of scCO$_2$, many compounds dissolve at degrees higher than the ones predicted by the ideal gas formulations. Since the solvating power of a SCF is directly proportional to its density, varying the temperature and pressure will make it possible to tune the density and thus control the solubility and separation of a specific material [12]. Table 1.3 illustrates some commonly used supercritical fluids together with their critical temperatures and pressures.

Table 1.2 Comparison of the general properties of liquid, gas and scCO$_2$ [16].

Phase	Density, (g/cm^3)	Diffusion Coefficient, (cm^2/s)	Viscosity, (poice) (g/cm.s)	Surface Tension, (dynes/cm)
Liquid	1	10^{-6}	10^{-2}	45-60
SCF	0.2-0.8	10^{-3}	10^{-3}	0
Gas	0.001	10^{-1}	10^{-4}	N/a

Table 1.3 Critical conditions for various supercritical solvents [17].

Fluid	Critical Temperature (K)	Critical Pressure (bar)
Carbon dioxide	304.1	73.8
Ethane	305.4	48.8
Ethylene	282.4	50.4
Propane	369.8	42.5
Propylene	364.9	46.0
Fluoroform	299.3	48.6
Ammonia	405.5	113.5
Water	647.3	221.2
n-Pentane	469.7	33.7

The solubility efficiency is closely related to the transport properties of a solvent. These properties are defined by the diffusion coefficient and the viscosity. When compared with those of liquid solvents, the diffusion coefficient (diffusivity) and viscosity of SCFs are several magnitudes higher and lower, respectively. Then the rate of diffusion of the species in a SCF will be faster than in a liquid solvent; this faster rate will directly contribute to a more efficient solubility in a SCF. Just as the density is affected by pressure changes, the diffusion coefficient also varies with changes in the pressure and temperature, and at the same time is affected by the change in the density and the viscosity [13].

scCO$_2$'s critical temperature below 35°C enables work at moderate temperatures; thus, scCO$_2$ is more convenient for processes carried out with thermally

unstable materials. In addition, removal of the supercritical solvent by simply releasing the pressure eliminates the costly solvent separations and provides solvent free high purity products. $scCO_2$ processes are also very important environmentally.

1.3.4.1 Difficulties and Drawbacks of $scCO_2$

In the compressed phase, $scCO_2$ has a low dielectric constant and a very low polarizability. The result of these two properties is the reduced ability for formation of sufficiently strong van der Waals interactions between the solvent and the solute [18]. Thus $scCO_2$ is a poor solvent for most of the non-polar compounds and for most of the polar non-volatile compounds. Likewise, most of the polymers having high molecular mass are not soluble in $scCO_2$. The known exceptions are poly (ether-carbonates) [19], fluorinated polymers and silicone based polymers. Figure 1.5 illustrates the categorization of the solubility of polymeric materials in $scCO_2$. These molecules have low cohesive energy density and low surface tension, which give them the relatively higher solubility efficiency [8]. Table 1.4 summarizes the main properties of $scCO_2$ that cause problems and difficulties when dealing with $scCO_2$ applications.

Table 1.4 Drawbacks and difficulties of CO_2 [15]

Difficulties	Drawbacks
Low dielectric constant	Capital cost of liquid pressure equipment
Low polarizability per volume	Lack of enough operation plants
Neither liphophylic, nor hydrophilic	Lack of innovative unit-operations to reduce utility consumption
	Understanding nature of reactions and solvency properties

1.3.5 Polymerization and polymer processing with CO_2

Some of the most successful commercial processes that employ CO_2 as solvent involve polymeric substrates, yet the vast majority of polymers produced worldwide are

produced in the complete absence of solvent. Indeed, polyolefins (polyethylene), vinyl polymers (styrenics, acrylontrile, butadiene), polyamides (nylons) and polyesters are generated principally in bulk polymerization processes [20]. Further, for the most part, commercial polymers are poorly soluble (many, in effect, are insoluble) in CO_2. However, even polymers that are poorly soluble in CO_2 will swell extensively under moderate CO_2 pressure, allowing for a number of applications using CO_2 as reversible diluent/plasticizer. CO_2 is used extensively in the foaming of polymers (both styrenics and polyurethanes), CO_2 has been used as the solvent in coating processes (Union Carbide's UniCarb process) and CO_2 is currently being explored at the pilot works level in fluoropolymer synthesis (DuPont) and powder coating processing (Ferro Industries)[20].

Polymerizations are typically classified by the mode of polymerization (ring-opening, free-radical, etc.), by the type of monomer used (styrenics, acrylates) or by the type of linkage formed during polymerization (polyamides, polyesters). In addition, polymerizations can be conducted in the bulk state, in solution, or in one of many so-called 'heterogeneous modes' namely precipitation, suspension, dispersion or emulsion. Because CO_2 is typically employed as a benign solvent, the following discussion of polymer formation and processing in CO_2 will focus on those applications.

1.3.5.1 CO_2 as a solvent for polymer systems

The compressed carbon dioxide is often promoted as an environmentally friendly solvent having useful properties for a wide range of technical and chemical processes [5]. A growing number of commercial operations and pilot activities illustrate that CO_2 (especially in its supercritical state) can combine ecological and economic benefits. But the poor solubility of many interesting target substances places a severe restriction on the widespread use of CO_2 as a solvent. Generally, polymers present special problems regarding dissolution in any solvent, the very low entropy of mixing in polymer/solvent binaries (owing to the long chains of the polymer) requires a very favorable enthalpic interaction between polymer segments and solvent to ensure dissolution of substantial polymer concentrations. This problem is magnified in the case of CO_2 owing to its weak solvent power [21].

A significant portion of academic polymer, SCF phase behavior, work has considered solutions where the polymer is the minor component. The solubilization of low concentrations of polymer in solvent will require the highest pressures. Swelling of the polymer by the solvent requires significantly lower pressures. Thus, in certain polymer–SCF mixtures one can observe very high degrees of swelling. High-pressure phase behavior studies of polymers and supercritical fluids have been conducted since the late 1940s; the early work was performed to support the high-pressure polyethylene process. Ehrlich's group performed some of the best early work on the phase behavior of polyolefins in supercritical alkenes and alkene [22]; these studies have been followed by numerous others on polyethylene: alkane or polyethylene:alkene mixtures [23].

In the late 1960s, Giddings suggested a simple correlation between solubility parameter and critical pressure that indicated the CO_2's solvent power should be similar to that of pyridine. Subsequent calculations performed during the early 1980s using CO_2's equation of state, strongly suggested that CO_2's solubility parameter should approach that of normal alkanes [24]. However, experimental work by Heller's group on the phase behavior of polymers performed during that time clearly demonstrated that CO_2's solvent power is inferior to that of *n*-alkanes. However, the strong quadrupole moment of carbon dioxide affects CO_2's pVT properties (including the critical pressure) without influencing its solvent strength. Consequently, early calculations of the solubility parameter were invariably inflated. This was actually confirmed by the very early study that proposed that CO_2's solubility parameter should approach that of pyridine; polymers that would dissolve in pyridine were not soluble in carbon dioxide. Very few polymers tested by Heller showed any significant solubility in carbon dioxide at moderate (<200 bar) pressures. Experimental work by Johnston et al. [25] suggested that solubility parameter was not the best means by which to characterize the solvent power of compressible fluids, such as carbon dioxide. Johnston suggested instead that polarizability /volume is a better measure of solvent power; by this standard CO_2 is judged to be a feeble solvent, in line with experimental evidence.

During this same time period, a number of researchers found that silicones [26] and fluorinated materials [27] exhibited miscibility with CO_2 at pressures well below those of alkanes of comparable chain length. In 1992, DeSimone et al. published the

first reports that describe a truly 'CO$_2$-philic' polymer, a fluorinated polyacrylate [28]. Further work [29] showed that block copolymers of fluorinated acrylates and 'CO$_2$-phobic' polymers were both soluble and able to form micelles in carbon dioxide. Samulski et al. [30] have found experimentally that fluorine interacts specifically with the electron-poor carbon on CO$_2$, which would explain why addition of one or two fluorine atoms to aryl phosphine ligands or chelating agents tends to enhance CO$_2$-solubility significantly. It is suggested that fluorine's role in the design of CO$_2$-philic materials is simply to lower the cohesive energy density [31]. Also, McHugh has recently suggested that fluorination can significantly enhance the 'CO$_2$-philicity' of polymers [32].

As interest in applications for CO$_2$-philic polymers exploded in the 1990s, a small group of researchers continued to probe the fundamentals of CO$_2$ behavior with special regards to polymer solubility. Johnston's and Eckert's groups, using IR spectroscopy and computer calculations, proposed that Lewis acid-base interactions between CO$_2$ and carbonyl groups could explain the high swelling of polyacrylates by carbon dioxide [6]. Further, the McHugh's group published several seminar papers on the phase behavior of CO$_2$ and various homo and copolymers in the mid-1990s[33]. Conventional understanding of the time would suggest that because CO$_2$ is a low dielectric, low cohesive energy density solvent, it should only solvate polymers of similar characteristics. However, for the case of ethylene–acrylate copolymers, McHugh found that increasing the acrylate content lowered miscibility pressures, despite the fact that the acrylate is the polar co-monomer. Johnston recently reported that polymers that exhibit low interfacial tensions (and hence low cohesive energy densities) tended to also exhibit low miscibility pressures in carbon dioxide [34].

Clearly, the phase behavior of polymers in CO$_2$ is tied to CO$_2$'s low cohesive energy density, but its Lewis acid character will also play a significant role if the polymer contains Lewis base groups. For example, Beckman found that polybutadiene, a very low cohesive energy density polymer, is more 'CO$_2$-philic' than other vinyl polymers of higher cohesive energy density [6]. However, both polypropylene oxide and polyvinyl acetate exhibit lower miscibility pressures than polybutadiene, likely owing to the presence of Lewis base groups in each of the latter polymers despite exhibiting higher cohesive energy densities than polybutadiene.

As summarized above, for a long period of time, the most effective CO_2-philes have been expensive fluorocarbons such as fluorinated polyethers. The high cost of these solubilizers, however, has limited the commercialization of the promising CO_2-based processes. But in the late 1990s, Beckman's group proposed a hypothesis for design of CO_2-philic polymers that incorporated the earlier conclusions reached by both McHugh and Johnston. They designed and synthesized a series of economical polymers that contain no fluorine and readily dissolve in CO_2 at low pressures [19]. Beckman et al. proposed that CO_2-philic polymers should incorporate monomers (or functional groups) that contain several features: high flexibility (and thus low Tg), low cohesive energy density and also Lewis base groups to provide loci for specific interactions between the polymer and CO_2. They demonstrated the effectiveness of the hypothesis by designing highly CO_2-soluble ether-carbonate copolymers from CO_2 and inexpensive oxiranes such as propylene oxide or ethylene oxide. The design of these non-fluorinated CO_2-philic polymers greatly enhances the potential for industrial application of CO_2, both in polymer science and general chemical processing. Among the CO_2-philic systems mentioned in Figure 1.5, the poly (ether carbonates) will be mentioned in the course of this study.

1.3.5.1.1 Non- fluorinated Polymer Design for scCO$_2$

In the below scheme, polymeric materials are summarized in terms of their solubility in scCO$_2$ media.

Polymeric Materials

Carbon dioxide - phylic

- Fluoropolymers
- Silicone based polymers
- Poly(ether carbonates)

Carbon Dioxide - phobic

- Hydrophylic
- Lipophylic
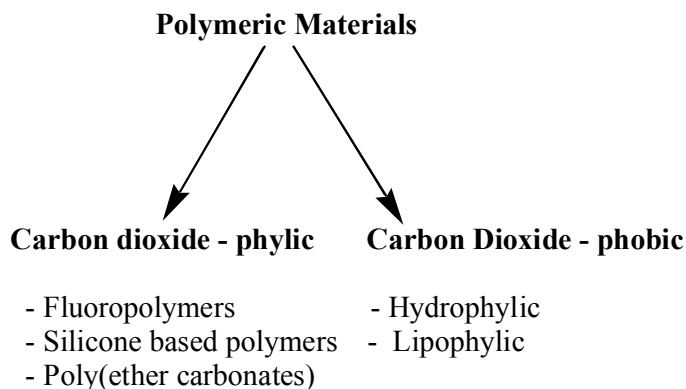
Figure 1.4 Solubility of Polymeric Materials in scCO$_2$ [35]**.**

As stated above, the CO_2-philic material may be a copolymer in which each structural unit has specific qualities that will optimize the copolymer's solubility in carbon dioxide. This requirements are fullfiled if the consistent monomers optimze the balance between ethalpy and entrophy of solute-copolymer and copolymer-copolymer interactions. The related data is given in Figure 1.5. Therefore, it should be proposed that a CO_2-philic hydrocarbon polymer should be a copolymer consisting of the following [19]:

(i) Monomer 1 (M1), which contributes to high flexibility, high free volume, and weak solute/solute interactions (low cohesive energy density or interfacial tension). Generally, low Tg and steric parameter values are used as evidence for high flexibility and free volume in polymeric materials. These factors combine to create a favorable entropy of mixing for the copolymer in CO_2, as well as weak solute/solute interactions, easing dissolution into CO_2.

(ii) Monomer 2 (M2), which produces specific solute/ solvent interactions between the polymer and CO_2 through a Lewis base group (e.g., carbonyl group) in the side chain or backbone of the polymer.

Ideally, interactions between M1 and M2 should be enthalpically unfavorable, further helping to promote dissolution in carbon dioxide. It is possible that this feature is a strong contributor to the low miscibility pressures of fluoroacrylate polymers in CO_2, in that interactions between the fluorinated side chains and acrylate backbone of this material are likely to be unfavorable. Because use of a homopolymer of either M1 or M2 only serves to optimize part of the free energy, if both monomer 1 and monomer 2 are chosen in the proper proportions, then the copolymer should be more soluble than either of the homopolymers. Figure1.6 presents the principles for designing CO_2-philic materials
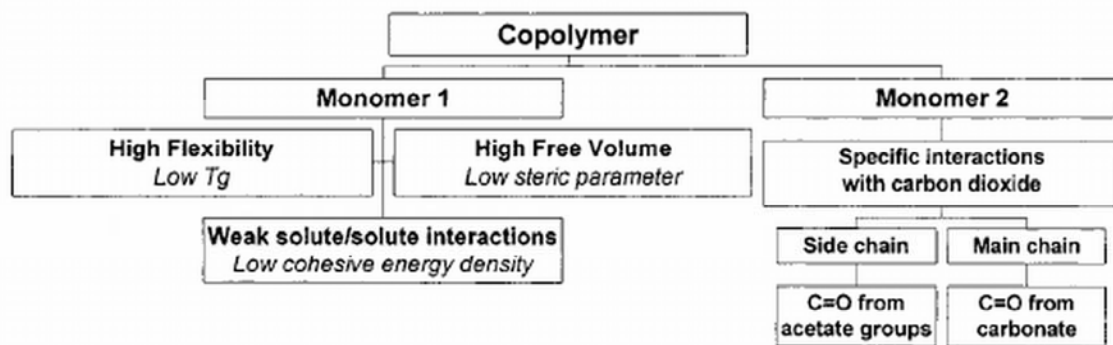
Figure 1.5 CO_2-philic material design [36].

Among the key characteristics of the poly (ether-carbonate) "CO_2-philes" are a low glass-transition temperature, weak interactions with other polymer chains, and a Lewis base functional group to create favorable interactions with the CO_2 solvent. To sum up, concerning the poly (ether carbonate) copolymer, the etheric moiety incorporates flexibility and subsequently low Tg to the structure, whereas, the carbonate group presents a Lewis base group to the polymer that are known to interact specially with CO_2.

1.3.5.2 Utilization of CO_2 in Polymerization Reactions

Three main categories can be given on account of utilization of CO_2 in polymerization reactions; utilization in chain and condensation polymerizations, as well as its utilization as a monomer. In the course of this thesis, the first two categories will be excluded, since it is out of the scope of the present study and the utilization of CO_2 as monomer will be discussed in detail.

1.3.5.2.1 Utilization of CO_2 in Chain Polymerizations

In chain polymerizations, an initiating species is formed which then contacts a monomer, creating the beginning of an active chain. This chain then grows rapidly to form the polymer molecule. Finally, a chain-terminating event may take place (or monomer may be depleted), ending growth of the chain in question. The various chain

polymerization types are then further subdivided based on the type of initiating species and also the relative rates of initiation and growth [37]. These polymerizations are categorized into two subtitles; free radical solution polymerization, heterogeneous free radical polymerizations including emulsion, dispersion and suspention polymerizations in $scCO_2$

. Carbon dioxide, while not a powerful solvent, is miscible with a large variety of volatile, low molecular weight vinyl monomers in these reactions.

1.3.5.2.2 Utilization of CO_2 in Condensation Polymerizations

Condensation polymerization [37] occurs through the step-wise addition of difunctional monomers to each other, usually in a reaction that produces a small molecule byproduct (water or alcohol, for example). Polyesterification (reaction of diol with diester or diacid) and polyamidation (diamine with diacid or diester) are two classic examples of great industrial importance. Because of the nature of these polymerizations, there are key differences with respect to chain polymerizations. Condensation polymerizations are usually endothermic, and hence heat must be applied to achieve high rate of reaction. Unlike chain polymerization, molecular weight builds slowly in condensation reactions. Indeed, the statistics of condensation polymerization show that the extent of reaction of the active end groups must reach at least 90% to create polymer chains of reasonable length. Because each condensation reaction is governed by equilibrium, removal of the small molecule byproduct is crucial in achieving high extent of reaction and hence high chain length.

Given the nature of condensation polymerizations, CO_2 has been applied as a diluent/plasticizer to enhance the removal of the small molecule, hence increasing molecular weight [38]. By dissolving in the polymer melt, CO_2 should reduce the viscosity and increase the rate of removal of the condensation byproduct. Clearly, for the process to be most successful, the small molecule should partition preferentially to the CO_2 phase. The green aspect of such a scheme is that use of CO_2 could allow better removal of the condensation byproduct at lower temperature, saving energy. The best example of this use of CO_2 is probably the work of Kiserow and DeSimone on the CO_2-enhanced solid-state polymerization of polycarbonate. In bisphenol A polycarbonate

production, diphenyl carbonate is reacted with bisphenol A to produce the polymer plus phenol. DeSimone showed that CO_2 could be employed to remove phenol from polycarbonate oligomers at temperatures well below the Tg of the polymer (420 K), raising molecular weight substantially [7]. A general problem with using CO_2 to enhance condensation byproduct removal is the low solubility of some common byproducts in carbon dioxide. Indeed, the use of CO_2 to plasticize polymer melts and remove condensation byproducts is sound, sustainable processing, but this technique will only be truly effective if the byproduct is designed to partition strongly to CO_2.

1.3.5.2.3   Utilization of Carbon dioxide as a monomer

As the literature reveals, the use of CO_2 on the other hand, has permeated almost all parts of the chemical industry, and that careful application of CO_2 technology can result in products that are cleaner, less expensive and of purity [5].

It has been known since 1969 that carbon dioxide can be copolymerized with oxiranes to form poly(ether-carbonates) [39]. Production of a polycarbonate using CO_2 instead of phosgene (the usual route) is indeed a green process, in that not only is a harmful chemical replaced with a benign alternative, but the production of substantial quantities of salt (the usual byproduct in polycarbonate production) is avoided. Poly(ether-carbonates) formed from oxiranes and CO_2 could be applied as degradable surfactants (using ethylene oxide) or low energy alternatives to polyesters polyols in polyurethane manufacture (using propylene oxide). They have also been found to be the most CO_2-philic, non-fluorinated materials yet identified [19] and hence they could enhance the wider use of CO_2 as a benign solvent. There are, however, some key technical obstacles that have substantially prevented the commercialization of a CO_2-based route to a polycarbonate to date:

> 1) Most of the catalysts developed to date have not demonstrated particularly high activity when used with either ethylene oxide or propylene oxide, the comonomers most likely needed to produce economically viable copolymers [40]. On the other hand, a number of catalyst systems have been shown to be highly effective in the copolymerization of CO_2 with cyclohexene oxide [41,

18

42], although this copolymer has not attracted any significant industrial interest owing to monomer cost versus polymer properties.

2) Those catalysts that *have* shown high activity in CO_2/propylene oxide co-polymerizations have not permitted significant incorporation of CO_2 into the copolymer (typically <10% carbonate) [43].

3) Catalysts developed so far tend to produce substantial amounts of low molecular weight and cyclic carbonate when used with either ethylene oxide or propylene oxide. In many cases, over 80% cyclic material is produced. The low molecular weight cyclic cannot be polymerized, and hence these catalysts could not be employed economically.

Clearly, the most pressing issue one must deal with to conduct a copolymerization in a supercritical fluid is that of catalyst and substrate solubility. Carbon dioxide is without question the most popular solvent of those with a readily accessible (<370 K) critical temperature. However, CO_2 is also a feeble solvent [44, 45], whose inability to effectively solvate compounds of interest has greatly inhibited commercial development in the past. Up to now, there have been many studies on the design and synthesis of CO_2-soluble catalyst with different organic molecules and their various metal forms, for instance, the metal porphyrin [46], metal carboxylate [42] and metal phenoxide [47] catalysts and their derivatives. More precisely, epoxides copolymerize with carbon dioxide, with metal containing catalysts such as zinc diethyl and additives, zinc carboxylates, and metal porphyrin complexes. The resulting copolymers have alternating epoxide and carbon dioxide groups, and are polycarbonates. These copolymers have found uses in many areas, such as ceramic binders, evaporative pattern casting, and adhesives [48]. Various attempts in the literature for the design of viable catalyst in these systems are discussed in detail below.

Early work (1970s–1980s) focused on the assessment of zinc catalysts for the copolymerization of oxiranes and CO_2. These catalysts typically employed a reaction between dialkyl zinc and a multi-hydroxyl containing compound to create the active catalyst. Polymerization times were relatively long, significant amounts of cyclic carbonate were produced, yet alternating copolymer (100% carbonate) could be generated. Molecular weight distributions in these polymerizations could be very broad, often >5.0. Nevertheless, a zinc system was eventually used to synthesize an ethylene

oxide–CO_2 alternating copolymer that was applied commercially (PC Corp., Wilmington, DE) as a ceramic binder (this copolymer degrades cleanly to gaseous byproducts at temperatures >470 K).

Recent work in this area has focused on the development of 'single-site' style catalysts to allow better control over molecular weight [49, 50]. However, while these new catalysts have proven to be very effective in the copolymerization of cyclohexene oxide and CO_2, none have been able to solve the problems observed during copolymerizations of CO_2 and either ethylene oxide or propylene oxide. In general, in copolymerizations of CO_2 and propylene oxide, catalysts derived from aluminum exhibit high activity and produce predominantly copolymer with a narrow molecular weight distribution, yet allow little CO_2 incorporation into the copolymer [43]. Zinc catalysts allow for high levels of CO_2 in the copolymer, yet produce predominantly low molecular weight alkylene carbonate.

Many metal-containing catalysts exhibit low solubility in carbon dioxide at moderate pressures, while, simple metal carbonyls are known to be miscible with CO_2 under relatively mild conditions [49] and have been used successfully to catalyze reactions in carbon dioxide.

Among the design of CO_2-soluble catalyst efforts, the U.S. patent of number 4.783.445 which improves catalysts for the copolymerization of epoxides with carbon dioxide can be counted up [48]. These catalyst systems are soluble in a variety of solvents are prepared by reacting zinc compounds with anhydrides in the presence of an alcohol or by reacting zinc salts with a monoester of a dicarboxylic acid. They can be added as a solution to a mixture of epoxides and carbon dioxide to prepare poly (ether carbonate)s. These soluble catalyst systems can also be charged to the reactor with other feedstocks without special equipment or handling requirements. Many solvents are suitable for the synthesis of the catalysts. When using anhydrides, the preferred solvents are the lower alcohols, such as methanol, ethanol, propanol, and butanol. The solvent should be low enough in molecular weight to be easily removed from the reaction mixture under vacuum. Therefore the soluble catalyst, obtained from phthalic anhydride and Zinc Oxide in the presence of ethanol, has been employed for the polymerizations in the course of this thesis.

Indeed, the generation of copolymers of CO_2 and either propylene or ethylene oxide would represent green chemistry, as these materials would have ready markets and alternative routes to their production (via phosgene) are highly problematic from a sustainable viewpoint. Until the technical difficulties to efficient copolymerization of CO_2-based route to aliphatic polycarbonates can be overcome, aliphatic polycarbonates will not enjoy widespread use. Whereas, a variety of other polymers have also been generated from CO_2, either the properties of these new materials have not been promising or the efficiency of the polymerization low. Hence, they are technical curiosities rather than potential avenues for green chemistry. Indeed, to achieve the highest impact (with respect to green chemistry), research should be directed at creating catalysts that target the efficient copolymerization of low cost epoxides and CO_2.

As mentioned above, many solvents are unpleasant but essential for industrial chemicals. Supercritical carbon dioxide would be a viable 'green' alternative but its use has been restricted by its limited solvent power. This is about to change and have found many uses as an industrial activity. The utilization of these copolymers is not negligible nowadays, and increasing each day. Some of these industrial applications can be counted as follows;

- PC Corp. (DE, USA) sells aliphatic polycarbonate (used as a ceramic binder) generated via the copolymerization of CO_2 and ethylene oxide.
- Xerox has patented [51] a process where bisphenol A polycarbonate is generated from bisphenol A and diphenyl carbonate using CO_2 to extract the residual phenol.
- Akzo-Nobel patented [52] the formation of a degradable surfactant via the copolymerization of ethylene oxide and CO_2, where the polymerization is terminated by a fatty acid.

It is important to state here that, every optimization in these copolymerization systems opens new applications.

2   CHAPTER 2

SYNTHESIS OF SIDE CHAIN LIQUID CRYSTALLINE POLYCARBONATES IN SUPERCRITICAL CARBON DIOXIDE MEDIA

2.1   Introduction

2.1.1   Historical Aspects of Liquid Crystals

Liquid crystals were discovered in 1888 by Austrian botanist Friedrich Reinitzer when he was studying the melting behaviour of cholesteryl benzoate. He observed that this material had two distinct melting points. He noticed the appearance of a turbid fluid at 146°C which did not form a conventional clear liquid until 178°C. During his studies the color of the turbid liquid also changed from red to bright blue-violet topale blue, and the whole process was reversible. Reinitzer sent his work to Otto Lehmann, a professor of natural philosophy (physics) in Germany. Lehmann had constructed a polarizing microscope with a stage to control precisely the temperature of this samples. He examined Reinitzer's substance with his microscope and noticed its similarity to other samples he was studying then. He concluded that a new state of matter had been discovered that was intermediate in ordering between the crystalline solid and isotropic liquid phases. Accordingly, this intermediate phase became known as the liquid crystal phase or mesophase [53]. The term 'liquid crystal' was coined by Otto Lehmann in 1900 (although at first he called them 'flowing crystals' (1889) and 'crystalline solids' (1890)) [53].

Much research in these early days provided information on the nature of the liquid crystal phase and many different types were discovered. However, the significance of

liquid crystals in technological devices (e.g., displays and thermography) was not realized until the 1960s. More importantly, it was not until the discovery of stable, room temperature, nematic liquid crystals by George Gray (an organic chemist at the University of Hull) in 1973 that liquid crystal displays could be made commercially viable [54]. Slowly, the phase studies to discover new and stable liquid crystals spread all over the world and there was an explosive growth during the 1980s and 1990s [55, 56]. Theories for the liquid crystal (LC) phases added a new dimension of study and the invention of liquid crystal displays gave the field a practical dimension. Scientific studies of LCs involve both the chemistry and physics of this state, concerned with liquid crystal synthesis and investigation of structure-property relationships. Many different liquid crystalline materials are now known and they generate a wide range of different liquid crystalline phase types. The intense research into the design, synthesis, evaluation and applications of liquid crystalline materials has provided a wide range of quality liquid crystal displays and a multitude of thermo chromic devices. Technologically, LCs have become a part of our lives, first showing up in wristwatches and calculators, but now being used for all kinds of advanced instrumentation , including laptops and flat panel displays. Their advantage was first their low power consumption and small size; now they are competitive with other technologies for attractiveness, ease of viewing, cost and durability.

2.1.2   The Occurrence of Liquid Crystalline Phases

So, liquid crystals are substances that exhibit a phase of matter that has properties between those of a conventional liquid, and those of a solid crystal. For instance, a LC may flow like a liquid, but have the molecules in the liquid arranged and oriented in a crystal-like way. The figure below explains the melting sequence for a liquid crystalline material.
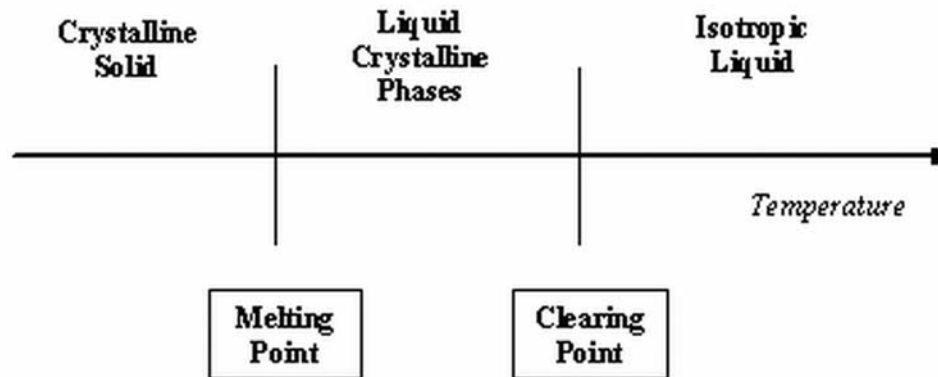
Figure 2.1 The possible melting sequence for a liquid crystalline material.
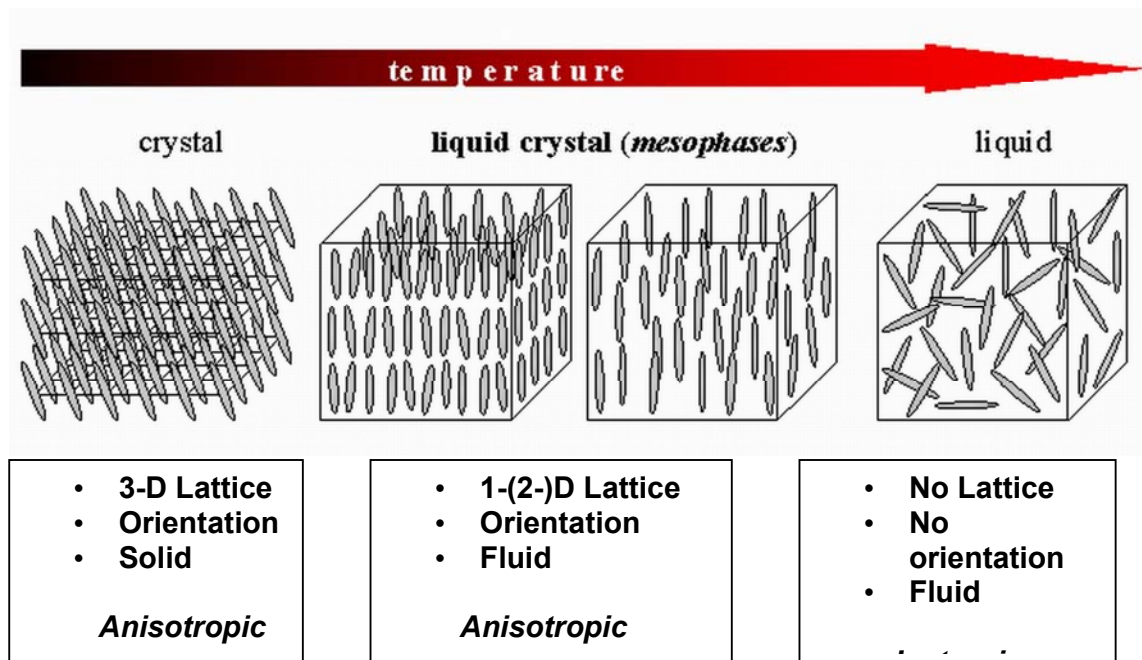
Figure 2.2 The molecular picture of solids, liquid crystals and liquids [57].

The distinguishing characteristsics of phases of condensed matter can be given as ;

    i. Positional order

    ii. Orientational order.

Positional order refers to the extent to which molecules or groups of molecules, on average, show translational symmetry. Orientational order refers to the extent to which the molecules align along a specific direction on a long-range basis [57].

As represented in Figure 2.2, molecules in a crystalline solid constraint to occupy certain positions in lattice sites and to orient themselves with respect to each other in specific directions. But, when this fully ordered molecular crystal is heated, the thermal motions of the molecules within the lattice increase and eventually the vibrations become so intense that the regular arrangement of molecules are broken down with the loss of long-range orientational and positional order to give the disorganized isotropic liquid. Thus, a crystal has orientational and three-dimensional positional order, whereas a liquid has none. The temperature at which this process occurs is called the melting point and the heat absorbed by the molecules is the latent heat of fusion. However, this process, which takes a compound from being very well ordered to being totally disordered in one step, is a very destructive one, which is not universal for all compounds. For many compounds, this process occurs by way of one or more intermediate phases as the temperature is increased. These phases are called mesophases and some of these mesophases are liquid crystalline. In contrast, for the liquid crystalline phases, the positional order could be lost but small degree of the orientation order remains as revealed in Figure 2.2.

So, liquid crystalline mesophases have properties which are intermediate between those of the fully ordered crystalline solid and the isotropic liquid; liquid crystalline mesophases are fluids which, due to partial orientational ordering of the constituent molecules, have anisotropic material properties (*i.e.*, their magnitude will differ from one direction to another)such as permittivity, refractive index, elasticity and viscosity. Depending on the degree of positional order, different liquid crystal phases arise, e.g. no positional order, giving rise to the nematic phase.

2.1.3   Classification of Liquid Crystals

There are two main classifications of liquid crystals, thermotropic and lyotropic, which are distinguished by the mechanisms that drive their self-organization [58].

2.1.3.1 Lyotropic Liquid Crystals (LLCs)

The LC behavior occurs when the mesogen is dissolved in a solvent above a certain critical concentration and the mesogens exhibit their phase transitions through the addition or removal of a solvent. In the lyotropic phases, solvent molecules fill the space around the compounds to provide fluidity to the system. Their organization is normally not based on mesogenic properties of a certain molecule but rather on the interaction between two, or even more, molecular units in solution. Therefore their sequence of phases rather depends on the concentration of the components added to the mixture than on temperature. These types of liquid crystal are very common in the biological world, for instance in cell membranes [59]. Since it is out of the scope of this work, this type will not be discussed in detail.

2.1.3.2 Thermotropic Liquid Crystals (TLC)

The LC phenomenon occurs in the melt phase and depends on the temperature. These are the molecules that show liquid crystalline behavior above their solid crystalline melting point. Liquid crystalline behavior is only seen over a limited temperature range. TLCs occur due to anisotropic dispersion forces between the molecular and packing interaction. The dipole-dipole interaction and Van der Waal's force are the primarily attraction force responsible for the mesophases [58]. Thermotropic mesophases have been found to be produced by two distinct types of molecular shape, rod-like called *calamitic liquid crystals* which were the first to be discovered, and disk-like called *discotic liquid crystals* which have been discovered relatively recently. The Columnar/discotic phases arise when disk-like molecules are stacked together in columns. These columns, which are liquidlike, are packed together to form a two-dimensional crystalline array. This type of LCs used in a wide range of applications, especially in the electro-optical displays. The discussion here will focus on TLCs that are calamatic. There are now many different types of liquid crystalline materials in addition to those generated by long and lath-like molecules. The Calamitic Liquid Crystals can be generally classified according to Figure 2.3.
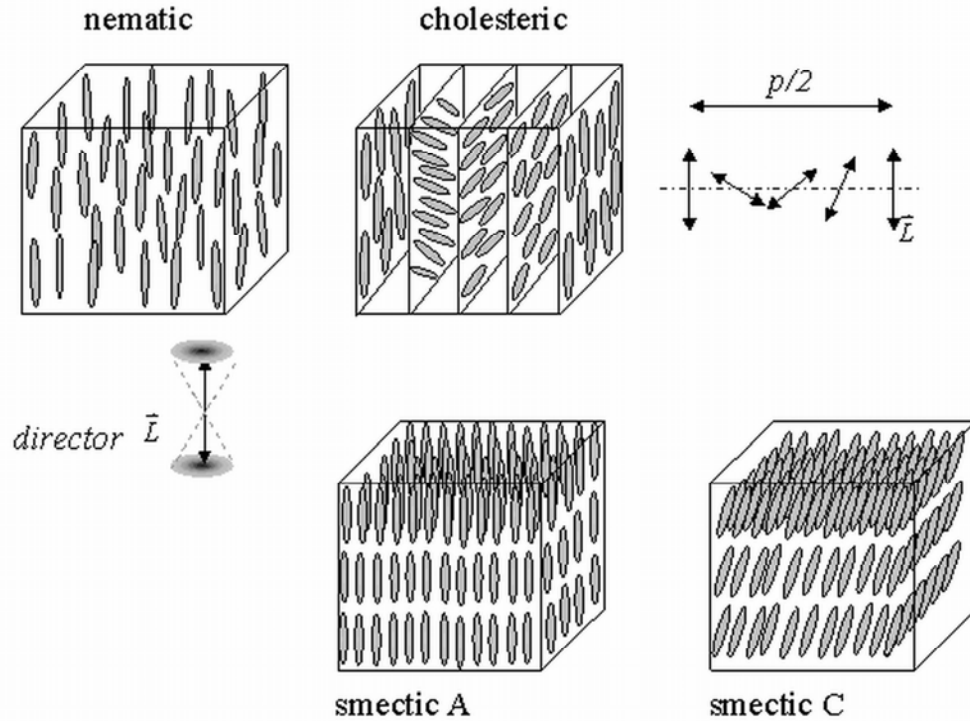
Figure 2.3 Molecular arrangement of some important thermotropic, calamitic liquid crystalline phases as intermediate state between solid and liquid [58].

2.1.3.2.1 Nematic phase

One of the most common LC phases is the nematic, where the molecules have no positional order, but they do have long-range orientational order. Thus, the molecules flow and are randomly distributed as in a liquid, but they all point in the same direction (within each domain). Most nematics are uniaxial: they have one axis that is longer and preferred, with the other two being equivalent. Some liquid crystals are biaxial nematics, meaning that in addition to orienting their long axis, they also orient along a secondary axis [60].

2.1.3.2.2 Smectic phase

The word smectic means 'soap-like' in Greek. Smectic liquid crystals exhibit long range orientational order like the nematics and, in addition, layering perpendicular to some direction. There are three main types of smectic phases: A, C and C* . In the

27

smectic A phase (SmA), the molecules point perpendicular to the layer planes, whereas in the smectic C phase (SmC), the molecules are tilted with respect to the layer planes. The (chiral) smectic C* phase is formed by optically active molecules or when smectic C is doped with a chiral substance. In this hexatic phase, the mesogens in a particular layer take on a roughly hexagonal close-packed ordering, with typically no registry between adjacent smectic layers. It is also possible to find examples of liquid crystals where the registry between layers is fairly strong; hence there are three dimensional positional (and possibly even orientational) orders. These phases are called crystal mesophases, and are in fact nearly as ordered as solid crystals (although they still exhibit fluid-like flow) [60].

2.1.3.2.3 Chiral phases

In the smectic C* phase, the molecules orient roughly along the director, with a finite tilt angle, and a twist relative to other mesogens. This results in, again, a spiral twisting of molecular axis along the director.
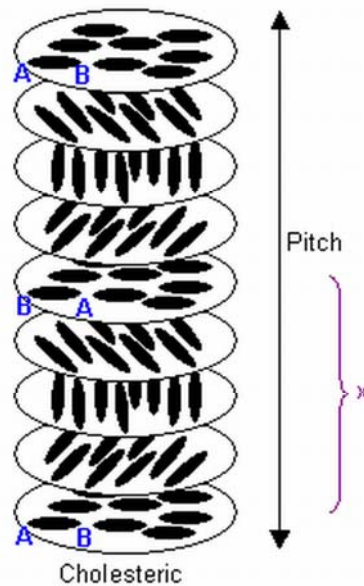
Figure 2.4 The representation of a cholesteric liquid crystalline and its pitch length [61].

The chiral nematic phase exhibits chirality (handedness). This phase is often called the cholesteric (N*) phase because it was first observed for cholesterol derivatives. Only chiral molecules (i.e.: those that lack inversion symmetry) can give rise to such a phase. The cholesteric (or chiral nematic) liquid crystal phase is typically composed of nematic mesogenic molecules containing a chiral center which produces intermolecular forces that favor alignment between molecules at a slight angle to one another. This leads to the formation of a structure which can be visualized as a stack of very thin 2-D nematic-like layers with the director in each layer twisted with respect to those above and below. In this structure, the directors actually form in a continuous helical pattern about the layer normal. The molecules are merely representations of the many cholesteric mesogens lying in the slabs of infinitesimal thickness with a distribution of orientation around the director [60]. The structure of a cholesteric LC is represented in Figure 2.4. This is not to be confused with the planar arrangement found in smectic mesophases.

An important characteristic of the cholesteric mesophase is the pitch. The chiral pitch refers to the distance (along the director) over which the mesogens undergo a full 360º twist (but it should be noted that the structure repeats itself every half-pitch, since the positive and negative directions along the director are equivalent). The half pitch distance of a cholesteric LC is illustrated on Figure 2.4. The pitch may be varied by adjusting temperature or adding other molecules to the LC fluid.

For many types of liquid crystals, the pitch is on the same order as the wavelength of visible light. This causes these systems to exhibit unique optical properties, such as selective reflection. These properties are exploited in a number of optical applications. A color will be reflected when the pitch is equal to the corresponding wavelength of light in the visible spectrum. This effect is based on the temperature dependence of the gradual change in director orientation between successive layers, which modifies the pitch length resulting in an alteration of the wavelength of reflected light according to the temperature. The angle at which the director changes can be made larger, and thus tighten the pitch, by increasing the temperature of the molecules, hence giving them more thermal energy. Similarly, decreasing the temperature of the molecules increases the pitch length of the cholesteric liquid crystal. This makes it possible to build a liquid crystal thermometer that displays the temperature of its environment by the reflected

color. Mixtures of various types of these liquid crystals are often used to create sensors with a wide variety of responses to temperature change. Such sensors are used for thermometers often in the form of heat sensitive films to detect flaws in circuit board connections, fluid flow patterns, condition of batteries, the presence of radiation, or in novelties such as "mood" rings. In the fabrication of films, since putting cholesteric liquid crystals directly on a black background would lead to degradation and perhaps contamination, the crystals are micro-encapsulated into particles of very small dimensions. The particles are then treated with a binding material that will contract upon curing so as to flatten the microcapsules and produce the best alignment for brighter colors. An application of a class of cholesteric liquid crystals which are less temperature sensitive is to create materials such as clothing, dolls, inks and paints. The wavelength of the reflected light can also be controlled by adjusting the chemical composition, since cholesterics can either consist of exclusively chiral molecules or of nematic molecules with a chiral dopant dispersed throughout. In this case, the dopant concentration is used to adjust the chirality and thus the pitch [58].

In the design of liquid crystal compounds the most important aspect is that they must exhibit the correct type of liquid crystalline phase over the desirable temperature, usually room temperature. Additionally liquid crystals must have a suitable combination of structural features to enable the generation of a rather subtle blend of physical properties. Clearly, to obtain everything from one material is not possible and so liquid crystals for commercial applications are all mixtures of appropriate materials that provide the best compromise of properties. A wide variety of synthetic organic chemistry techniques are used to prepare liquid crystal materials. An equally wide range of techniques are used to assess the materials both as single compounds and in mixtures. Many liquid crystalline materials are synthesized for fundamental reasons, *i.e.*, to determine the relationship between the molecular structure and the physical properties; others are synthesized directly for applications (*e.g.*, display devices and thermo chromic devices).

2.1.4   Chirality (Handedness) in Liquid Crystals

In certain cases, organic molecules can be chiral or handed. A chiral object has such a shape that it can not be superposed on its mirror image; rather like a left hand and a right hand. The two non-superimposable, mirror-image forms of chiral molecules are referred to as enantiomers. Each chiral center of the enantiomers is labeled as *R* or *S* [62]. In the following figure, the two enantiomers of a bromochlorofluoromethane are given, representing the chirality of the molecule by possessing an asymmetric carbon atom.
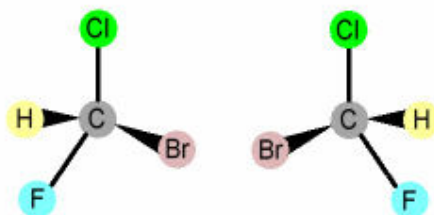
Figure 2.5 The two enantiomers of bromochlorofluoromethane [63].

The study of chirality falls in the domain of stereochemistry, which is a subdiscipline of chemistry involving the study of the relative spatial arrangement of atoms within molecules. Chiral compounds exhibit optical activity, i.e., when polarized light is passed through a substance containing chiral molecules, the direction of polarization can be changed. This phenomenon is called optical rotation or optical activity. On the other hand, a 50/50 mixture of the two enantiomers of a chiral compound is called a racemic mixture and does not exhibit optical activity [62].

The isolation of one particular isomer gives a chiral material and this type of chirality is often described as molecular chirality. However, liquid crystals are ordered phases that are also fluid and when certain liquid crystal phases are composed of chiral molecules then the whole phase becomes chiral or handed; this type of chirality is often called form chirality where some macroscopic feature of the bulk phase has a handed structural feature [62]. As already described, chiral mesogens usually give rise to chiral mesophases. For molecular mesogens, this means that the molecule must possess an asymmetric carbon atom. An additional requirement is that the system not be racemic,

31

in other words, a mixture of right- and left-handed versions of the mesogen will not cancel the chiral effect [63].

An object is either chiral or achiral (it either lacks or has mirror symmetry); it cannot be both. If a liquid crystalline substance consists of chiral molecules we denote this by putting a star after the phase labels, for instance N* or C*. Chirality is *not* a state of matter and there can thus be no phase transition from chiral to achiral, or vice versa. For instance, a nematic phase made up of chiral molecules cannot turn into an achiral phase at a certain temperature. Chirality has important consequences on the macroscopic arrangement of the liquid crystal molecules and this in turn affects the optical behavior of the substance [64]. Chiral phases usually have a helical twisting of the mesogens. In the figure below, the helical axis of the N* and the SmC* liquid crystals are given. The chiral twisting that occurs in chiral LC phases also makes the system respond differently to right- and left-handed circularly polarized light. These materials can thus be used as polarization filters.
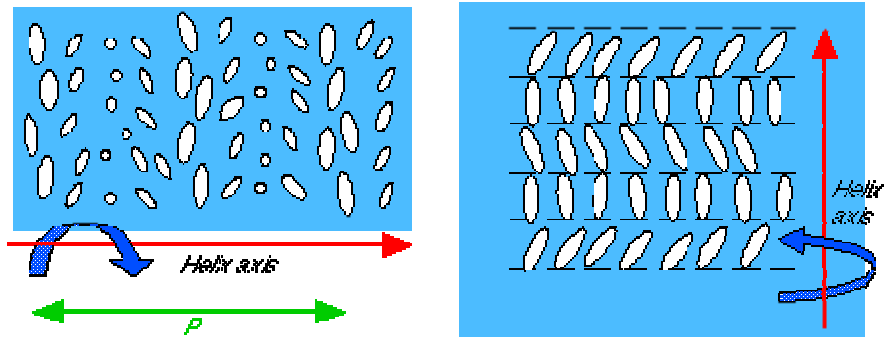
Figure 2.6.a. The chiral nematic, or cholesteric, phase forms a helical structure. The molecules twist in a plane perpendicular to the screen.

Figure 2.6.b. The helical structure of the chiral smectic C* phase. The tilted molecules precess in a plane perpendicular to the screen.

Figure 2.6 The helical structure of **a)** Cholesteric phase **b)** Smectic C* [65].

The most common liquid crystalline phase that exhibits form chirality is the cholesteric (N*) phase or in other words the cholesteric (Ch) phase as stated before. .In the cholesteric phase the chirality manifests itself in the form of a helical arrangement of molecules as illustrated in Figure 2.6. As previously mentioned, the molecular alignment is identical to that found in the nematic phase except that the molecular chirality causes a slight, sequential change in the direction of the rod-like molecules

through a section of material. This gradual change in molecular direction in other words, is the pitch of the material. For a particular chiral material the direction of the helix is opposite for each isomer but the pitch length is the same. As it is seen in the above figure, the helix axis, around which the molecules twist, lies perpendicular to the local director. Since the twist has a constant strength throughout the sample, a periodic structure along the helix axis is obtained. It is not a positional periodicity but a directional. Every half turn of the helix the molecules are oriented the same way. If we shine light with a wavelength corresponding to the pitch, through the sample along the helix axis, the circularly polarized component with the same handedness is totally reflected [66]. This gives the substance a beautiful intense color, easily observable by the naked eye. Consequently, interesting optical interference effects will be observed. Since the pitch varies with temperature, the color of the substance will also vary [65].

The chiral smecticC (SmC*) phase also exhibits form chirality as a helical macrostructure. In the achiral SmC phase the constituent molecules are tilted with respect to the layer normal and the helix in the chiral variant is generated by a slight, sequential change in the direction of the tilt within each layer as shown in Figure 2.6. Due to the layered structure, no twist can be admitted within the layer. Without breaking the layers, the orientation of the director can vary continuously only between the layers, thus when going from one layer to the next. Hence, the helix axis must now lie perpendicular to the layer planes. The pitch of the helix of the SmC* phase is also temperature dependent but at high temperatures the pitch is long and at low temperatures the pitch is short. The combination of chirality and tilt in the SmC* phase reduces the symmetry of the system and the constituent molecules are spontaneously polarized; this phenomenon has great technological implications for very fast-switching ferroelectric light shutters and display devices [66].

2.1.5 Identification of Liquid Crystalline Phases

The presence of a liquid crystalline phase is usually quite easy to identify but the identification of the phase type is often very difficult. Liquid crystal phases can be identified by a variety of techniques like optical polarizing microscope, differential

33

scanning calorimetry, X-ray analysis, miscibility studies [53]. These techniques are described below.

2.1.5.1 Optical polarizing microscopy

It is the most common method used to identify liquid crystal phases. A small sample of liquid crystal is placed on a microscope slide with a cover slip. The sample slide is placed in a hot-stage of variable temperature which is placed under a microscope between crossed polarizers. In a polarising microscope, the light is polarized by passing it through a polarizing filter. It then passes through the sample, and then through a second polarizing filter called the analyzer. When viewed between crossed polarizers an isotropic liquid will appear black because polarized light will be extinguished by the second crossed polarizer. LCs have a certain ordering of their constituent molecules as mentioned before, and are birefringent. Accordingly plane polarized light is affected by the liquid crystal material and does not get extinguished by the second crossed polarizer; this generates a colored texture or pattern. Cooling the liquid can also yield these textures when liquid crystal phases are present [57].
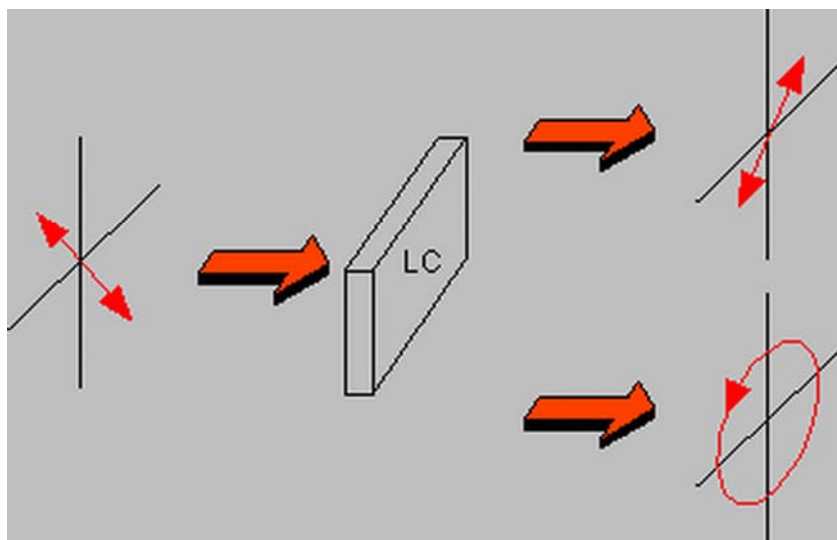
Figure 2.7 When light passes through a liquid crystalline cell, it may change its state of polarization [65].

It is easy to identify some of the simple and common liquid crystalline phases (such as nematic, SmA and SmC) but some of the others are quite difficult to identify and a great deal of experience is required. If a sample with an unknown liquid crystalline phase is mixed with a known and fully characterized liquid crystal then complete miscibility across the phase diagram indicates that the two phases are identical. Such miscibility studies are frequently employed in the identification of liquid crystal phases [54, 57].

2.1.5.2 Differential Scanning Calorimetry (DSC)

A small sample of a material can be subjected to differential scanning calorimetry. This technique measures the enthalpy change associated with a phase transition and displays the information as a graph with a peak for each transition temperature. The position of the peak gives the transition temperature and the area below the peak represents the enthalpy change involved. Although, this technique does not identify a particular phase type it provides valuable information like the exact transition temperatures and the enthalpy change different phase structures [54].

2.1.5.3 X-ray Diffraction

X-ray diffraction is the ultimate tool for the identification of liquid crystal phase type. This technique maps out the exact molecular positions within the structure at each given temperature and thus identifies the liquid crystal phase type at each temperature [54].

2.1.6 Liquid Crystalline Polymers

Liquid crystalline polymers (LCPs) are a class of materials that combine the properties of polymers with those of liquid crystals. These "hybrids" show the same mesophases characteristic of ordinary liquid crystals, yet retain many of the useful and versatile properties of polymers [67].

The two main units of a liquid crystalline material are the spacer and the mesogenic units. The spacer unit is the flexible section of polymer chain between two mesogens or the mesogen and the backbone of a polymer which generally composed of ethylene units. The mesogenic compounds on the other hand, generally consist of long, narrow, lath-like and fairly rigid molecules. Usually, the mesogenic unit is made up of a rigid core of two or more aromatic rings joined together by a functional group. It is the alignment of these groups that causes the liquid crystal behavior. A simple demonstration of a polymeric liquid crystalline structure is given below.

Spacer Unit   Mesogenic Unit
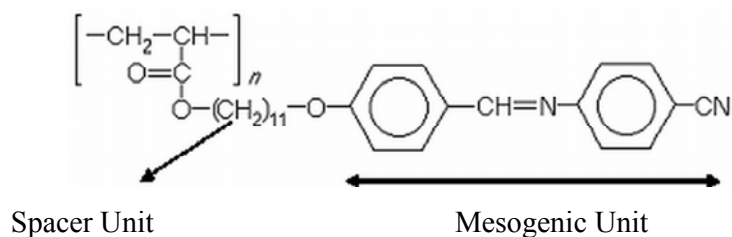
Figure 2.8 The representation of the units of a liquid crystalline in a, liquid crystalline polymer.

In order for normally flexible polymers to display liquid crystal characteristics, the mesogens must be incorporated into their chains. The placement of the mesogens plays a large role in determining the type of LCP that is formed. Main chain liquid crystalline polymers (MCLCPs) are formed when the mesogens are themselves part of the main chain of a polymer. Conversely, side chain liquid crystalline polymers (SCLCPs) are formed when the mesogens are connected to the polymer by the flexible spacer unit as side chains.

They show superior chemical stability, mechanical property and rheological behavior when compared to conventional polymers. LCPs can find applications as high stiffness and high-strength fibers, films with excellent barrier properties, novel composites, processing aids in the melt, endoscopic surgical instruments, electro-optical displays [67].

2.1.6.1 Main Chain Liquid Crystalline Polymers (MCLCPs)

Main chain liquid crystalline polymers are formed when rigid elements are incorporated into the backbone of normally flexible polymers. These stiff regions along the chain allow the polymer to orient in a manner similar to ordinary liquid crystals, and thus display liquid crystal characteristics [67]. There are two distinct groups of MCLCPs, differentiated by the manner in which the stiff regions are formed.

The first group of main chain liquid crystalline polymers is characterized by stiff, rod-like monomers. The following figure shows an example of this kind of MCLCP.
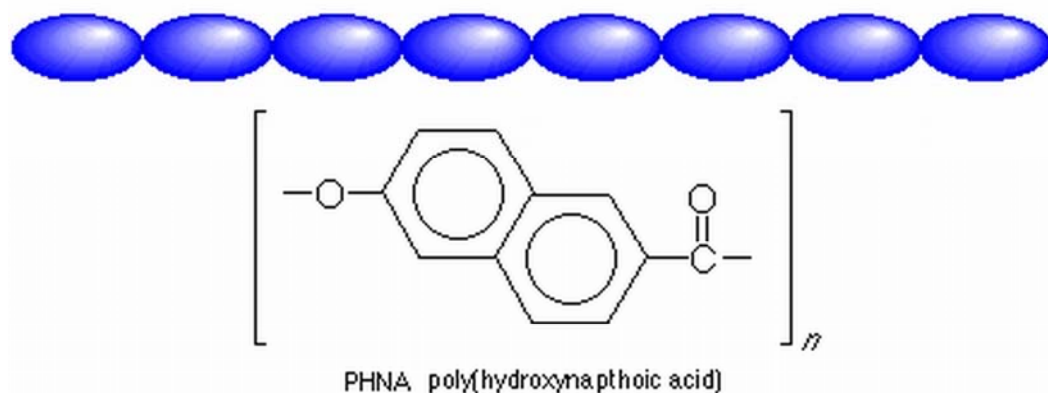
Figure 2.9 Representation of the first group MCLCPs and its example [68].

In this group the mesogenic unit is incorporate directly into the chain and the mesogen acts just like the stiff areas in the group. Generally, the mesogenic units are made up of two or more aromatic rings which provide the necessary restriction on movement that allow the polymer to display liquid crystal properties. The stiffness necessary for liquid crystallinity results from restrictions on rotation that are caused by steric hindrance and resonance. Another characteristic of the mesogen is its axial ratio. The axial ratio is defined to be the length of the molecule divided by the diameter ($x = L/d$). Experimental results have concluded that these molecules must be at least three times long as they are wide. Otherwise, the molecules are not rod-like enough to display the characteristics of liquid crystals [68].

The second group is different from the first in that the mesogens are separated or "decoupled" by a flexible bridge, called a spacer. Decoupling of the mesogens provides

for independent movement of the molecules which facilitates proper alignment. The following is a figure of this type of MCLCP, which consists of a flexible spacer unit of methylene groups and the stiff mesogenic unit of aromatic ring and double bonds.
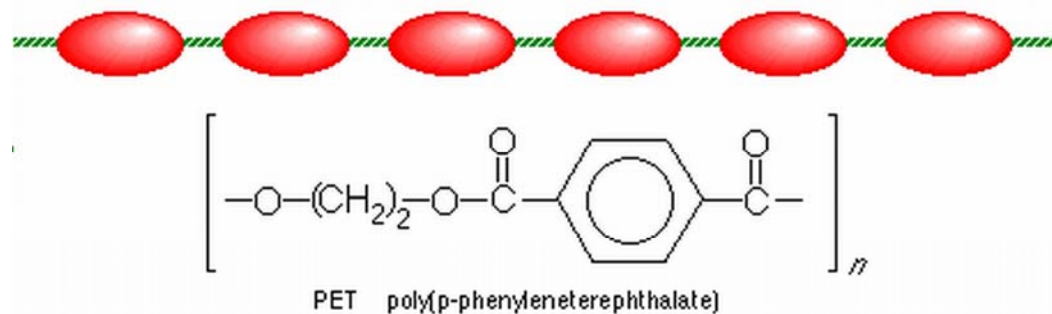
Figure 2.10 Representation of the second group MCLCPs and its example [68].

It is difficult to create polymer liquid crystals that show mesogenic behavior over temperature ranges which are convenient to work with. In fact, many times the temperature of the liquid crystalline behavior is above the point where the polymer begins to decompose. This problem can be avoided in one or more of the following ways [68].

i. The first method of lowering polymer melting temperatures involves the arrangement of the monomers in the chain. If the molecules are put together in random orientation (head-to-tail, head-to-head, etc.) as given in the below representation, interactions between successive chains are minimized. This allows for a lower melting temperature.

ii. Another method to bring the temperature down to a useful range involves copolymerization. If a random copolymer can be created, the regularity of the chains is greatly reduced. This will help to minimize the interactions between the chains by breaking up the symmetry, which in turn will lower polymer melting temperature. The following

38

picture shows the irregularity of polymer substituents that can lead to decreased interactions.
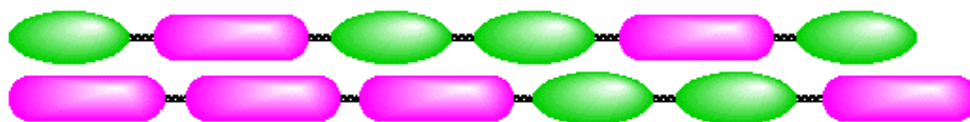
iii.   Finally, defects can be introduced into the chain structures which lower the polymer melting temperature. In the representation below, such a structure is exemplified. This method creates 120 degree "kinks" in the chain which disrupt the ability for neighboring polymers to line up. Unfortunately, this also decreases the effective persistence length so too many kinks can destroy any liquid crystal behavior.
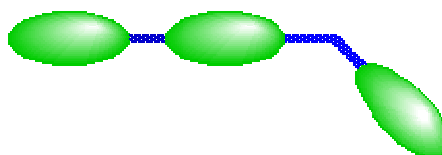
2.1.6.2   Side-Chain Liquid Crystalline Polymers (SCLCPs)

These polymers consist of a mesogen attached to the polymer backbone though a spacer chain that is typically a few carbon atoms long. Recently, side-chain liquid crystalline polymers (SCLCPs) have been receiving increasing attention, both from a scientific and a commercial point of views [69]. The possible uses for these materials take advantage of their physical properties. The most important potential uses are: non-linear optical devices (fiber optics), optical data storage, ferroelectric organic compounds, and the like [67].
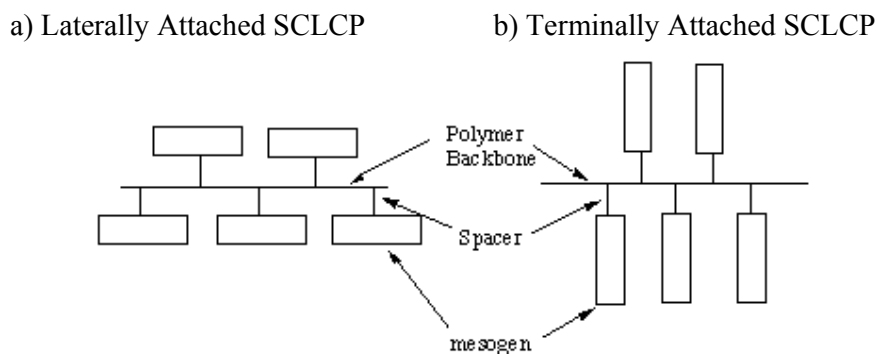
Figure 2.11 A schematic diagram of SCLCPs [70].

Side chain liquid crystalline polymers have three major structural components: the backbone, the spacer, and the mesogen. The versatility of SCLCPs arises because these structures can be varied in a number of ways. The structure of the backbone can be very important in determining if the polymer shows liquid crystal behavior. Polymers with rigid backbones typically have high glass transition temperatures, and thus liquid crystal behavior is often difficult to observe. In order to lower this temperature, the polymer backbone can be made more flexible. It is the alignment of mesogenic groups that causes the liquid crystal behavior. Usually, the mesogen is made up of a rigid core of two or more aromatic rings joined together by a functional group. Like their main chain counterparts, mesogens attached as side groups on the backbone of side chain polymer. These liquid crystals are able to orient because the spacer allows for independent movement. Even though, the polymer may be in a tangled conformation, orientation of the mesogens is still possible because of the decoupling action of the spacer.

The structure of the spacer is an important determining factor in side chain polymer liquid crystals. Generally, the spacer consists of two to four methylene (CH_2) groups attached together in a line. Accordingly, the spacer length has a profound effect on the temperature and type of phase transitions. Usually, the glass transition temperature decreases with increasing spacer length. Short spacers tend to lead to nematic phases, while longer spacers lead to smectic phases [70].

Among these polymers optically active SCLCPs have attracted much attention due to the wide range of their potential applications, in particular in the fields of optics

and electro optics [71]. Many applications of liquid crystals (LCs) require chiral and optically active materials, e.g., doping nematics with such materials to give better response in displays, [72, 73] and ferroelectric properties of smectic LCs are only observed with chiral mesogenic molecules [74, 75].

Chirality can be introduced in SCLCPs at various levels. Although, such a center in the backbone appears particularly interesting, in most polymers in the literature, these chiral centers are located in the terminal position of the pendant mesogenic units. Few reports have dealt with the synthesis of liquid crystalline polymers having chiral centers in the spacer [76] groups or in the macromolecular backbone [77]. Chirality in the backbone appears particularly interesting for two reasons: (1) the presence of a chiral center in the main chain allows one to study the influence of both chirality and tacticity of the macromolecular backbone on the mesomorphic behavior; (2) the introduction of chirality in the polymer backbone may give information about the magnitude of decoupling between the mesogenic units and the arrangement of polymer backbone through the spacer group [78].

2.1.7 Applications of Liquid Crystals

By far the most important application of liquid crystals is in display devices. Apart from liquid, in a liquid crystal the orientation of the molecules is well determined such that they all point in a certain direction. This property can be exploited to make different kinds of displays (called LCD for short). LCDs are now used in a wide range of equipment and apparatus such as watches, calculators, portable color televisions, lap-top computer screens, car, ship and aircraft instrumentation.

Although each of the above mentioned displays are different in detail and application, the basic principle behind their operation is similar. Vertical and horizontal alignments of liquid crystal molecules have different optical properties. Accordingly, liquid crystals are ideal for display devices because;

(i) the mesophase is fluid and therefore the molecules are easily moved by the application of an electric field (1-3 V),

(ii) the phases are structured, and the alignment of the molecules in a thin film of mesophase can be controlled either by boundary conditions (treatment of the glass plates) or by the application of a small electric field.

The elongated liquid crystal molecules are aligned in one direction and give one optical property and when an electric field is applied the fluid molecules reorient to give a different optical property and hence the different usage in displays [79].

The simplest example is the type of display used in a digital watch or a pocket calculator. In this case one uses liquid crystals with molecules that are optically active, which means that they can change the polarization of light.
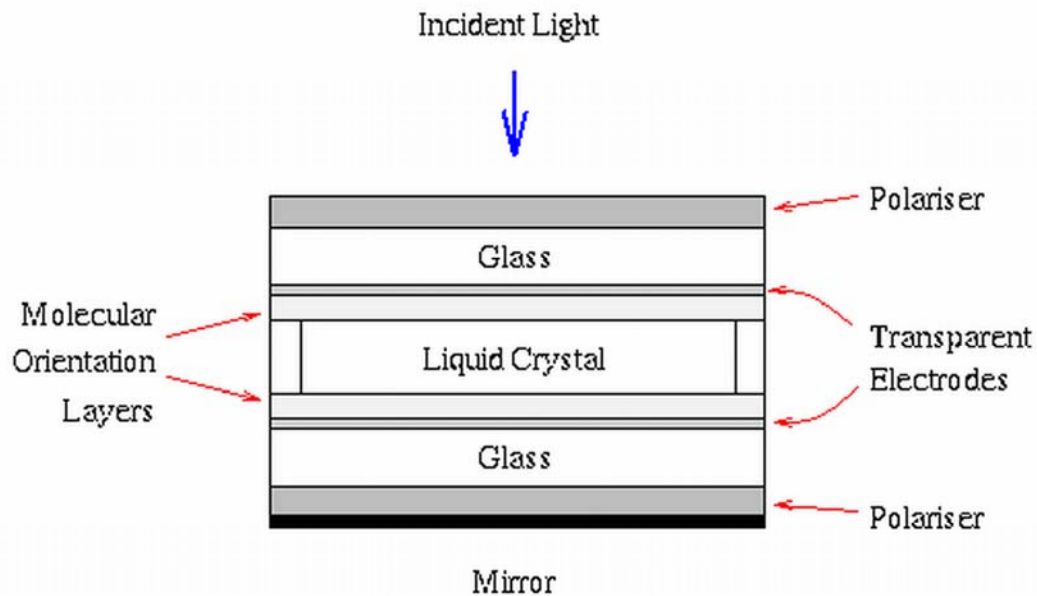
Figure 2.12 The Twisted Nematic Display Device [80].

The Twisted Nematic Display Device given in Figure 2.12 consists of two parallel glass plates spaced ~5-10 mm apart, the gap being filled with a nematic liquid crystal of a specific molecular design. Each glass plate carries a transparent, electrically conducting layer [indium oxide and tin oxide (ITO)] which is etched to leave the switchable areas of the display. The surfaces are then coated with a special molecular orientation layer (usually polyimide) which is rubbed with nylon or velvet in a unidirectional manner and the nematic molecules align parallel to this direction. The

rubbing directions of the upper and lower glass plates are arranged mutually perpendicular and because of the fluid nature of the nematic phase a 90° twist of the nematic director is induced over the cell thickness. The cell is placed between crossed-polarizers which are parallel to the rubbing direction (and therefore to the nematic director)[66].
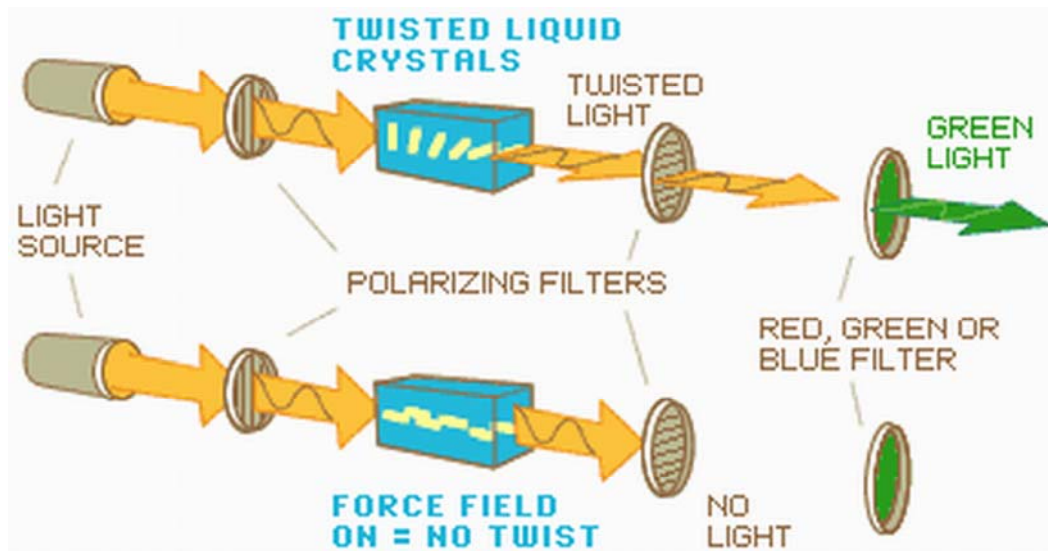
Figure 2.13 The operation of the twisted nematic display device (TNDD) [81].

Usually the TN-cell is used which can rotate the polarization of the light a quarter of a turn given that the length of the cell is long enough compared to the wavelength of the light. By placing a vertical polarization filter before the cell and a horizontal one after the cell a system is obtained which lets through light. This property can be changed by applying an electric field across the TN-cell which makes the molecules change direction so that they no longer change the polarization of the light. This way no light comes through the system since the two polarization filters are perpendicular to each other. In a simple display this property is used together with the polarization filters. By placing a mirror behind the second filter one gets a "light-cell" which either reflects light and thereby looks bright or absorbs the light and becomes black. With the help of transparent electrodes one can apply different electric fields to different parts of the display and thereby create a pattern [79, 81].

Liquid crystal display devices offer excellent features not provided by other types of display. LCDs are of a flat-panel design and have low power consumption, accordingly they can be small and compact and hence used where portable displays are desirable or essential. The compact design is also useful where displays are used in small spaces or where weight needs to be minimized, for example, in aircraft, cars and caravans. In fact, more recently displays have been developed for use inside helmets (head-up displays) for fighter pilots and racing drivers. Other important features of LCDs are the fast switching speed and the low power consumption. All of the small, compact portable equipment that has been developed as a result of improved computer technology would not be possible without liquid crystal displays because no other display technology offers small, compact design with very low power consumption. Now that LCDs are widely used and well developed they are also very cheap and very reliable [79, 81].

On the other hand, the smectic liquid crystal phase is rather viscous and so when used as a material for a display device the power consumption is too high and the switching speed is too slow. However, a very promising new display technology (ferroelectrics) based on the SmC* phase offers extremely fast switching speeds at low voltages. The mode of switching is different from that of the TNDD and involves a switching around a cone through 45° from one tilt direction to the other. The difference in optical properties between the two tilt directions gives the contrast in the display. A ferroelectric liquid crystalline display has many other advantages over the TNDD besides that of switching speed, e.g., the switched states remain stable when the electric field is removed and so power is only used when a change in the display is required.

Cholesteric (N*) materials are of great technological importance because of their ability to selectively reflect light of a wavelength equal to that of the pitch length (as illustrated in Figure 2.4). So as previously discussed, if the pitch length is of the order of the wavelength of colored light then colored light will be reflected. Additionally, since the pitch length of the helix of a cholesteric phase changes with temperature, an adjustment can be made. At high temperature the pitch becomes wound up and short and hence the light reflected is blue but at lower temperature the pitch unwinds and becomes long which causes the reflection of red light. Accordingly, a cholesteric material with a suitable pitch can be used as a thermometer which reflects different

colors at different temperatures. Such materials can be encapsulated into a polymer or an ink and can be used in great variety of items. For example, the polymers can be used to make decorative items, clothing and paints that changes color with temperature. The inks can be used for printing onto paper or clothing that changes color with temperature. However, cholesteric liquid crystal mixtures can be used to make accurate thermometers that consist of a plastic strip with a fixed legend. These thermometers are very convenient for use in fish tanks and display refrigerators. They also give an accurate indication of body temperature. Other areas of use include the detection of structural flaws, the detection of hot spots in electronic circuits and in aerodynamic testing for the cooling of engine parts [79].

Additionally, liquid crystal polymers are still very much in the research stage but some liquid crystal polymers are in commercial use. If a polymer is extruded in the liquid crystal phase, the anisotropic ordering of molecules confers an extremely high strength to the polymer. Kevlar is a good example of such a high strength liquid crystal polymer and is used in bullet-proof vests and for car body panels. Liquid crystal polymers are also useful as a data storage medium. For example, a laser beam can be used to write onto an ordered liquid crystal phase and produce an isotropic liquid which on cooling gives a dotted liquid crystal ordering. The written area can be changed simply by cooling the ordered liquid crystalline phase from the isotropic liquid but applying an electric field during the cooling process. This type of technology can produce both erasable and write once only devices.

Liquid crystals is an exciting and unique field that draws upon the skills of scientists from a wide range of disciplines, including chemistry, physics, engineering, biology, mathematics and computation. Liquid crystals are very special materials and their research and development is of great technological importance.

Due to the presence of orientation order in liquid crystals electrical, magnetic, optical and rheological properties exhibit anisotropic characteristics. Presence of an external electric field E causes the mesogens to orient either parallel or perpendicular to E, leading to the dielectric constants measured with E parallel or perpendicular to director differ. Concerning that property, LCs find extensive usages as displays .

45

2.2   Motivation

As mentioned previously, optically active side chain liquid crystalline polymers (SCLCPs) have attracted attentions due to their wide range of applications, in particular in the fields of optics and electro optics. For the polymer to be optically active, the chiral center can be introduced either into the backbone or into the side chains of a SCLCP. In order to monitor the chirality transfer from the backbone to the liquid crystalline mesophase experimentally, the chirality in the polymeric structure is introduced in the main chain of the polymer.

On the other hand, it is known that prominent among the current efforts, the utilization of carbon dioxide chemically in $scCO_2$ media result in products that are cleaner, less expensive, and of purity. In comparison to the alternative route involving the use of highly toxic phosgene, polycarbonate synthesis in $scCO_2$ media presents a single-step reaction and an environmentally benign approach.

Armed with these informations, a desire to combine these three valuable aspects (liquid crystallinity, chirality, and supercritical carbon dioxide application) has mainly motivated us to synthesize a SCLC Polycarbonate with a chiral backbone. More importatntly, the incorporation of the carbonate group in the backbone is expected to provide enough flexibility to the mesogenic unit to introduce liquid crystallinity, and the ether moieties in the backbone further enhance flexibility. Therefore, SCLCPs with a flexible backbone have been prepared for the possibility of obtaining better electro-optical properties than those of their non-flexible analogues.

The results of this study are not only of interest for the synthesis of optically active SCLCPs, which potentially provides a short optoelectronic response time, but also the synthesis method offers a single-step reaction which does not cause an environmental damage compared to the alternative routes.

2.3 Experimental

2.3.1 Reagents

2.3.1.1 Materials

Zinc oxide (ZnO, MW = 81.37 g/mol, purity > 99.99%), 4'-4 Hydroxybiphenyl-carbonitrile (HOC$_6$H$_4$C$_6$H$_4$CN, MW = 195.22 g/mol, purity > 97%), Cesium Fluoride (CsF, MW = 151.9g/mol, purity > 99.99%), (S)-(+)-Epichlorohydrin (C$_3$H$_5$ClO, MW = 92.53 g/mol, purity > 98%), and Triethylamine ((C$_2$H$_5$)$_3$N, MW = 101.19 g/mol, purity > 99.5%) were all supplied from Aldrich Chemicals, Germany. On the other hand, Phthalic Anhydride (C$_8$H$_4$O$_3$, 148.12, purity >99%), (S)-(+)-Glycidyl Nosylate (C$_9$H$_9$NO$_6$S, MW = 259.23 g/mol, purity > 98%), 6-chloro-1- hexanol (C$_6$H$_{13}$ClO, MW = 136 g/mol, for synthesis), Potassium Carbonate (K$_2$CO$_3$, MW = 138.21g/mol, anhydrous), were purchased from Acros Organics. Finally, the acryloyl chloride (C$_3$H$_3$ClO, MW = 90.5 g/mol, for synthesis grade and stabilized with Phenothiazine), used in the synthesis of LC$_6$ intermediate was obtained from Merk Laboratories. All the materials were used as received.

2.3.1.2 Solvents and Drying Agents

N,N-Dimethylformamid (DMF) (C$_3$H$_7$NO, MW = 73.1 g/mol, anhydrous) and Ethanol ((C$_2$H$_6$O, MW = 46.07 g/mol, 99% grade and denaturized with 1% MEK) were supplied from Aldrich Chemicals Company and used under an inert atmosphere. The Dimethyl Sulfoxide (DMSO) (C$_2$H$_6$OS, MW = 78.13 g/mol, HPLC grade) was obtained from Labkim and distilled over CaH$_2$, before its use. Also, the Dichloromethane (CH$_2$Cl$_2$, 84.9 g/mol, analytical grade) and the Ethylacetate (EtOAc) (C$_4$H$_8$O$_2$, 88.11 g/mol, analysis grade) were gotten from Labkim Corporation, Turkey. Other solvents, Hexane (C$_6$H$_{14}$, MW= 86 g/mol, analytical grade), Tetrahydrofuran (THF) (C$_4$H$_8$O, 72.11 g/mol, analytical grade) and

Hydrochloric acid (HCl) (36.46 11 g/mol, 37% extra pure), were purchased from Riedel-de Haen Chemicals and used as they received.

2.3.2 Characterization Methods

Characterizations of the catalyst monomer and polymer were performed using ATR method by Fourier transform infrared spectroscopy (FT-IR) recorded on Equinox 55/S Fourier transform (Bruker). ^{1}H-NMR and ^{13}C-NMR were recorded on Unity Inova 500 MHz nuclear magnetic resonance (Varian AG, Switzerland). DSC thermal analyses were run at N_2/N_2 atmosphere with a heating rate of 10ºC/min. using Netzsch Phoenix differential scanning calorimeter 204 (Selb, Germany). The number-average molecular weights (M_n) and polydispersity index (M_w/M_n) were measured with gel permeation chromatography (GPC) on a Agilent Model 1100 instrument containing a pump, a refractive index detector and four Waters Styragel columns HR 5E, HR 4E, HR 3, HR 2; and THF was used as eluent at a flow rate of 0.3 mL/min at 30ºC. Data analysis was performed with PL Caliber software. The system was calibrated with narrow polystyrene standards (Polymer Laboratories). The optic microscope images were obtained by the Nikon Eclipse MD600 microscope. The controlled heating was maintained by Mettler Toledo FP90 central processor and FP82 HT- Hot-stage. Samples were gradually heated by 2°C/min in a temperature range of 40-120.

The XRD pattern was recorded on an x-ray powder diffractometer (Bruker AXS-D8, Karlsruhe, Germany). The measurement was performed in the 2θ range of 1° - 25° at 40 kV and 40 mA, using Cu-K_α radiation. In the measurement, the step size was 0.02° and data collection period was 2 second in each step.

The sample for the XRD experiment was prepared by rapid quenching of the polymer annealed at its liquid crystalline state [82]. The experimental procedure for the sample preparation is given below: A film of the polymer cast on a single crystal silicon wafer was heated in a furnace to its isotropic state, at which the sample

annealed for 10 min. Subsequently the sample was cooled to its liquid crystalline state and annealed there for 10 min, the silicon wafer was thrown into a liquid nitrogen Dewar flask. The wafer was taken out from the flask and warmed to room temperature.

Polymerizations held in $scCO_2$ were performed by P-50 High Pressure Pump Contrivance (Thar) in a 100mL high-pressure stainless-steel vessel. Heating was achieved with a heating band and temperature was controlled by a thermocouple adapted to the vessel.

2.3.3   Synthesis Methods

2.3.3.1   Synthesis of the Catalyst

The catalyst is prepared as in the reference [48] by reacting zinc oxide with a phthalic anhydride in the presence of an alcohol. In a typical reaction to a 500 cc three-necked round bottom flask equipped with a thermometer, reflux condenser and nitrogen inlet was charged with 25 g of phthalic anhydride and then flushed with N_2. The phthalic anhydride was heated, then 200 cc of anhydrous ethanol and 10 g of zinc oxide, which had been flushed with N_2, was transferred to the flask. The reaction mixture was magnetically stirred while being heated to 65°C. After 5 hours, the heat was removed and the mixture was filtered by vacuum. The product was vacuum dried at 50 °C overnight to recover 4.8 g of solid catalyst. 'H-NMR ($CDC1_3$): δ 1.1 (t, CH_3), 4.24 (m, -(C=O)-OCH_2), 7.48 and 7.55 (d, 2a-CH~), 7.93 ppm (s, 2a-CH~). ^{13}C-NMR: δ 13.760, 62.005, 127.698, 130.147, 130.269, 130.662, 133.427, 133.980, 169.695, 175.634. IR (ATR) 1725, 1611, 1591, 1551, 1443, 1406, 1287, 1128, 1081, 1040, 878, 844, 749, and 707 cm-^{1}.

2.3.3.2 Synthesis of (S)-[(4-cyano-4'-biphenyl)oxy]methyloxirane (LC$_0$ monomer)

In the synthesis of highly enantiopure monomer the well documented procedure is followed. In a typical reaction, CsF (19.9 mmol) was added to a solution of 4-cyano-4'-hydroxybiphenyl (6.6 mmol) in anhydrous DMF (5 ml). The reaction mixture was stirred for 3 hours and (S)-glycidyl 3-nitrobenzenesulfonate (nosylate) (6.6 mmol, 98.8% ee) was added. The reaction mixture was stirred at 25 °C overnight, under an inert atmosphere. After water was added, the solution was extracted with EtOAc. The organic phase was dried over MgSO$_4$ then filtered, and finally evaporated. The residue was purified by column chromatography on silica gel (1:1, hexane/EtOAc) to give (S)-monomer with a 95% yield. 'H-NMR (CDC1$_3$): δ 2.77 (dd, 1H), 2.92 (t,1H), 3.36 (m,1H), 3.98 (dd,1H), 4.28 (dd,1H), 7.09 (dd, 2a-CH~), 7.51 (dd, 2a-CH~), 7.66 (m, 4a-CH~). ^{13}C-NMR: 44.611, 50.055, 68.833, 110.190, 115.103, 115.202, 119.028, 127.050, 127.126, 128.385, 128.419, 128.533, 132.031, 132.554, 145.046, 159.039. IR (ATR) 2222, 1601, 1524, 1491, 1448, 1289, 1261, 1181, 1115, 1033, 1000, 971, 912, 857, 833, 817, 752, 679, 661 cm^{-1}.

2.3.3.3 Synthesis of the 4-cyano-4'-(6-hydroxyhexyloxy)biphenyl (LC$_6$ intermediate)

The LC$_6$ intermediate has been synthesized due to the following well-documented procedure. Prior to the reaction, the nitrogen gas was flushed through the reaction system. Into a 500 cc three-necked round bottom flask equipped with a thermometer, reflux condenser, magnetic stirring bar and nitrogen (N$_2$) inlet 4'-hydroxy-4-biphenylcarbonitrile (15.4 mmol) in 150 ml of dry DMSO was injected. After complete dissolusion, the system was charged with anhydrous K$_2$CO$_3$ (14.5 mmol) and stirred for further 20 minutes at room temperature. Subsequently, the temperatre of the system was elevated to 120°C and the 6-chloro-1-hexanol (20 mmol) was added dropwise under N$_2$ atmosphere. Then the reaction mixture was added dropwise to 400 ml of 10% NaOH solution at room temperature. The resultant was then filtered and dried at 40°C under vacuum. Finally, it was recrystalized from benzene and the obtained white crystalline product was again dried under vacuum (yield 75%). 'H-NMR (CDC1$_3$): δ 1.46 (m, 2H),

1.53 (t, 1H), 1.62 (m, 2H), 1.83 (m, 2H), 3.67 (m, 2H), 4.01(t, 2H), 6.99 (m, 2a-CH~), 7.51 (m, 2a-CH~), 7.67 (m, 4a-CH~). ^{13}C-NMR (CDC1$_3$): 25.668, 29.170, 32.649, 62.878, 67.974, 110.019, 115.039, 119.104, 127.053, 128.311, 131.294, 132.545, 145.245, 159.709. IR (ATR) 3327, 2941, 2871, 2225, 1645, 1601, 1525, 1494, 1472, 1291, 1269, 1181, 1060, 1011, 825, 803, 731, 660 cm^{-1}.

2.3.3.4 Synthesis of the (S)-[(4-cyano-4*-biphenyl) hexyloxy] methyloxirane (LC$_6$ monomer)

Into a three-necked flask fitted with a magnetic stirrer, a reflux condenser, and a rubber septum were introduced 1 g (0.0034 mol) of prepared 4-cyano-4'-(6-hydroxyhexyloxy) biphenyl and 0.38 g (0.0068 mol) of powdered KOH. Then, 5 ml of anhydrous DMSO and 0.8 ml (0.01 mol) of distilled epichlorohydrin were added. After 4 hr, a further portion of epichlorohydrin (0.4 ml) was introduced. The reaction mixture was stirred at 20°C for 15 hr, then poured into an excess of water. The precipitate was recovered by centrifugation, washed several times with water. Purification by chromatography on silica gel (dichloromethane /ethyl acetate /hexane: 2/1/1) gave of a waxy white solid. ^{1}H-NMR (CDCl$_3$): δ 1.25 (m, 2H), 1.44 (m, 2H), 1.82 (m, 2H), 2.60 (dd, 1H), 2.79(dd, 1H), 3.15 (m, 1H), 3.36 (dd, 1H), 3.49 (m, 2H), 3.71(dd, 1H), 4.01 (t, 2H), 6.99 (m, 2a-CH~), 7.51 (m, 2a-CH~), 7.67 (m, 4a-CH~). ^{13}C-NMR (CDC1$_3$): 25.678, 29.146, 29, 634, 44.280, 50.909, 60.301, 67.996, 71.490, 110.012, 115.055, 119.113, 127.061, 128.305, 131.272, 132.546, 145.262, 159.725. IR (ATR) 2937, 2870, 2225, 1600, 1525, 1492, 1469, 1399, 1292, 1250, 1184, 1116, 1089, 1032, 998, 940, 895, 853, 823, 759, 732, 660 cm^{-1}.

2.3.3.5 Synthesis of the LC$_0$ polymer (LCP$_0$)

To obtain the copolymer in a 100 ml stainless steel reactor, 2.4 g catalyst (40% of the monomer by weight percentage) and 6 g of the mesogenic epoxide were added and small amount of dichloromethane was used as co-solvent. The schematic representation of the supercritical set-up is given in Figure 1.1. The reaction mixture was then pressurized by carbon dioxide up to 4500 psi and stirred magnetically at 90°C. After a

definite time, the volatile fractions were removed from the reaction mixture at R.T. under reduced pressure and the residue was obtained [48]. 'H-NMR (CDCl$_3$): δ 4.06 (m, 2H), 4.23 (m, 2H), 4.98 (d, 1H), 7.01 (dd, 2a-CH~), 7.71 (dd, 2a-CH~), 7.87 (m, 4a-CH~). ^{13}C-NMR (CDCl$_3$): 159.045, 156.710, 145.072, 132.572, 132.550, 132.050, 131.676, 129.267, 128.407, 127.145, 119.050, 116.067, 115.213, 110.186, 72.652, 70.493, 69.238, 68.307, 66.880, 63.539, 62.08. IR (ATR): 2874, 2222, 1747, 1602, 1522, 1494, 1454, 1400, 1246, 1180, 1115, 1036, 915, 820, 734, 701 cm^{-1}

1 – Heat Exchanger (Precooler)
2 – Thar Model P-50 Pump
3 – Refrigerated Circulator Bath
4 – On-off Valve
5 – Pressure Gauge
6 – Syringe Pump (High-Pressure Generator)
7 – Line Filter
8 – Check Valve
9 – Reactor/View cell
10 – Thermocouple and Temperature Read-out
11 – Pressure Transducer
12 – Pressure Read-out
13 – Rupture Disk
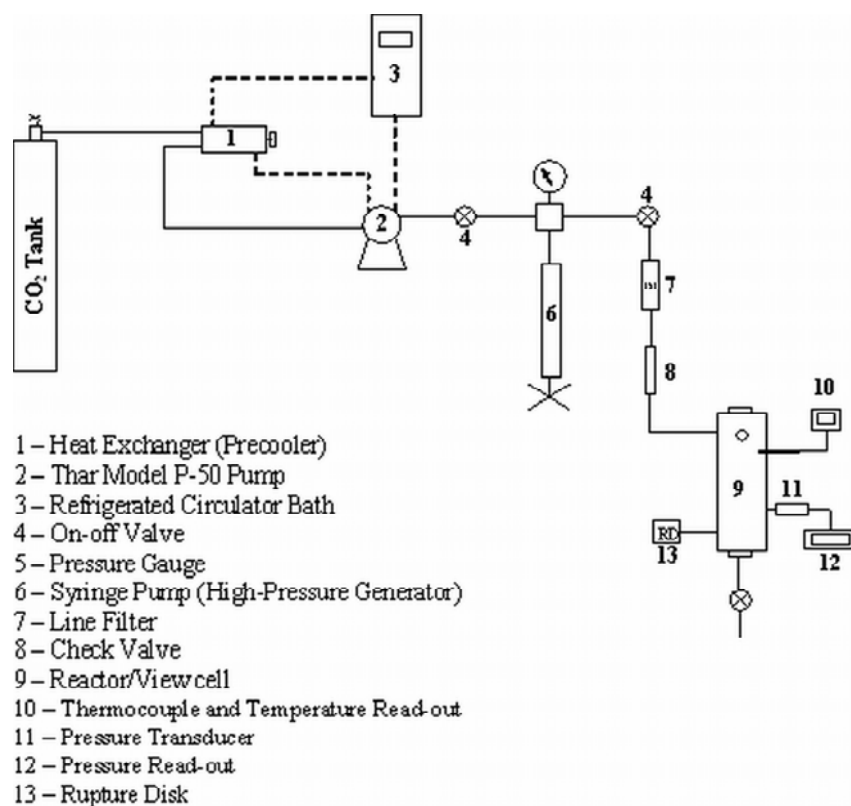
Figure 2.14 Schematic representation of the supercritical set-up.

2.3.3.6 Synthesis of the LC$_6$ polymer (LCP$_6$)

The corresponding LC$_6$ polymer was synthesized according to the same procedure with LC$_0$ polymer. ^{1}H-NMR (CDCl$_3$): δ 0.7-1.34 (m, 6H), 3.27 (m, 2H), 3.53 (m, 4H), 4.01 (t, 2H), 4.37 (m, 1H), 6.99 (m, 2a-CH~), 7.51 (m, 2a-CH~), 7.67 (m, 4a-CH~). ^{13}C-NMR: 25.678, 29.146, 29, 634, 60.301, 67.996, 71.490, 110.012, 115.055, 119.113,

127.061, 128.305, 131.272, 132.546, 145.262, 154.52, 158.18. IR (ATR): 2937, 2870, 2225, 1743, 1600, 1525, 1492, 1469, 1398, 1246, 1182, 1116, 1089, 1032, 998, 940, 895, 823, 732, 660 cm^{-1}.

2.4   RESULTS AND DISCUSSION

2.4.1   Synthesis and Characterization of the Catalyst

A catalyst, which is prepared in the presence of an alcohol by reacting zinc oxide with a phthalic anhydride [48], is used to prepare the aliphatic polycarbonates. The proposed reaction of zinc oxide catalyst is given in Scheme 2.1.
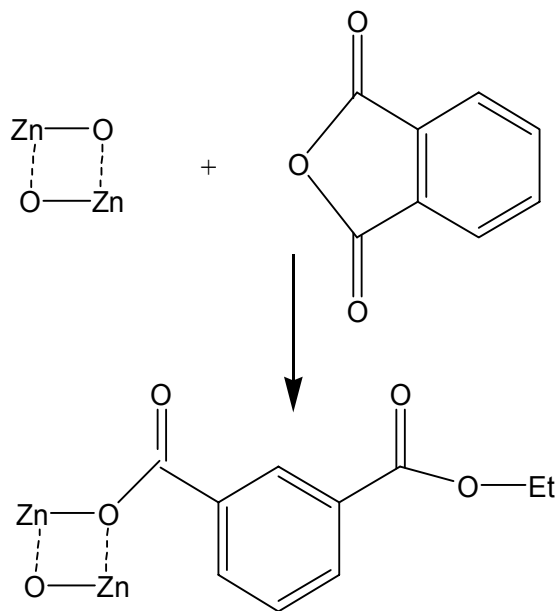
Scheme 2.1 The proposed reaction of zinc oxide catalyst.

More detailed mechanism of the catalyst will be discussed in the following chapter. On the basis of mechanistic studies, reported in Chapter 3, we have proposed that the epoxide ring is opened by nucleophilic attack from the backside. In order to rationalize this proposal, several different functional group polycarbonates from either

racemic or chiral epoxy monomers have been synthesized and microstructure investigations have been conducted on them.
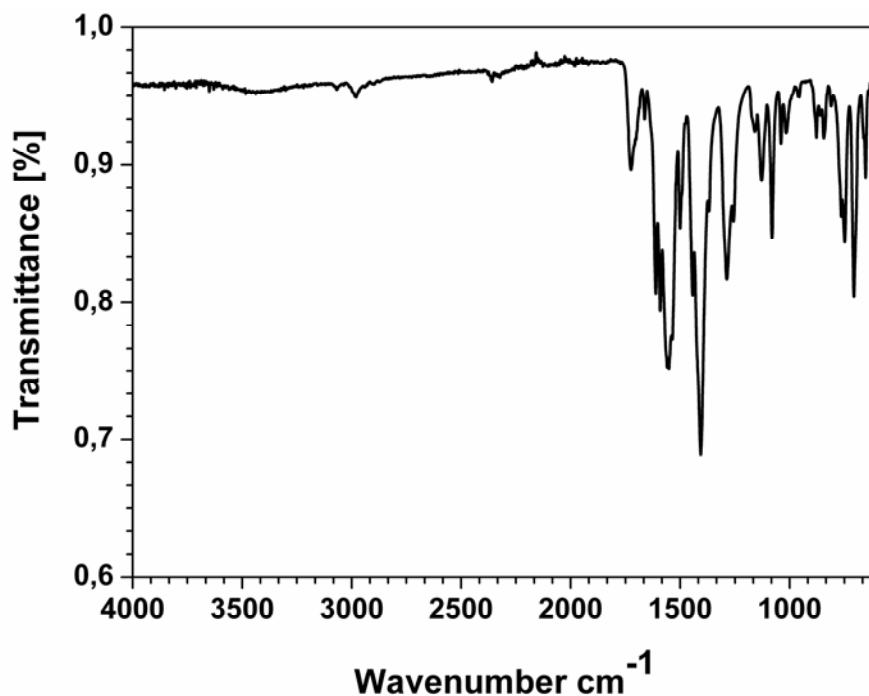
Figure 2.15 The FTIR spectrum of the catalyst

Above, the FTIR (ATR) spectrum of catalyst is given. Concerning the mechanism illustrated in Scheme 2.1, the disappearance of anhydride bands at 1810 and 1760 cm^{-1} and appearance of the ester peak at 1725 cm^{-1} is indicative of the ring opening of the phthalic anhydride by ester formation at one end of the coordination bond. Owing to the aryl substitution a shift to lower frequencies is observed for the carbonyl peak of the resulting ester. On the other hand, the coordination characteristic absorption peaks of the catalyst are detected specifically at 1591 cm^{-1} (COO-antisymmetric stretching), 1551 cm^{-1} (COO- antisymmetric stretching), 1406 cm^{-1} (COO-symmetric stretching), 1443 cm^{-1} (CH$_2$ scissoring). Strong absorptions in the range from 1300 to 1000 cm^{-1} (1287, 1128, 1081 and 1040 cm^{-1}) are indicative of the C-O stretching.
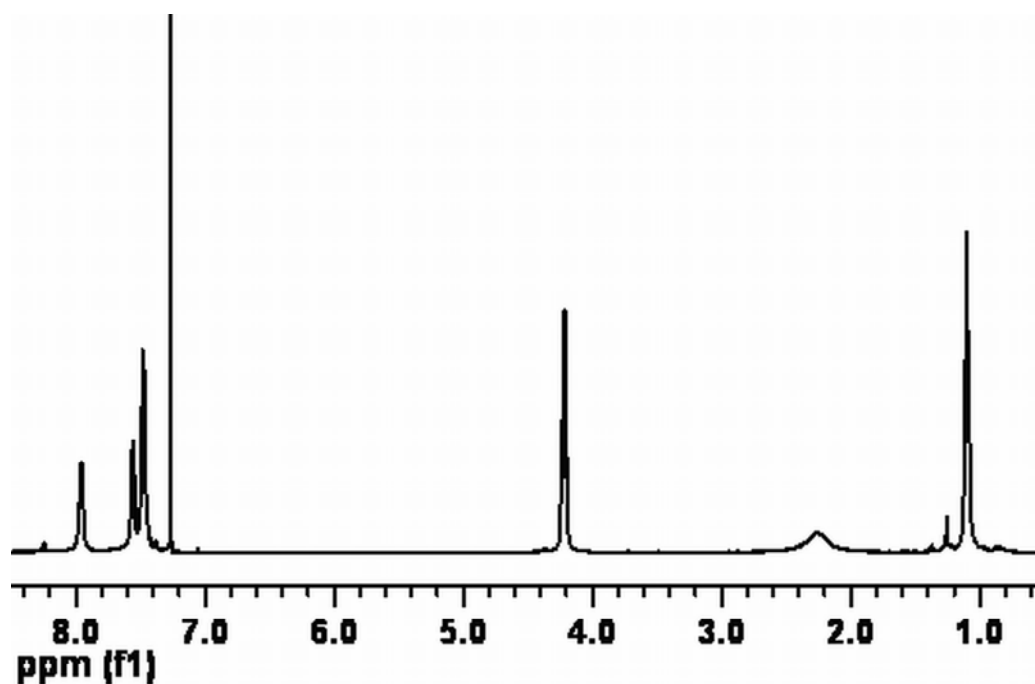
Figure 2.16 ^{1}H-NMR spectrum of the catalyst

The ^{1}H-NMR spectroscopy of the catalyst confirms the ring opening of the phthalic anhydride and the formation of the ester bond, depending on the peak at 4.24 ppm. The analysis of the purified catalyst in $CDCl_3$, gives other peaks as a triplet at 1.1 ppm and a doublet at 7.5 ppm, a singlet at 7.98 ppm corresponding to the CH_3 and aromatic hydrogens respectively.
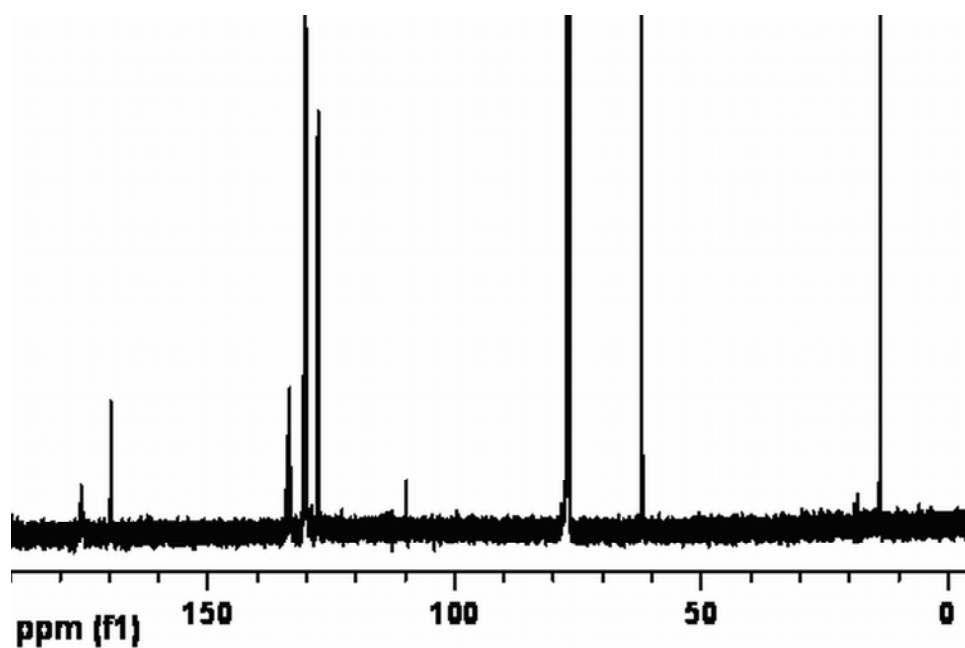
Figure 2.17 ^{13}C-NMR spectrum of the catalyst

The most conclusive data can be obtained from the [13] C-NMR spectra in terms of the synthesized catalyst. Owing to the appearance of two different carbonyl peaks, one can estimate that one end of the opened phthalic anhydride forms a coordination bond with the ZnO while the other end bonds with the ethoxy group. The downfield shift of the carbonyl peak to the 176 ppm is due to formation of coordination bond with ZnO. Other peaks that are between 127.7 and 134 ppm are assigned to aromatic carbons and the ones at 62 and 14 ppm are due to ethylene and methyl carbons. Forming a coordination bond with ZnO, the catalyst provides an intermediate in which CO_2 and the epoxide can insert alternatively. The polymer can propagate in between those two specious.

It is important to mention herein that, the values obtained from the spectra are in great agreement with those obtained in the study of Beckmann et al. who synthesized a catalyst from maleic anhydride, ZnO and a fluoro alcohol [41].

2.4.2   Synthesis and Characterization of LC$_0$ Monomer
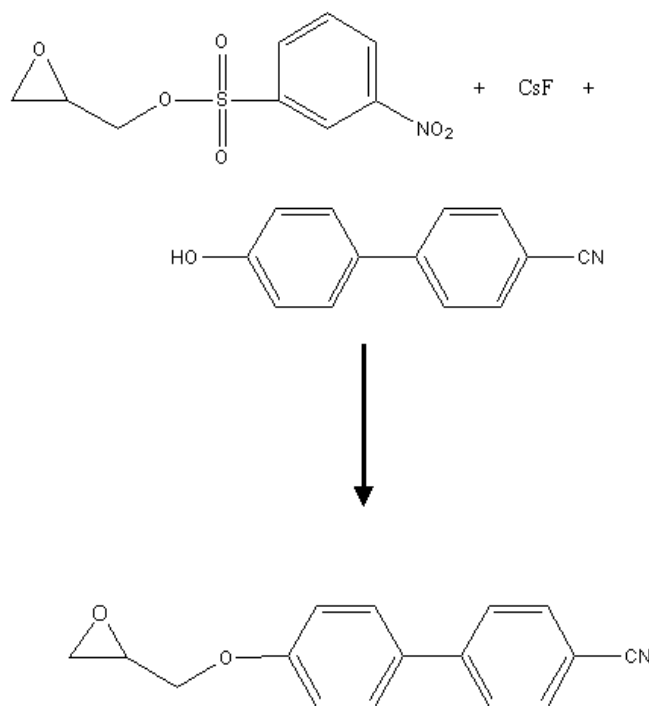
Scheme 2.2 The schematic representation of the monomer synthesis.

The mesogenic epoxide was prepared by a nucleophilic reaction between the 4-cyano-4′-hydroxybiphenyl and glycidyl nosylate. To ensure the enantiopurity of the mesogenic epoxide, a completely controlled reaction by cesium fluoride (CsF), providing convenient excess to enantiopure materials, is used [83]. Among various methods reported so far, the most simple and promising one is the protocol of Kitaori et al., which makes use of nucleophilic attack of phenols to oxiranes. We adapt the above protocol and synthesize the enantiopure mesogenic epoxide that is precursor for the synthesis of optically active SCLC polycarbonate in scCO$_2$. The reactions of oxiranes with nucleophiles are constituted basically by two types of transformations, ring opening and nucleophilic substitution. The substitution leads to the retention of the chiral center while the chirality sense is reversed upon the ring opening. Since a decrease in enantiomeric purity is caused by the competition of ring opening (C-3 attack) with the nucleophilic attack (C-1attack), glycidyl nosylate, displaying an enhanced leaving character, is employed to force the reaction in the favor of nucleophilic substitution.

Correspondingly, Kitaori et al reported that controlling the modes of the paths by CsF, the reaction of oxiranes with phenols undergoes exclusive substitution at C-1 position with glycidyl nosylate whereas, the ring opening (C-3 attack) occurs with epichlorohydrin, glycidol and 1,2-epoxyalkanes [83].
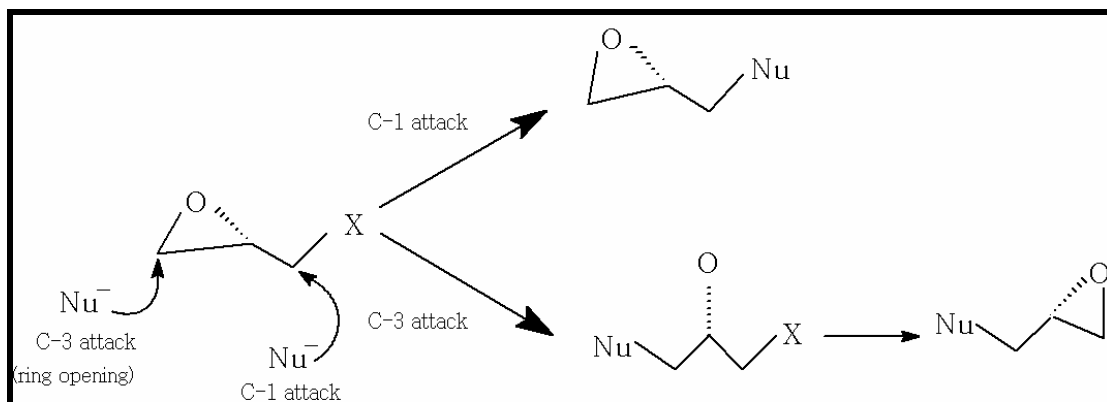
Scheme 2.3 The types of transformations for the reactions of oxiranes and nucleophiles [83].

A considerable attention has been directed towards the synthesis of enantiomerically pure monomer. Since the synthesis of such optically active glycidyl

ether containing mesogenic group, will lead to an optically active polymer that is precursor for scCO$_2$ applications.
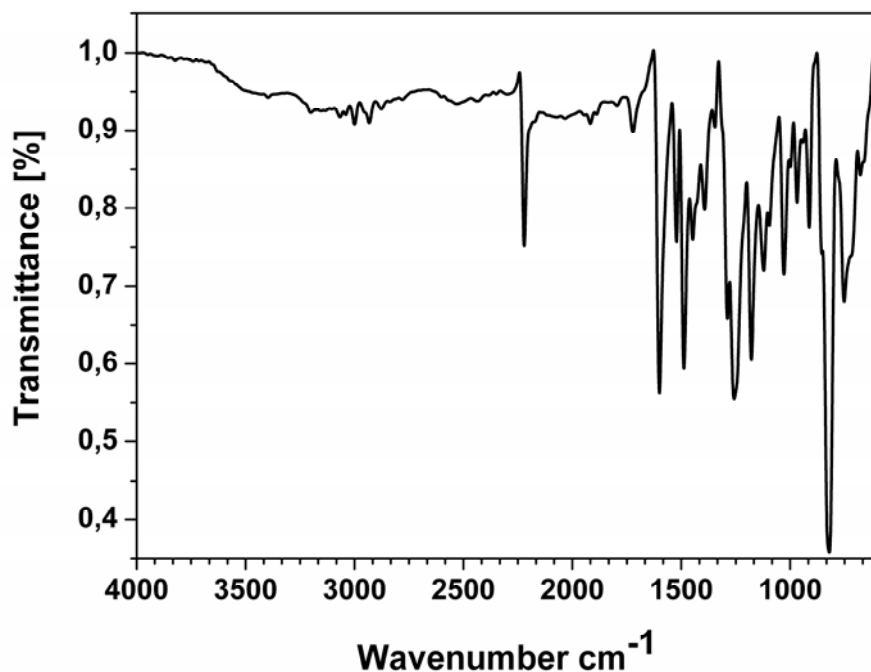
Figure 2.18 FTIR spectra of the monomer

The spectrum data obtained for the monomer, illustrate that the reaction mechanism prefers the nucleophilic substitution reaction instead of the ring opening transformation. In the FTIR spectra the three membered ring compounds of epoxides usually give three bands, and for the utilized monomer, the following values are observed; a medium intensity symmetric stretching vibration at 1261 cm^{-1}, an asymmetric vibration at 857 cm^{-1}, and a strong absorption at 833 cm^{-1}. The strong absorption at 2222 cm^{-1} is indicative of the CN bond stretching. The stretch which is to the downfield of 3000 cm^{-1} and the absorptions occurring in pairs at 1601 cm^{-1} and 1490 cm^{-1} on the other hand, are indicative of the aromatic rings.

In the ^{1}H-NMR in Figure 2.19, the disappearance of the nosylate's aromatic hydrogen peaks and the hydroxyl peak of the 4-cyano-4$^{'}$-hydroxybiphenyl is a clear evidence of the success in the nucleophilic reaction. The peak assignments have been done on the spectrum as illustrated in the following. In order to have a better

visualization of the chirality of the monomer, a three dimensional structure is given. The integration of the spectra reveals that nosylate and 4-hydroy-4-biphenyl carbonitrile reacted at 1:1 ratio.
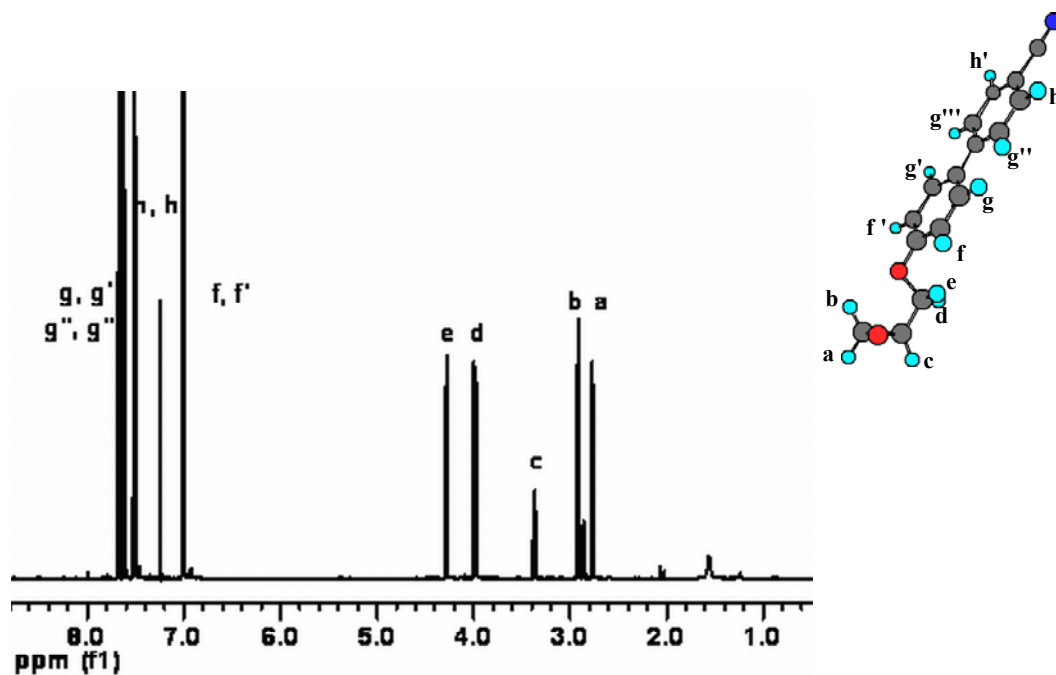
Figure 2.19 ^{1}H-NMR spectrum of the monomer

In agreement with the analytical data obtained from IR and ^{1}H-NMR spectra, ^{13}C-NMR spectrum provides another evidence for the successive nucleophilic reaction giving epoxy ring peaks at specifically 50.0 and 44.6 ppm and a peak corresponding to the spacer ethylene unit at 68.8 ppm. Additionally, the peaks that are observed at 119.2 and 159.09 ppm are due to the cyano carbon and biphenylic carbon that is adjacent to the oxygen, respectively. Other peaks at 145.6, 132.8, 128.3, 127.7, 115.8 and 110 ppm correspond to the biphenylic carbons. This data illustrates that the reaction mechanism prefers the nucleophilic substitution reaction instead of the ring opening transformation. In the following the ^{13}C-NMR spectrum is given and the peak assignments have been done on the structure.

59
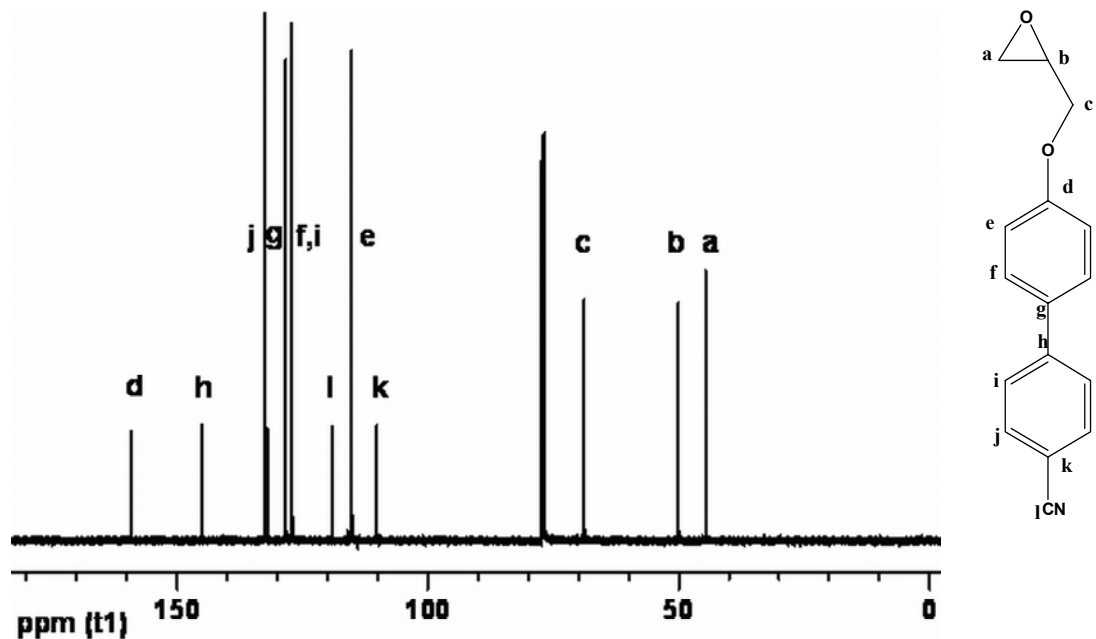
Figure 2.20 ^{13}C-NMR spectrum of the monomer.

Having two different planar structures (the biphenyl unit and the epoxy ring) around an oxygen atom, the synthesized mesogenic epoxide offers a chiral center from the methine carbon of the epoxide. As revealed in the literature, mesogenic molecules with short spacer units tend to present a nematic LC mesophase, whereas the ones with longer spacer units present a smectic LC mesophase [78]. Hence, having only one spacer unit and a chiral center, the monomer should give a chiral nematic (cholesteric) texture. The LC phase of the synthesized monomer is observed clearly under the optical microscope as shown in Figure 2.21 (a). In the second heating cycle, the so-called oily-streaks texture, which is the most commonly observed appearance of cholesteric phases, is obtained for the monomer at about 79°C. The other cholesteric oily streak texture is captured on cooling form the isotropic at 81°C and given in Figure 2.21 (b).

(a)
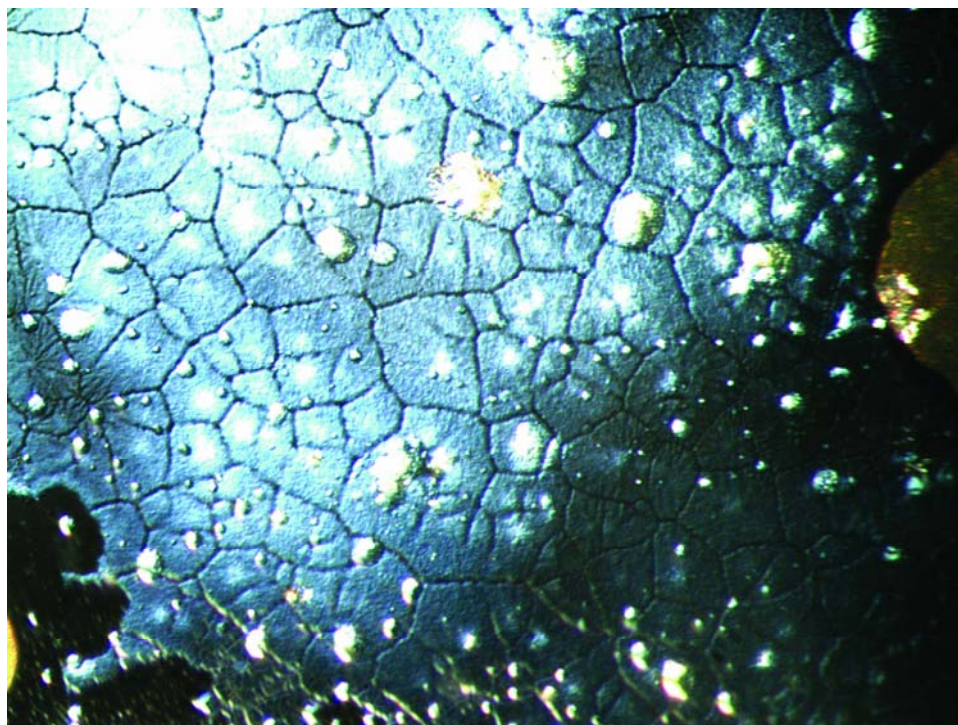
(b)
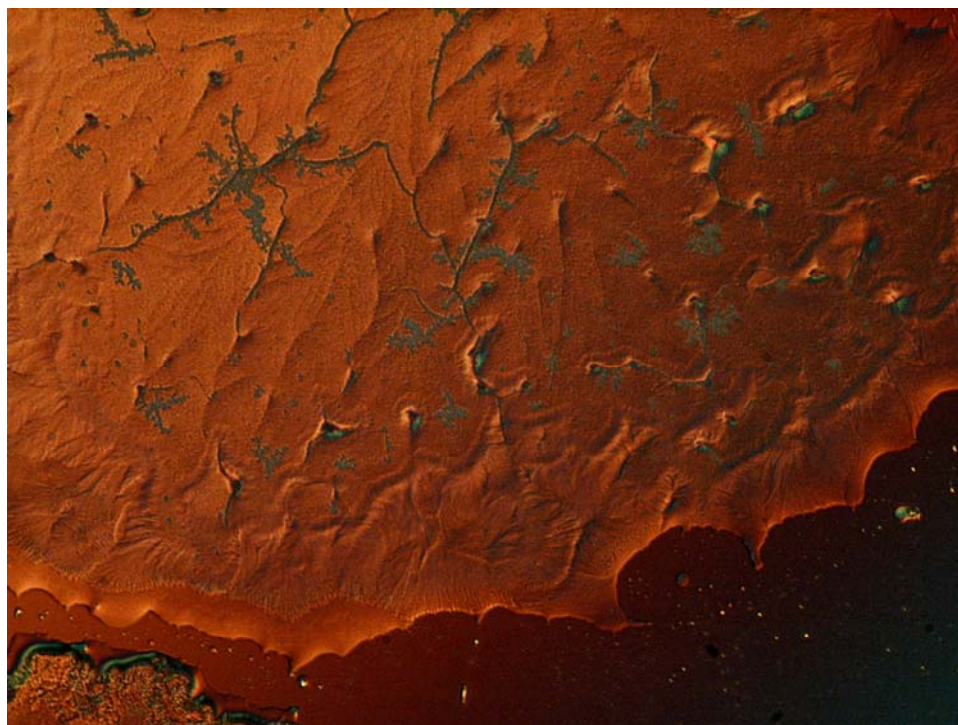
Figure 2.21 The chiral nematic (cholesteric) transition of the monomer **(a)** obtained in the second heating cycle at 79°C **(b)** obtained on cooling from isotropic state at 81°C. For both textures, original magnification calibration is 10x 20.
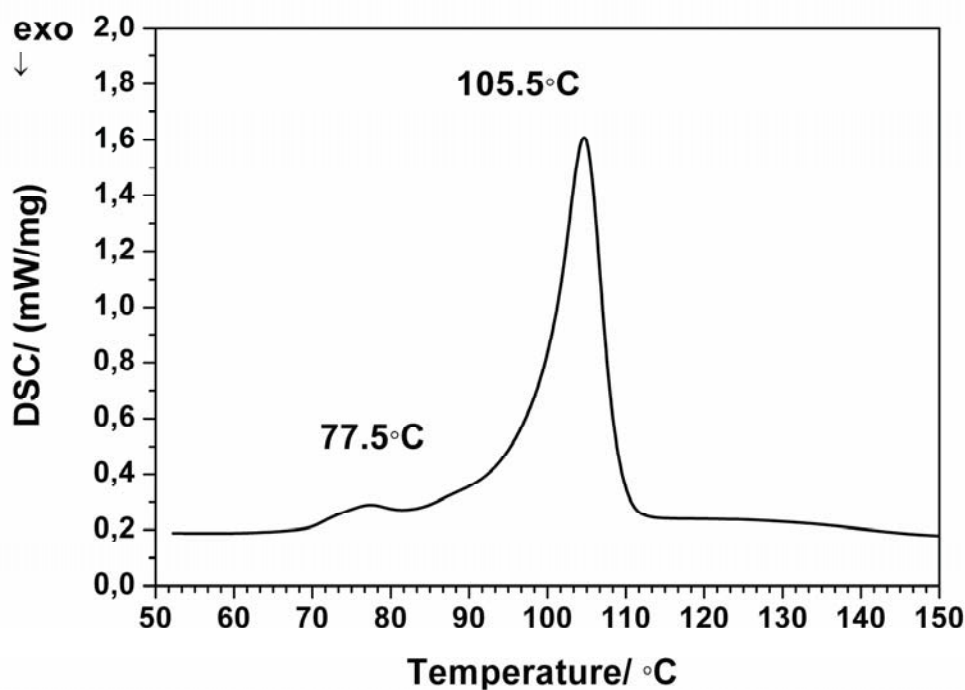
Figure 2.22 DSC thermogram of the monomer

On the other hand, the DSC thermogram of the monomer in Figure2.22 shows a small shoulder at about 77.5°C and a clearing point at 105.5°C which is consistent with the monomer phase transition at 105.9°C as reported by Taton et al. [78]. It is important to mention herein that, the monomer synthesized in the study of Taton et al. differes from our synthesized monomer in terms of optical activity. By using the stated CsF method, obtaining an enantiomerically pure monomer is guaranteed. Attributable to the optic microscope textures, the DSC data illustrates that the crystalline-cholesteric transition involves a very small change in enthalpy, whereas the transition from the ordered cholesteric mesophase to the disordered isotropic state results in a larger change in enthalpy at 105.5°C.

2.4.3 Synthesis and Characterization of the LC$_0$ Copolymer
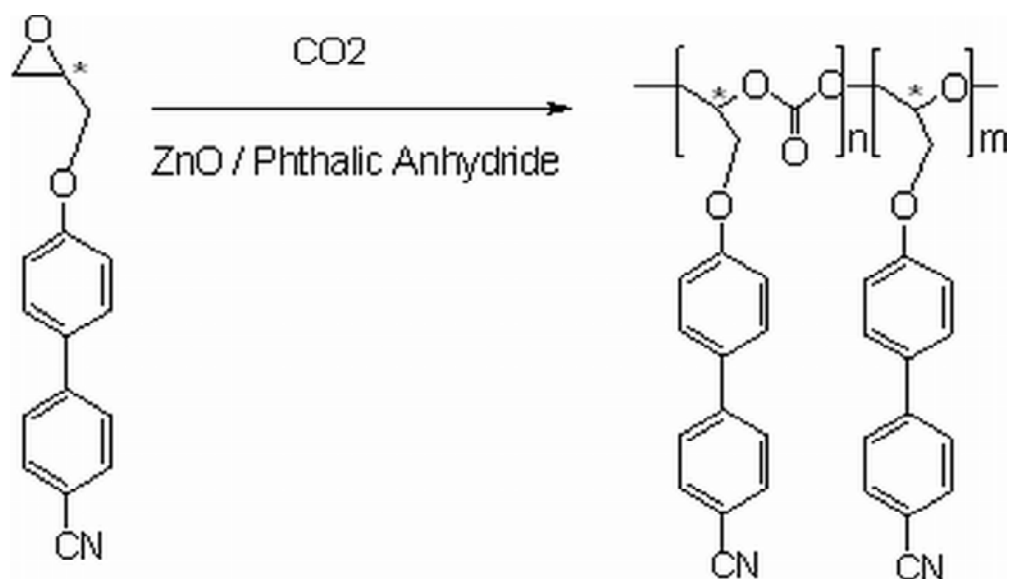
Scheme 2.4 The copolymerization is done under the conditions of 24 hours in scCO$_2$ with a small amount of dichloromethane as co-solvent. The reaction mixture is pressurized by CO$_2$ up to 4500 psi.

As illustrated in Scheme 2.4, polymerization of epoxides in supercritical carbon dioxide (scCO$_2$) media result in block copolymers consisting of both etheric and carbonate units. The star on the scheme 2.4 represents the chirality on that carbon atom. Such structures have been obtained in the literature by employing different kind of catalyst systems [84-87]. The m:n ratio of the obtained copolymer has been determined as 1:10 by comparing the methine hydrogen of the ether and the carbonate groups in ^{1}H-NMR.

As proposed in the literature optically active polymers can be synthesized by using either optically active monomers or optically active catalysts [62, 88]. Much depends on the optical activity of the monomer. The polymerization of optically active monomers is interesting not only because optically active polymers can be obtained but also monomer's optical activity can affect polymer tacticity. This fact is reported by Taton et al. [88], who illustrated that for chiral mesogenic epoxides, cholesteric SCLC polyethers were obtained, whereas for racemic epoxides nematic mesophases were observed.

By using this highly enantiopure monomer and the synthesized achiral catalyst we obtain an isotactic polymer. Specifically, in the copolymerization with CO_2, racemization does not take place [89, 90], and the polymerization does not proceed via the enantiomorphic site control [91]. So being aware of these advantages of polymerization in $scCO_2$ media, by using the mentioned catalyst system, chiral epoxides should give chiral polymers. Since the catalyst is not chiral and the polymerization does not proceed via the enantiomorphic site control, a special stereoregularity is expected for our polymer. Owing to the fact that the monomer we used is highly enantiopure and also the ring opening of the epoxide results always from the backside attack [92, 93], this special stereoregularity can be rationalized as isotactic. In other words, since our catalyst is said to be steriospecific the optic center in the monomer, when incorporated into the polymer, directs the placement of the next monomer unit to occur with the same configuration. The isotacticity of polymer is illustrated by a single carbonyl resonance at 156.7 ppm in Figure2.23, representing a single chiral environment [94].
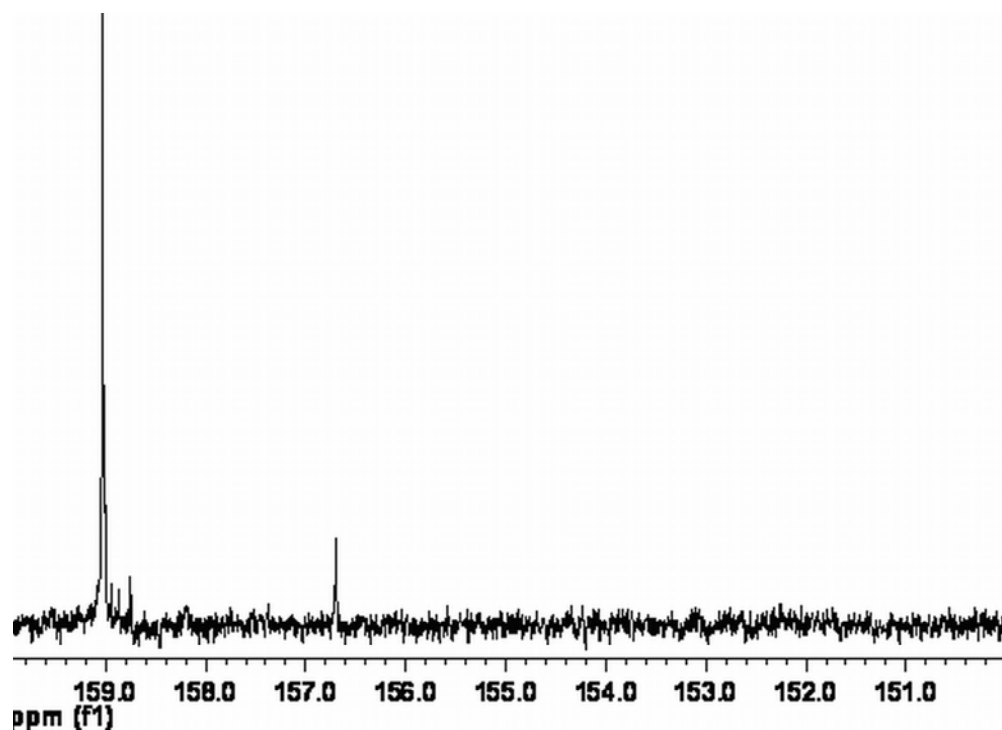
Figure 2.23 The expanded portion of the ^{13}C NMR spectrum of the polymer in the range of 160 and 150 ppm.
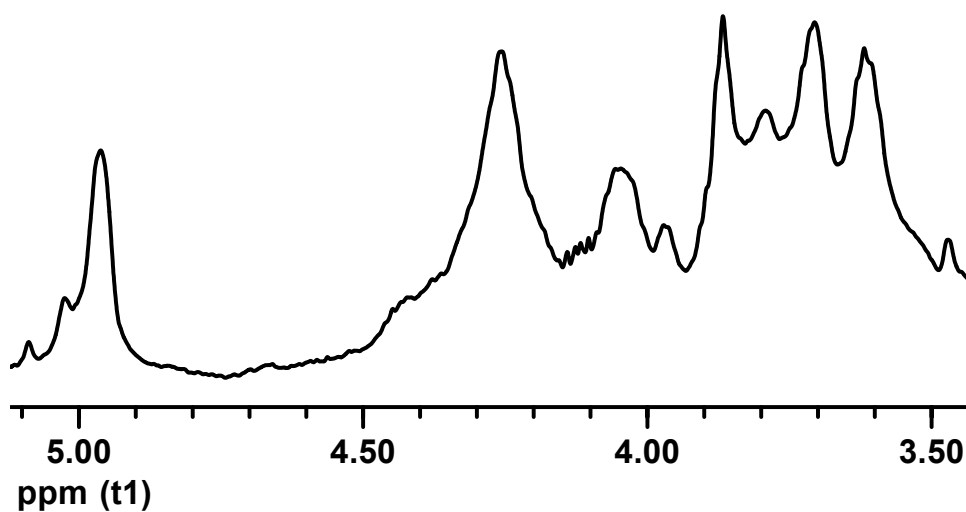
Figure 2.24 The expanded portion of the ^{13}C NMR spectrum of the polymer in the range of 3.4 and 5 ppm.

In the ^{1}H-NMR spectrum, the shift to lower fields is observed for the epoxy protons. The methylene and the methine protons are shifted to 4.23 ppm and 4.98 ppm, respectively. This downfield shift of the protons in the backbone is caused by the strong deshielding effect of the carbonate group in comparison with the monomeric epoxy group. Additionally, the methylene units in the spacer groups give a broad band at 4.06 ppm. These results are comparable with the findings of Inoue et al. who synthesized polycarbonate with aluminum porphyrin catalyst system [49].
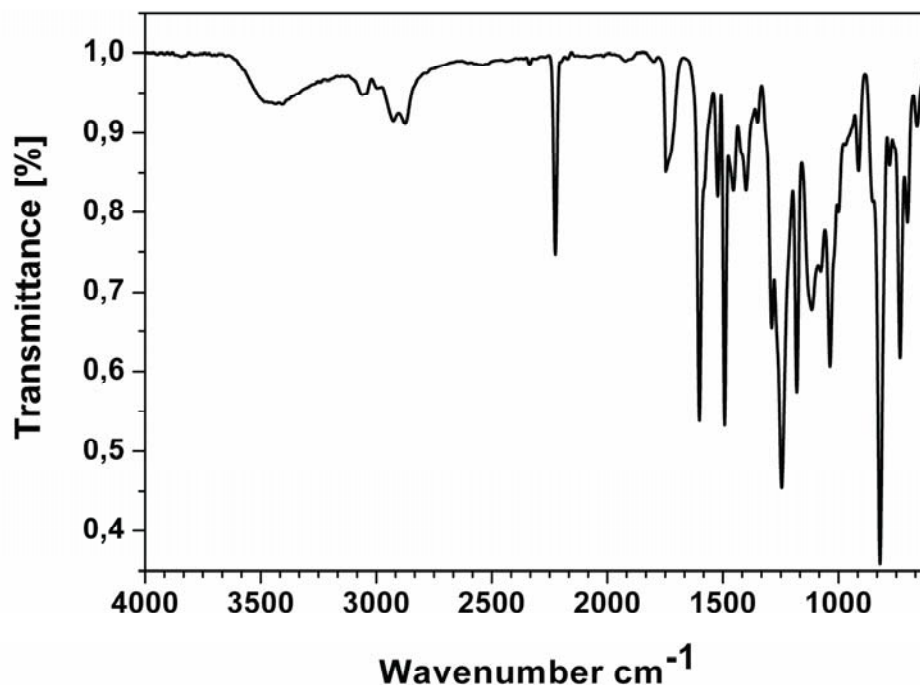
Figure 2.25 FTIR spectra of the copolymer

Being a valuable structural characterization method, the FTIR, is also in agreement with the synthesis of the copolymer. In the spectrum the most characteristic change, going from monomer to polymer, is the appearance of a sharp peak at 1747 cm^{-1}, originating from the C=O stretching of the carbonate group in the polymer. Also the other characteristic stretching vibration of the carbonate group depending on the C–O–C bond vibrations is observed at 1246 cm^{-1}. The strong absorption at 2222 cm^{-1} is due to the cyano bond stretching in the spacer unit.

In Table 2.1, different polymerization conditions and their corresponding polymerization conversions are given. The polymerization conversions are calculated by comparing the unreacted nosylate's methylene peak and the biphenyl methylene peak in ^{1}H-NMR. Using more catalyst tends to increase the polymer conversion, whereas short reaction times yield a low polymerization conversion. On the other hand, longer reaction times tend to decrease the molecular weight of the synthesized polymer [86]. This decrease in the molecular weight, is due to the relatively slow initiation and rapid propagation reaction, while the cyclic carbonate is formed in a simultaneous side reaction and by depolymerization of the already formed polymers. For this reason, the

optimum reaction conditions to be used with the mesogenic epoxide appear to be a temperature of 90°C, a pressure of 4500 psi, and a reaction time of 24 hours.

Table 2.1 Polymerization conditions of LC_0 monomer and their corresponding conversions.

Polymer	Polymerization Conditions	Molar Feed Ratio (N_{cat} / N_{mon})	Polymerization Conversions	Mn Value	Polydispersity
P-1	T=90°C, P=4000 psig, t = 20 h	1/5	%36	5.3×10^4	1.17
P-2	T=90°C, P= 4500 psig, t = 20 h,	2/5	%50	_	_
P-3	T=90°C, P= 4500 psig, t = 24 h	2/5	%61.5	2.1×10^5	1.26

The mesogenic properties have been determined both by optic microscope investigation and XRD measurements. The LC phase of the bulk polymer was unambiguously defined by textural observation by optical microscope. On cooling from the isotropic melt, the cholesteric phase transitions are observed at 83.7 and 85.9°C. The droplets are characteristics of nematic mesophase since they occur nowhere else [82, 95]. For a chiral nematic (cholesteric) mesophase, different colors in the droplet correspond to different twist states of the cholesteric liquid crystalline polymer. Such cholesteric droplets, representing different colors, are observed at 83.7 °C in Figure 2.26 (a). Therefore the coexistence of a cholesteric structure was verified by textural observation.

Since the coupling is strong between the mesogenic unit and the polymer backbone (due to the short spacer length), a transfer of chirality from the backbone to the mesophase is expected. The optic microscope textures confirm this chirality transfer and consequently we observe a cholesteric texture for the copolymer.
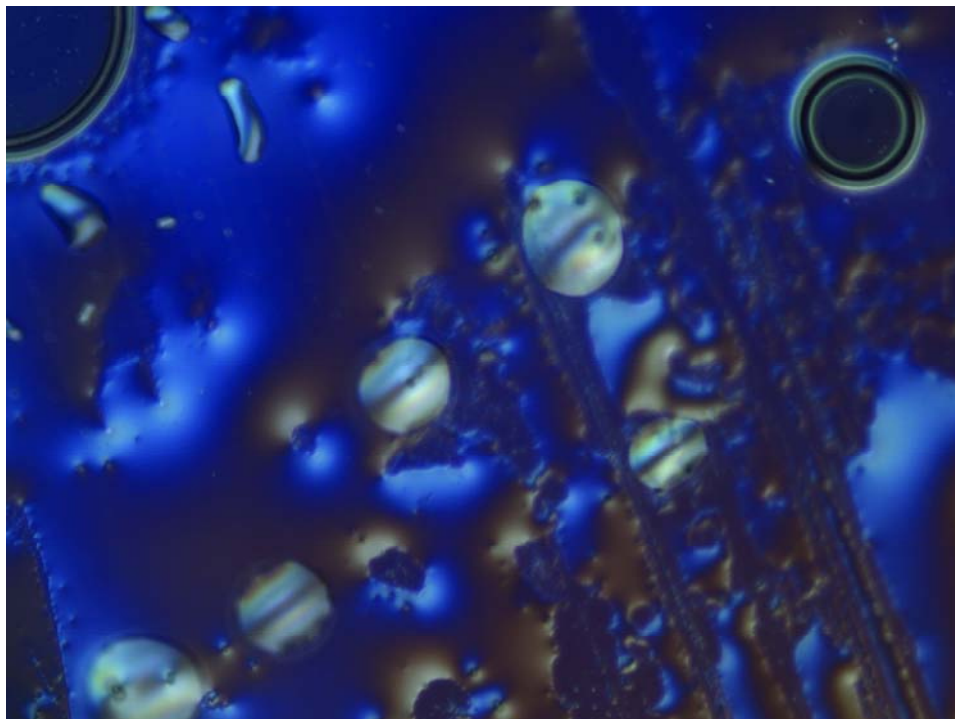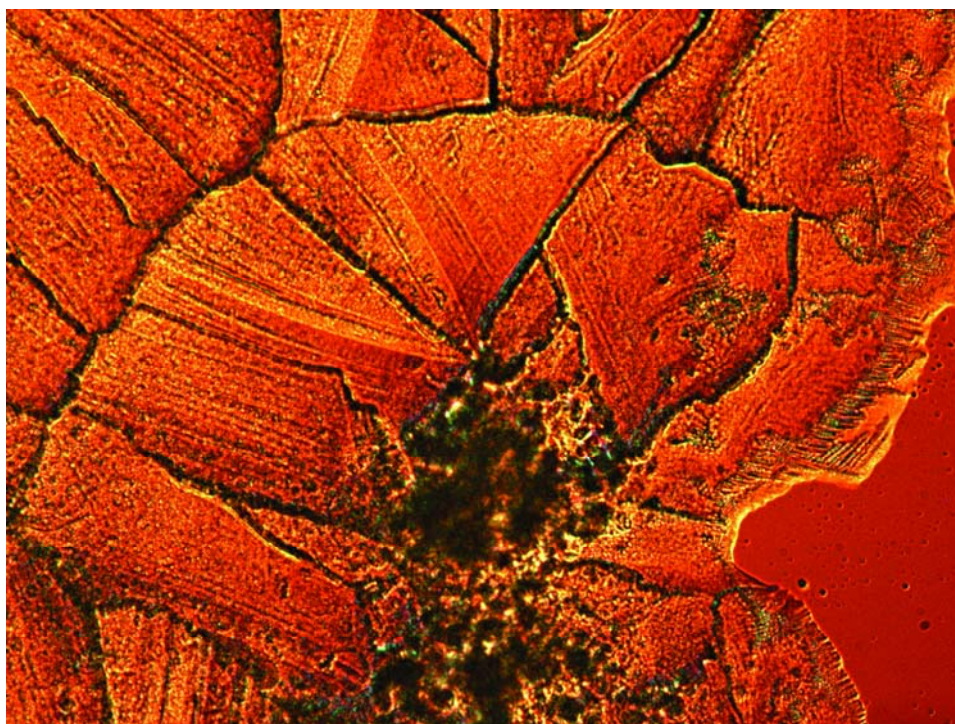
Figure 2.26 The cholesteric textures of the bulk polymer observed by polarized light microscopy in the second cooling cycle **(a)** at 83.7°C (the original magnification calibration 10x 20) **(b)** at 85.9°C (the original magnification calibration 10x 50).

In order to gain more information on the mesomorphic structure of the copolymer we carried out X-ray diffraction .The polymer sample for the X-ray diffraction experiment was prepared by freezing the molecular arrangements in the liquid crystalline state by liquid nitrogen as previously reported in the literature [82, 96, 97].

In Figure 2.27, no reflections are detected at low angles, indicating that there is no layer ordering within the mesophase which takes the polymeric mesophase out of smectic classification. The copolymer shows an X-ray diffraction pattern consisting of two mid–angle reflections and one high-angle reflection. The two mid-angle reflections at about $2\theta = 5.6°$ and $2\theta = 14.53°$ are characteristic peaks of the copolymer which are observed in the crystalline form as well and correspond to the average intermolecular distance about 15.73 Å and 6.12 Å respectively. The peak at high angle region which centered at about $2\theta=21.36°$ gives the average distance of the shorter preferred spacing of 4.15 Å. The appearance of a broad or sharp peak furnishes a qualitative indication of the degree of order [95]. Explicitly, the sharp peak at high angle region implies an ordered side chain structure between the main chains.
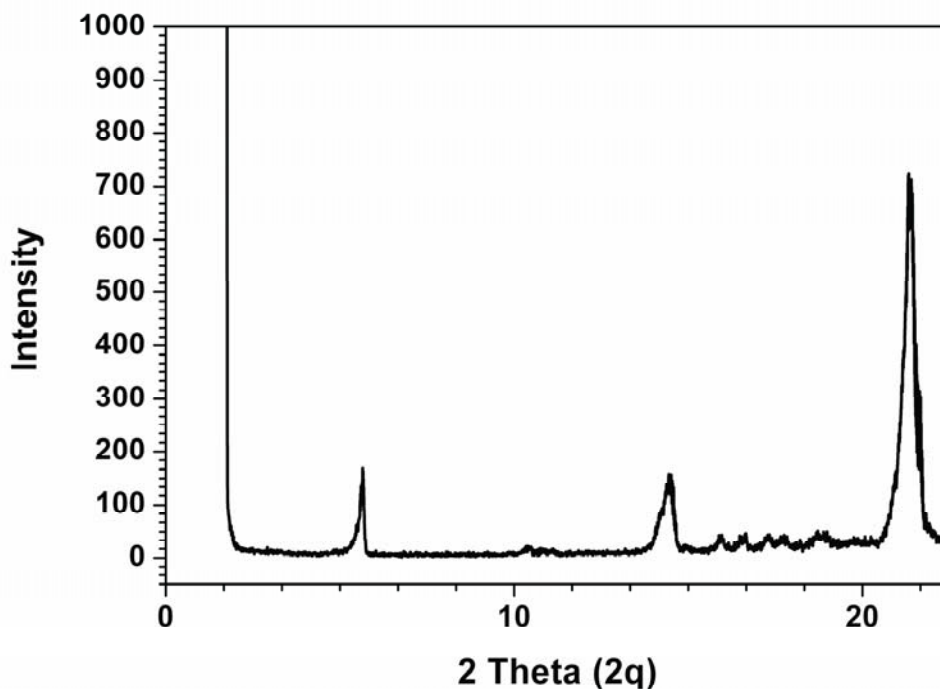
Figure 2.27 The X-ray measurement for the copolymer at room temperature.

The phase assignment was conducted by optical polarizing microscopic observation and X-ray diffraction measurement. The results correlate with each other and the coexistence of a cholesteric structure was verified.
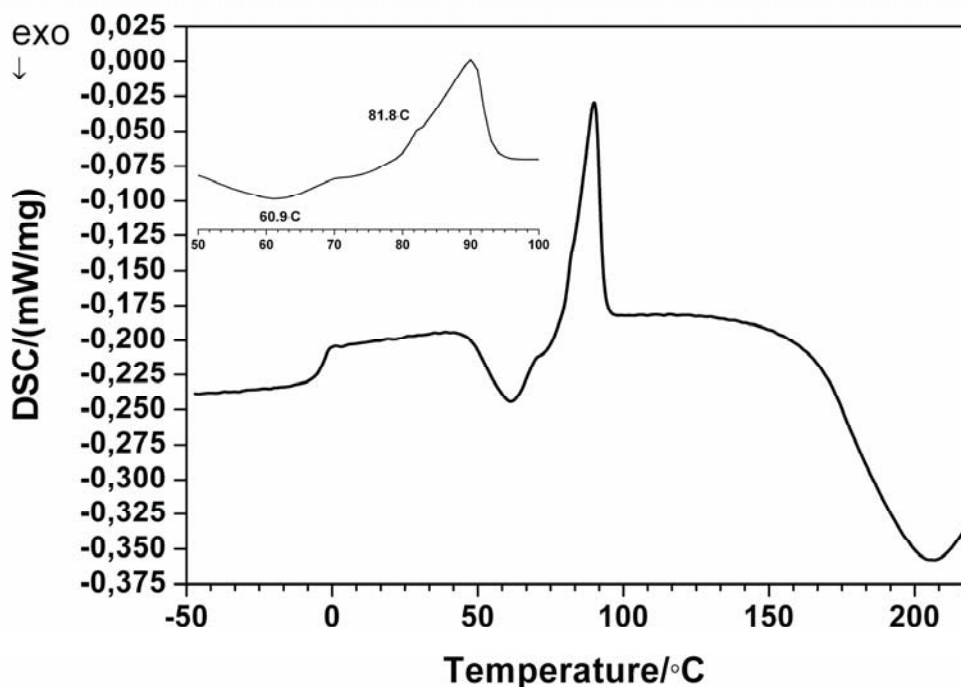
Figure 2.28 The DSC thermogram of the copolymer in second heating cycle with a heating rate of 10ºC/min.

Moreover, from the DSC thermogram above, a glass transition (Tg) curve at -3.3°C and a decomposition peak at 203.4°C are observed. It is meaningful to state that depending on the side groups and the catalyst utilized, different Tg values have been reported in the literature for such kind of copolymers ranging from -19°C to 145°C [93, 98-100]. The exothermic peak at 60.9°C, on the other hand, represents the crystallization of the polymer (k→ k$^{'}$ transition). As the temperature increases, the crystal packing transforms to a better ordered subphase, thus releasing heat to the surrounding [96]. The big endothermic peak at 90.1°C actually involves two transitions: a crystal-to-cholesteric transition and a cholesteric-to-isotropic transition. The polarized optical microscopy observation is in agreement with these transitions as well. When the DSC thermogram of the copolymer is expanded, a small shoulder on the peak at 90.1°C is observed which represents the two overlapping peaks. Same overlapping peaks are observed for the

copolymers having different m:n ratio in Table 2.1 and their DSC thermograms are given in Figure 2 29.

(a)
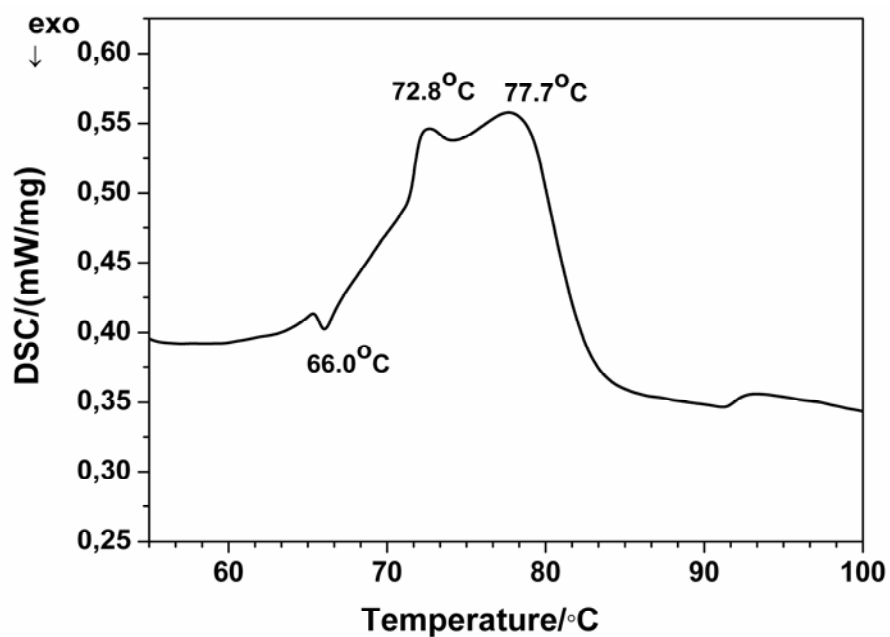
(b)
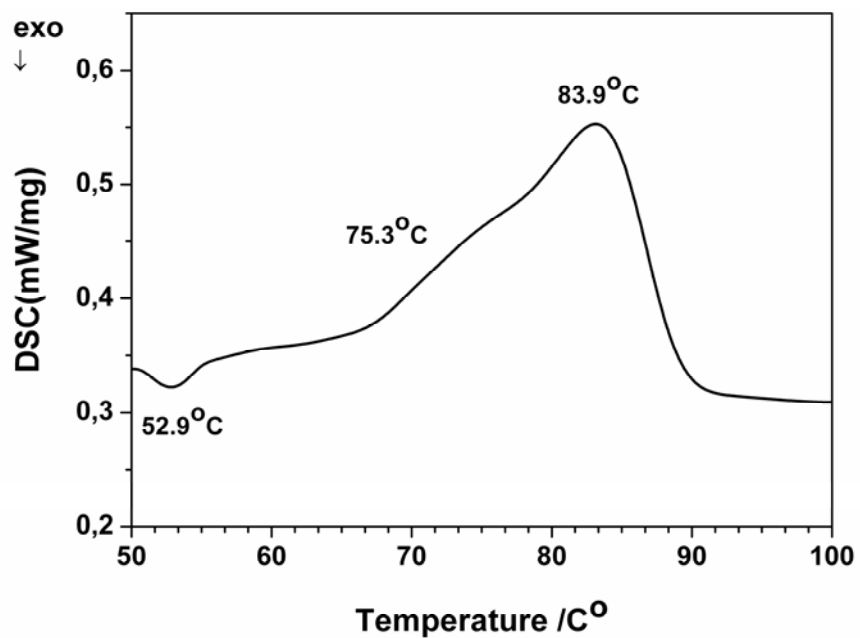
Figure 2.29 The DSC thermograms of the copolymers having different carbonate contents (n/m ratio of the copolymer), **(a)** 60/ 100 **(b)** 74/100 respectively, obtained with a heating rate of 10ºC/min., in their second heating cycle.

On the other hand, the mesomorphic temperature range is an indicative of the processing window of a liquid crystalline material. The mesomorphic temperature range is denoted as (ΔT) and defined as follows; (ΔT= Ti-Tg) [101].As it is shown in Table2.3, for the obtained polymer, the Ti value does not change dramatically, whereas a pronounced decrease in Tg value is observed from that of its acrylic analogues [102] . Hence, the present study exhibits another practical benefit in terms of liquid crystallinity by widening the mesomorphic temperature range) [103].

2.4.4 Synthesis and Characterization of LC_6 Monomer.

After the synthesis of 4-cyano-4'-(6-hydroxyhexyloxy) biphenyl (LC_6 intermediate), which is illustrated in Scheme 2.5, S-epichlorohydrin is reacted with it to yield the LC_6 monomer. Below the schematic representation of LC_6 monomer synthesis reaction is given. The hydrogen assignment in ^{1}H-NMR has been done on the LC_6 monomer structure in Scheme 2.6, as well.
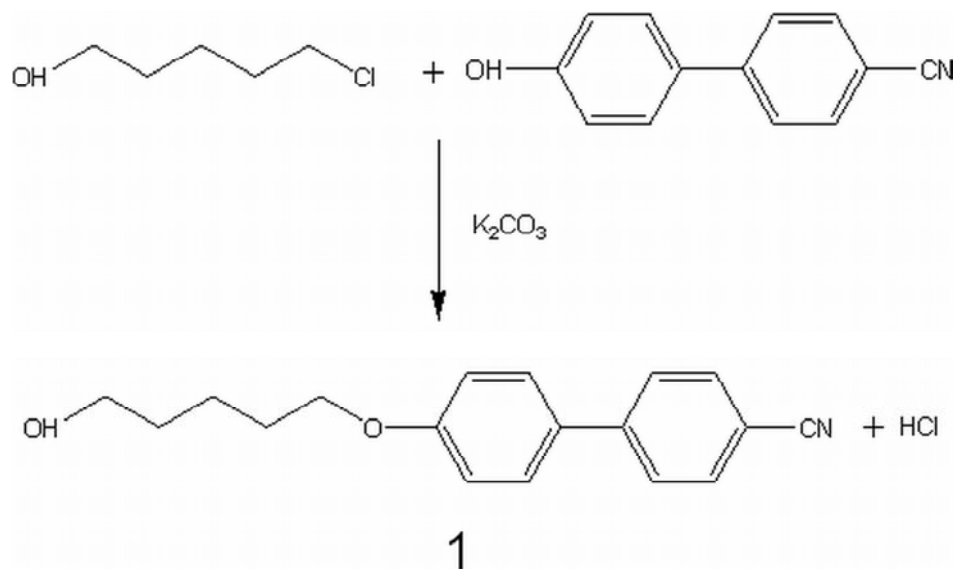
Scheme 2.5 The representation of the LC_6 intermediate synthesis.
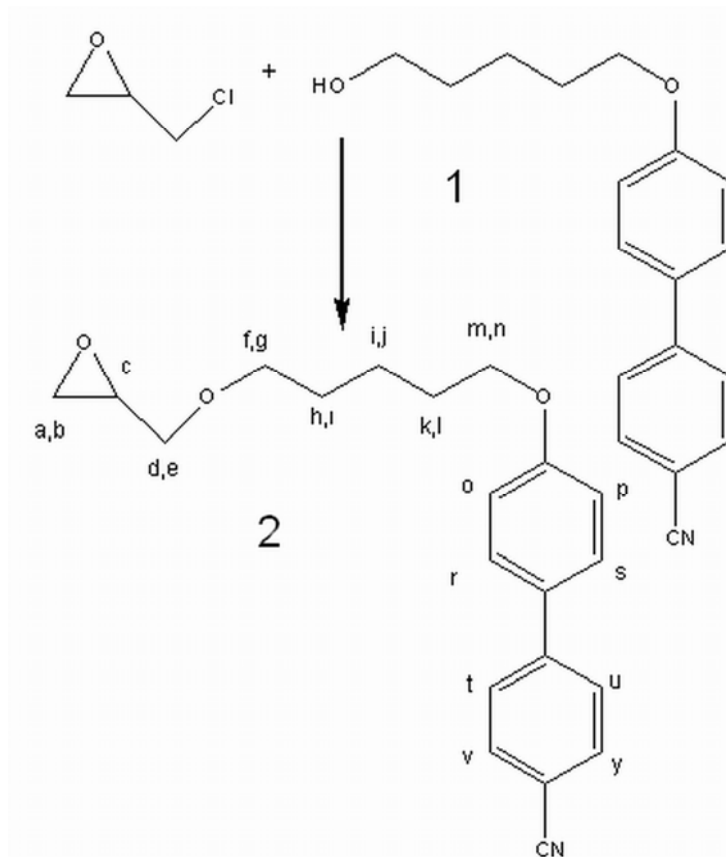
Scheme 2.6 The representation of the monomer synthesis reaction.

In order to synthesize the mesogenic LC_6 monomer (2) from 4-cyano-4'-(6-hydroxyhexyloxy) biphenyl (the LC_6 intermediate) (1), several attempts have been made. Owing to the ring strain of epoxides, reaction mechanism favors ring opening in comparison to nucleophilic substitution reaction. As a result of this fact, the reaction conversion is found to be very low. To increase the yield, various nucleophiles and different reaction conditions have been tried. Since DMSO is miscible both with organic solvents and water it is chosen as the reaction media for all of the trials to dissolve both the organic phase and the inorganic phase simultaneously. After the complete dissolution of the inorganic salt of LC_6 intermediate, epichlorohydrin is added drop wise, in two portions. As an epoxy specious, presenting a better leaving group than epichlorohydrin, glycidyl nosylate is employed in the first two trials. For that reason, there is no need to use the nosylate in excess. Whereas, using both nosylate and potassium tertier butoxide has yielded a more complex reaction mixture, since another

organic soluble material (tertier butoxy sulfonate) is yielded in the organic phase. Hence, the isolation of the product become more difficult, and as a consequence very low yields have been obtained.

Another attempt to increase the yield and to simplify the product isolation, is using epichlorohydrin and less complex nucleophilic specious. It is important to note that, metallic sodium can open the epoxy ring so the stochiometry must be purposefully adjusted to 1:1:1 in order to avoid excess of it in the reaction media. As can be draw from the table, powdered KOH is more successful in terms of the reaction conversions.

As a consequence of these trials, the exact reaction procedure is decided as follows; Into a three-necked flask fitted with a magnetic stirrer, a reflux condenser, and a rubber septum were introduced 0.5 g of 4-cyano-4'-(6hydroxyhexyloxy) biphenyl prepared according to reference [78] and 0.19 g of powdered KOH. Then, 5 ml of anhydrous DMSO and 0.4 ml of distilled epichlorhydrin were added. After 4 hours, a further portion of epichlorohydrin (0.2 ml) was introduced. The reaction mixture was stirred at 20°C for 15 hours, then poured into an excess of water. The precipitate was recovered by centrifugation, and washed several times with water. Purification by chromatography on silica gel (dichloromethane/ ethyl acetate/hexane:2/1/1) gave of the product as white solid. The following table summarizes all the trials and gives their reaction conditions and conversions.

Table 2.2 Polymerization conditions and conversions for LC$_6$ monomer (2).

Trial no	Epoxy Type	Nucleophile Type	Stochiometry (alcohol/ nucleophile /epoxide)	Reaction Condition	Reaction Conversion
1	Nosylate	Potassium Tertier Butoxide	1:2:1	Refluxed under argon atm.	Hydrolysis of the C≡N group and %0 conversion
2	Nosylate	Potassium Tertier Butoxide	1:2:1	Room temp.	%4 conversion
3	Epichlorohydrin	Powdered KOH	1:2:5	Room temp.	%9 conversion
4	Epichlorohydrin	Metallic Sodium	1:1:1	Room temp.	%7 conversion
5	Epichlorohydrin	Powdered KOH	1:2:5	Refluxed under argon atm.	% 10 conversion
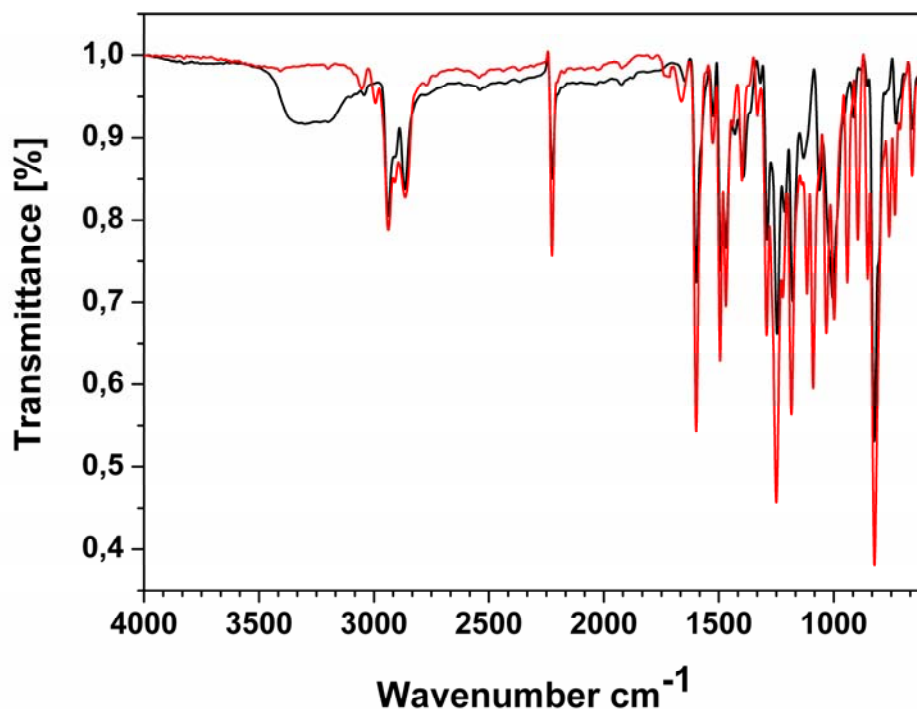
Figure 2.30 Comparison of the FTIR spectra of the LC$_6$ intermediate (1) with the glycidyl LC$_6$ monomer (2).

Figure 2.30 illustrates the comparison of the IR spectra of the LC$_6$ intermediate (1) with the glycidyl LC$_6$ monomer (2). In the spectrum above, the first and the second specious are represented as dark blue and red respectively. Depending on the data obtained from the IR characterization, the nucleophilic reaction is said to be successful. The disappearance of the hydroxyl signal at about 3300 cm^{-1} for LC$_6$ intermediate, indicates the conversion to the LC$_6$ monomer. In comparison to the LC$_6$ intermediate, the increase in the absorption intensity for the LC$_6$ monomer at 1250 cm^{-1} is a direct consequence of the epoxy ring. Furthermore, the strong absorption at 2225 cm^{-1} and the absorptions occurring in pairs at 1600 and 1492 cm^{-1}, can be assigned to the cyano and aromatic stretching respectively.

(a)

(b)
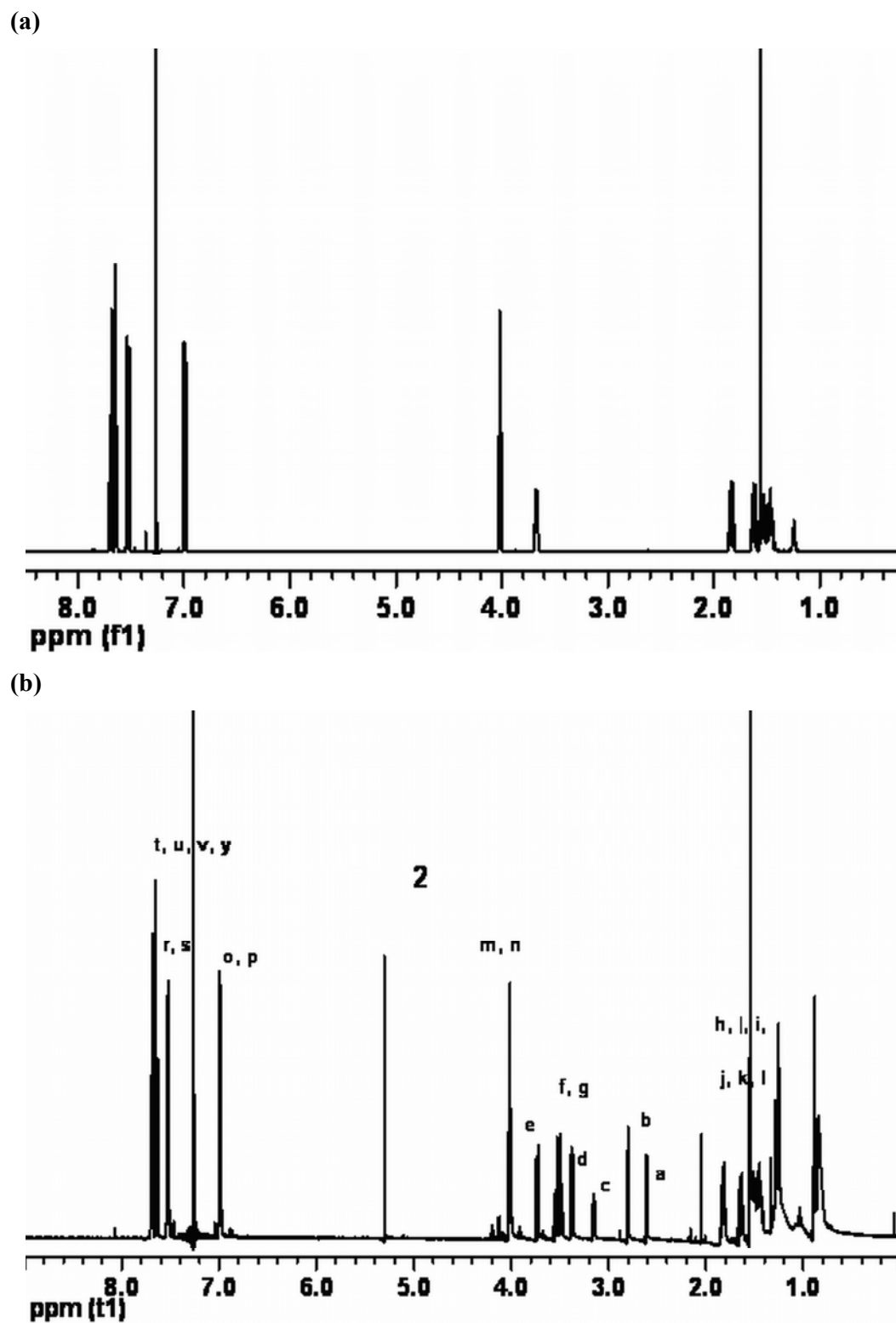
Figure 2.31 ¹H-NMR of the hydroxyl LC6 intermediate (1) and the glycidyl LC6 monomer (2).

Figure 2.31 also shows that the synthesized LC$_6$ monomer has an expected structure in correspondence to the assignments of the peaks on the figure to the hydrogen atoms. The chemical shift of the ethylene hydrogen's more to the upfield in the ^{1}H-NMR spectra is due to the shielding effect of the epoxy ring. Due to the comparison of the integration constants, it is revealed that the nosylate and the 4-cyano-4'-(6-hydroxyhexyloxy) biphenyl have reacted in 1:1 ratio.
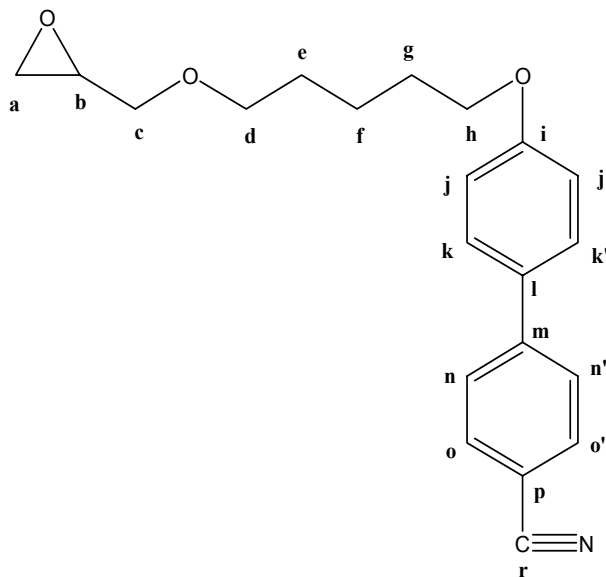
Scheme 2.7 Carbon assignment on the LC$_6$ monomer structure.

(a)
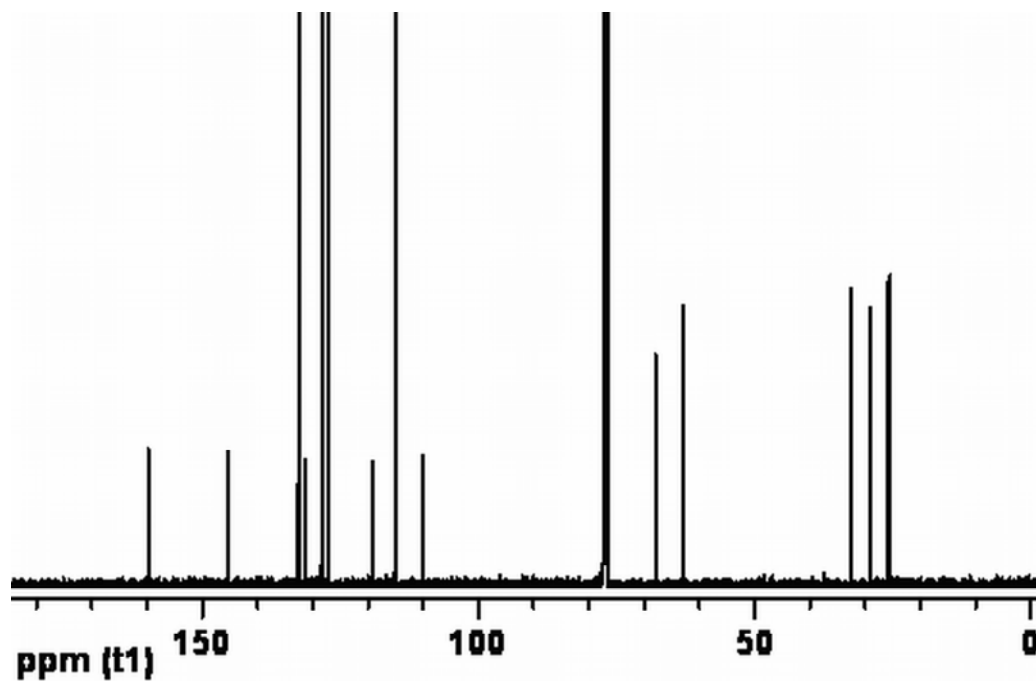
(b)
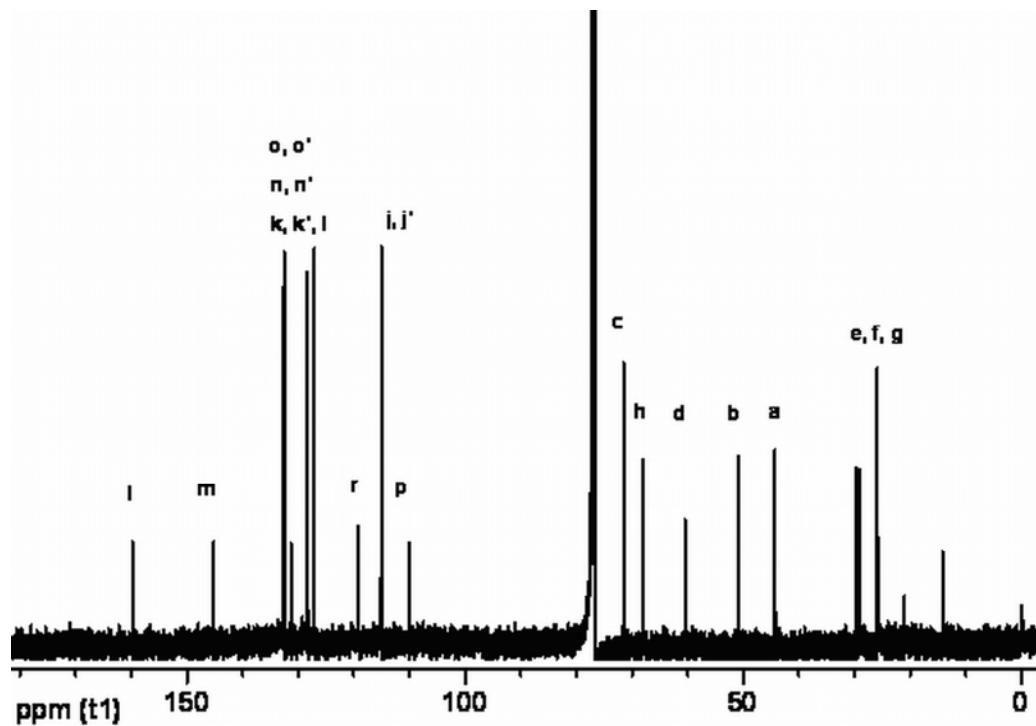
Figure 2.32 ^{13}C-NMR of the hydroxyl LC6 intermediate (1) and the glycidyl LC6 monomer (2).

The ^{13}C-NMR (CDCl$_3$) characterizations of LC$_6$ intermediate (1) and LC6 monomer (2) also confirm the successful nucleophilic substitution reaction as well. In Figure 2.32 (a), the peaks at exactly 29.63, 29.14, and 25.88 ppm are due to the aliphatic ethylene groups in the spacer unit. Moreover, the chemical shift for the cyano group is detected at 119.1 ppm. There are two ethylene groups in the spacer unit, which are adjacent to the oxygen atom, for LC$_6$ monomer. The one adjacent to the phenoxyl group is found further downfield (71.9 ppm), as this carbon is more deshielded by the attached phenoxyl group in comparison to the one which is close by the hydroxyl group. The additional peaks for the specious (2) in comparison to the specious (1) comes from the epoxy ring carbons.

(a)
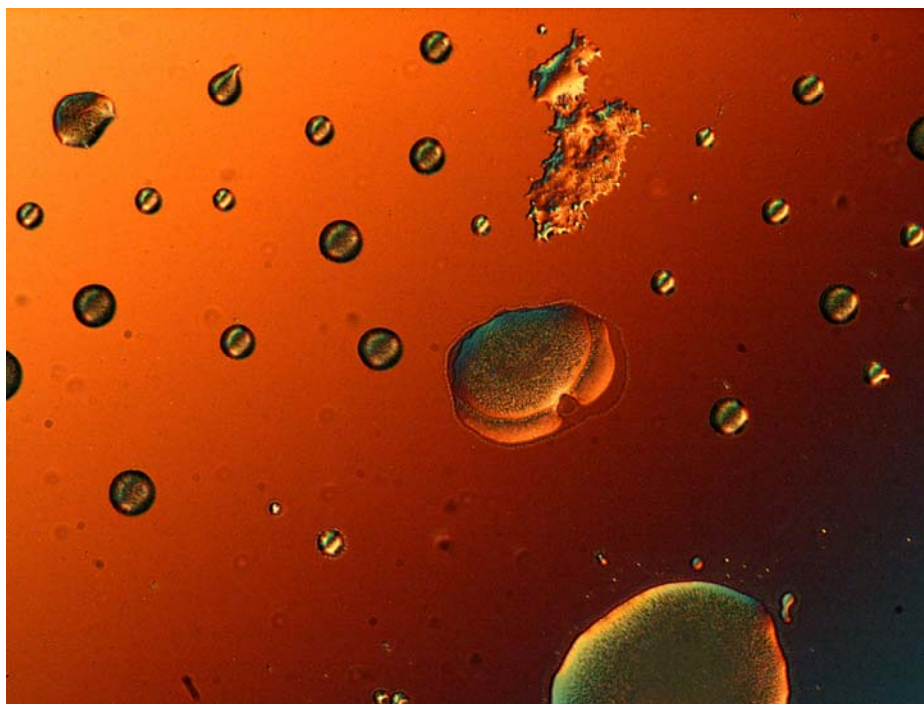
(b)
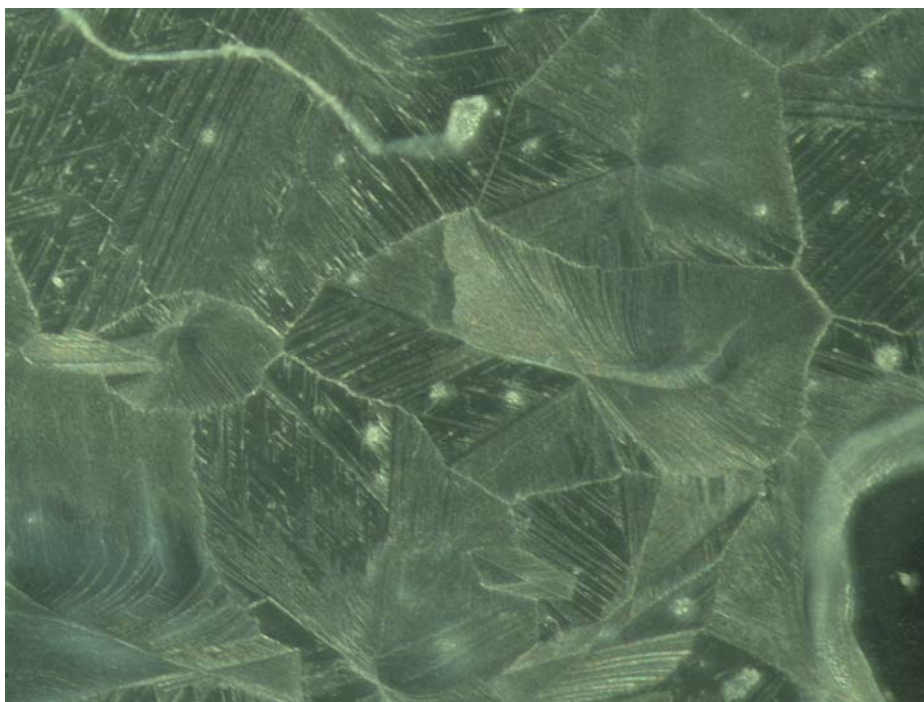
Figure 2.33 The cholesteric textures of the LC_6 monomer observed by polarized light microscopy in the second heating cycle **(a)** at 27°C (the original magnification calibration 10x 10) **(b)** at 32°C (the original magnification calibration 10x 20).

The two planar structures (the biphenyl unit and the epoxy ring) of the synthesized LC_6 mesogenic monomer, present a chiral center from the methine carbon of the epoxide. The chirality originates from the highly enantiopure S-epichlorohydrin which is employed in the monomer synthesis reaction. The LC phase of the synthesized LC_6 monomer is observed clearly under the optical microscope in Figure 2.33. In the second heating cycle, around room temperature the spherulitic cholesteric domains are observed as birefringent spheres with green and orange interference colors. And again in the second heating cycle, the most well-known cholesteric transition, oily streak, is monitored at 32°C. These findings are consistent with the study of Taton et al. [78] in which the monomer phase transitions were reported as I 33 Ch 15.8 K. The original magnification for both images is approximately 200x.

2.4.5 Synthesis and Characterization of LC_6 Copolymer
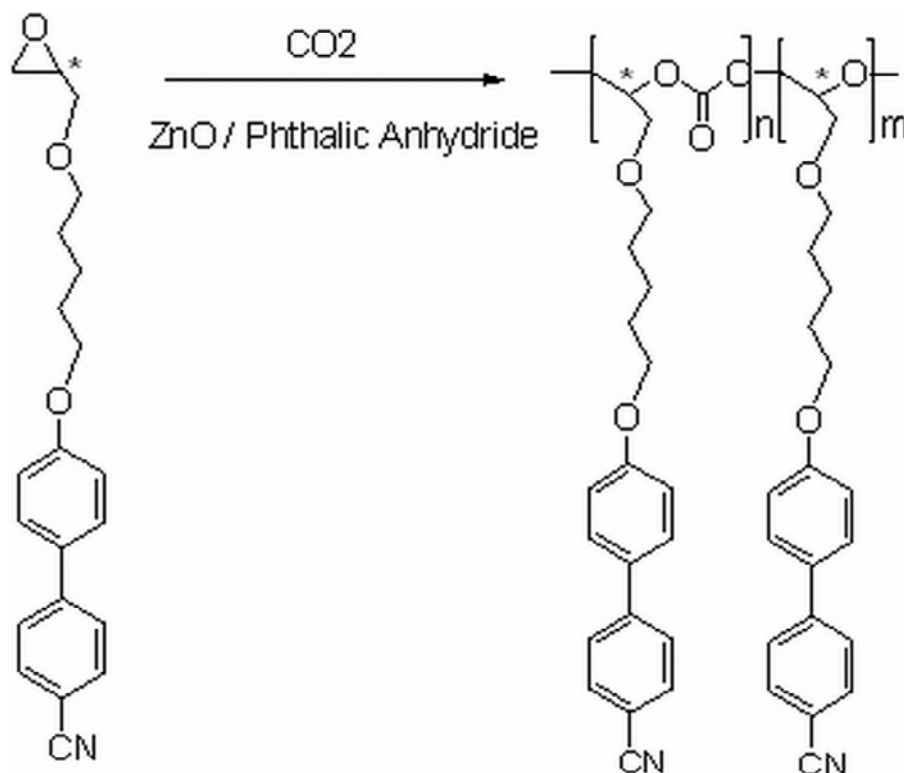
Scheme 2.8 The schematic representation of the copolymerization reaction. The copolymerization is done under the conditions of 24 hours in $scCO_2$ with a small amount of dichloromethane as co-solvent. The reaction mixture is pressurized by CO_2 up to 4500 psi.

By using the mesogenic epoxide with six spacer units and the catalyst synthesized from ZnO and phthalic anhydride, the copolymer illustrated in Scheme 2.8 is obtained in scCO$_2$ media. The star on the structures represents chirality on that carbon atom. As illustrated, the obtained copolymer consists of both the etheric and carbonate units. Actually, as a by product of such reactions in scCO$_2$ media, a cyclic carbonate formation is observed. This cyclic carbonate has been proposed to form through a back-biting reaction [104]. However, as evidenced by IR characterization below, no by-product is yielded as the LC$_6$ monomer copolymerized. Additionally, the structure and thermal analysis, as well as the optical analysis have been carried out for the obtained copolymer.
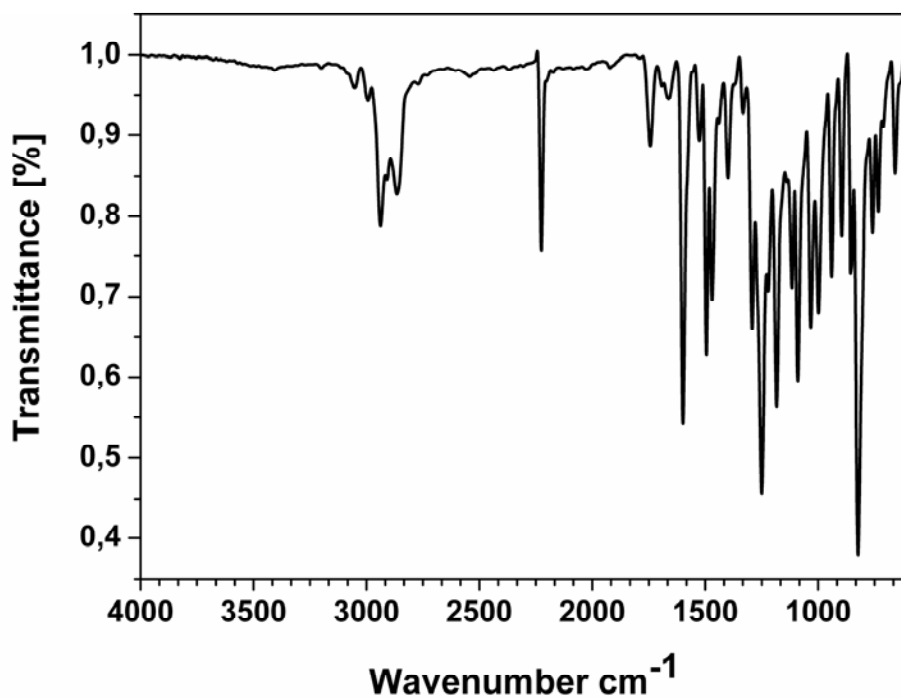
Figure 2.34 The FTIR spectrum of the copolymer

In the FTIR spectrum the most prominent change, going from LC$_6$ monomer to the polymer, is the appearance of a sharp peak at 1743 cm^{-1}, originating from the C=O stretching of the carbonate group, in the copolymer. Also the other characteristic stretching vibration of the carbonate group depending on the C–O–C bond vibrations is observed at 1246 cm^{-1}. The strong absorption at 2225 cm^{-1} is due to the cyano bond stretching in the spacer unit. The aromatic -CH- stretching can be observed (at a

frequency of 3043 cm^{-1}) as well as the aliphatic stretching. Also, the absorption bands at about 2865 and 2938 cm^{-1} is due to the ethylene units in the side chains of the polymer.

Attributable to the FTIR spectrum of the copolymer, no cyclic carbonate is observed at nearly the frequencies 1800 cm^{-1} [105]. As previously mentioned, this cyclic carbonate has been proposed to form through a back-biting reaction of the formed carbonate specious.
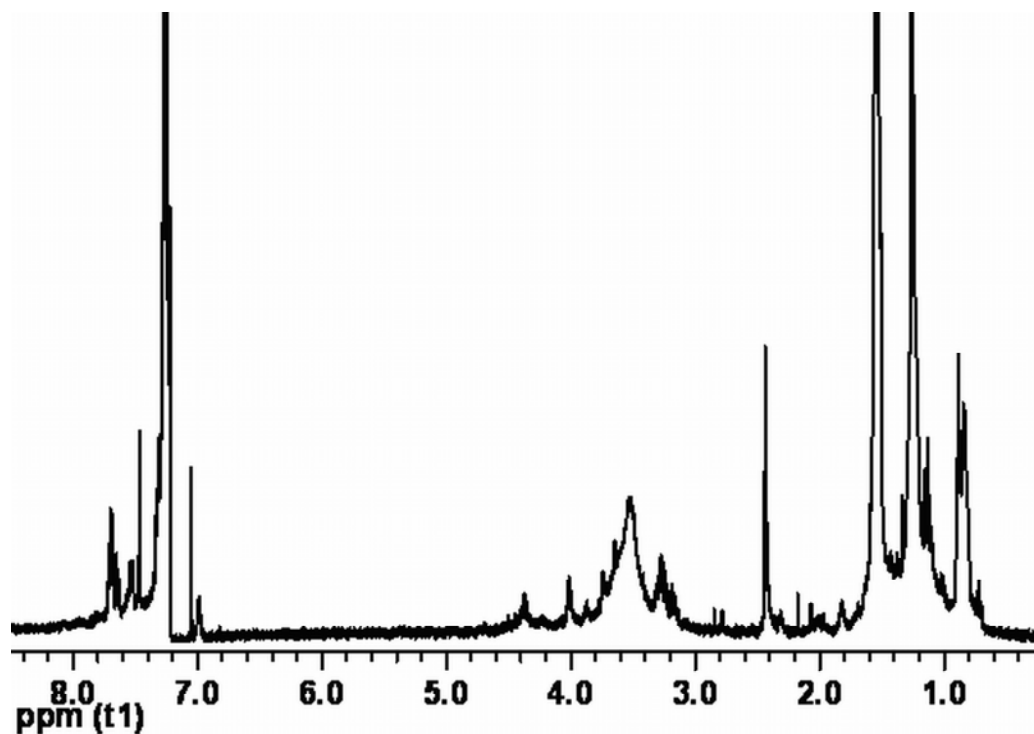
Figure 2.35 ^{1}H NMR spectrum of the copolymer

Additionally, in the ^{1}H-NMR spectrum, the shift to lower fields is observed for the epoxy protons. The methylene and the methine protons of the carbonate group are shifted to 3.53 ppm and 4.37 ppm, respectively. This downfield shift of the protons in the backbone is caused by the strong deshielding effect of the carbonate group in comparison with the monomeric epoxy group. Furthermore, the methylene units in the spacer groups give a broad band at 3.27 ppm.

The conversion of the LC$_6$ monomer to the copolymer is said to be completed since a very negligible peak is obtained for the methine proton of the monomer at 2.85

ppm. As the spectrum above is expanded and the unreacted methine peak of the monomer is integrated, the exact polymerization conversion can be calculated as 99.8%.
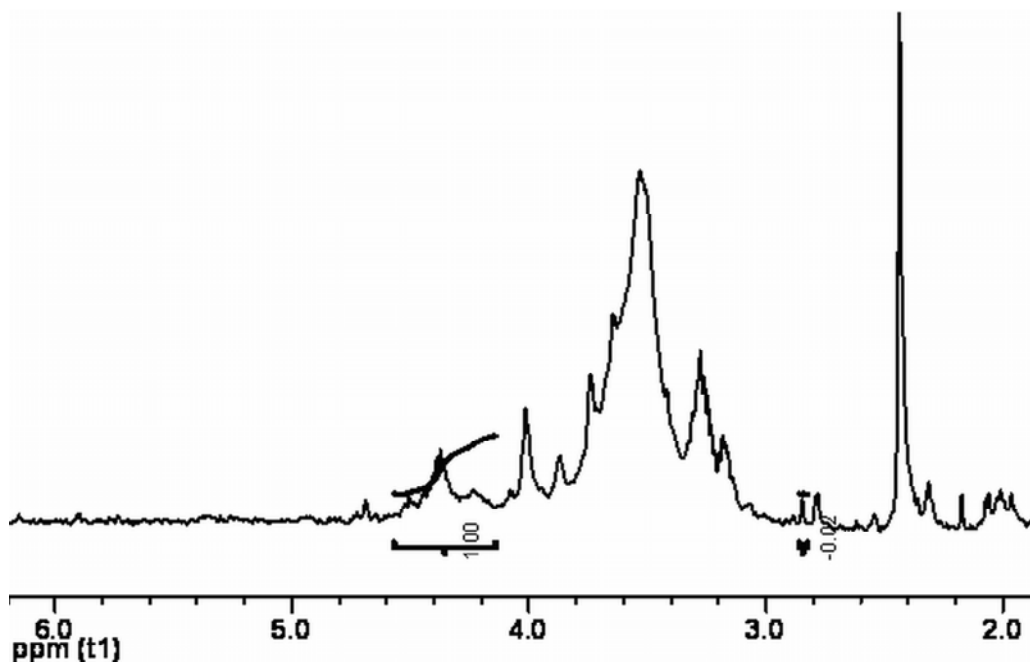
Figure 2.36 The expanded portion of ^{1}H NMR spectrum of the copolymer in the range of 6 and 2 ppm.

On the other hand, this work presents an experimental support to the previous study on the synthesis of a copolymer from a monomer without spacer unit (LC0 monomer). The ultimate goal of the current work is to achieve the synthesis of an optically active poly(ether carbonate) copolymer with LC_6 monomer in $scCO_2$ media, and to provide another proof for the final conclusion on the copolymerization mechanism. Moreover, the findings in the work with LC_0 monomer presented that, by using a highly enantiopure monomer, this polymerization mechanisim yields an isotactactic polymer. The reasonable explanations of this assertion are; specifically in the copolymerization with CO_2 racemization does not take place [89, 90] and the polymerization does not proceed via the enantiomorphic site control [91]. So being aware of these advantages of polymerization in $scCO_2$ media, by using achiral catalysts, chiral epoxides should give chiral polymers.

Furthermore, factors such as stereoregularity, tacticity and backbone chirality can have an important influence on the phase behavior of SCLCPs. Much depends on the

optical activity of the monomer. The polymerization of optically active monomers is interesting not only because optically active polymers can be obtained, but also because monomer optical activity can affect polymer tacticity. This fact is reported by Taton et al. [88], who illustrated that for chiral mesogenic epoxides cholesteric SCLC polyether were obtained, whereas for racemic epoxides, nematic mesophases were observed. Since, the catalyst is not chiral and the polymerization does not proceed via the chain-end control mechanism [86], a special stereoregularity is expected for our polymer . Owing to the fact that, the monomer used is highly enantiopure and also the ring opening of the epoxide results always from the backside attack [92, 94] this special stereoregularity can be rationalized as isotactic. The isotacticity of copolymer is illustrated by a single carbonyl resonance at 154.52 ppm in Figure 2.37, representing a single chiral environment [95].
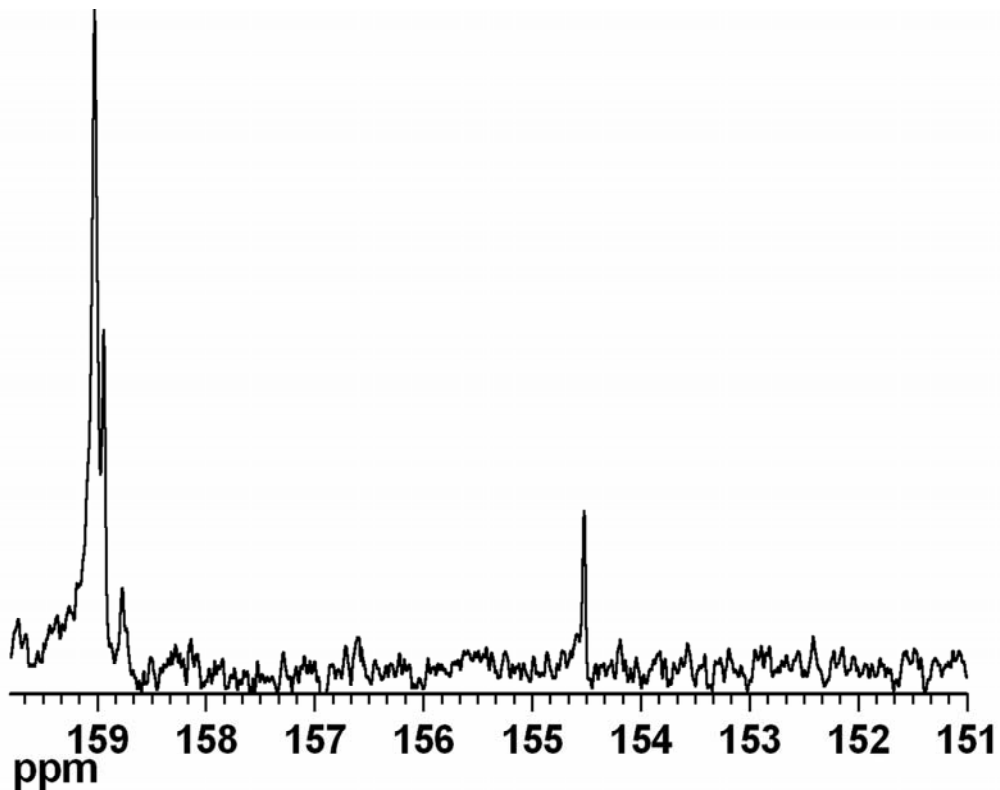
Figure 2.37 The expanded portion of the ^{13}C NMR spectrum of the copolymer in the range of 159 and 151 ppm.

As revealed in the literature, mesogenic molecules with short spacer units tend to present a nematic LC mesophase, whereas the ones with longer spacer units present a smectic LC mesophase [88]. Increasing the spacer length of the mesogenic unit to six, still stabilizes the consistency for the nematic mesophase as evidenced in Figure2.38.

It is essential to note that, in the literature for the polymers with a longer spacer group, the effect of the chiral centers of the polymer backbone is not detected [78]. Whereas, the coupling between the mesogenic unit and the polymer backbone, turn out to be strong for this polymer. Consequently, a transfer of chirality from the backbone to the mesophase is detected for $PolyLC_6$ (polymer with 6 spacer unit) as in $PolyLC_0$ (polymer without a spacer unit). The optic microscopy textures confirm this chirality transfer and as a result, a chiral nematic texture for the copolymer is detected as shown in the following figure.

(a)
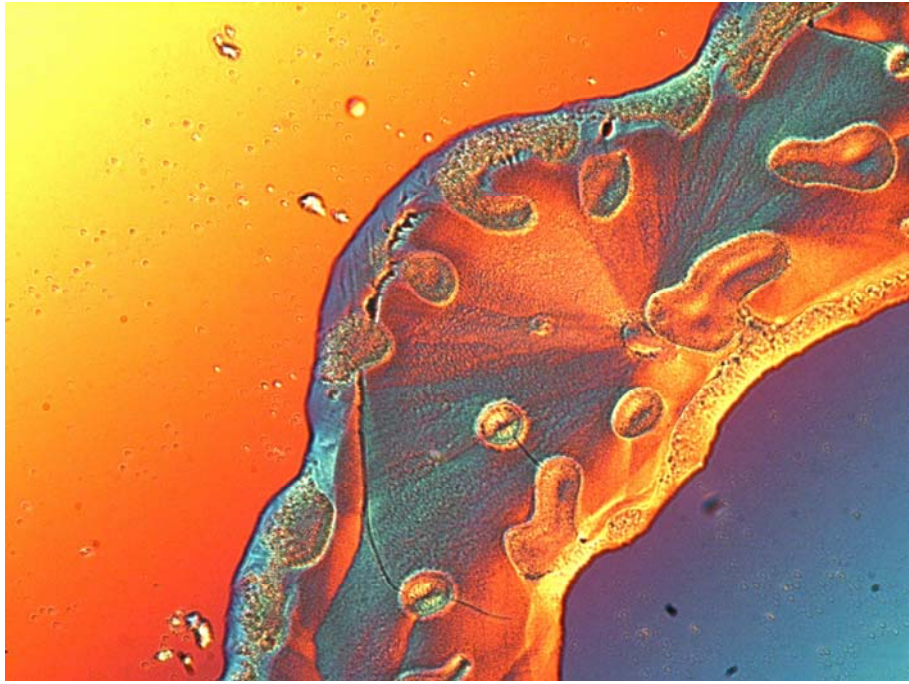
(b)

(c)
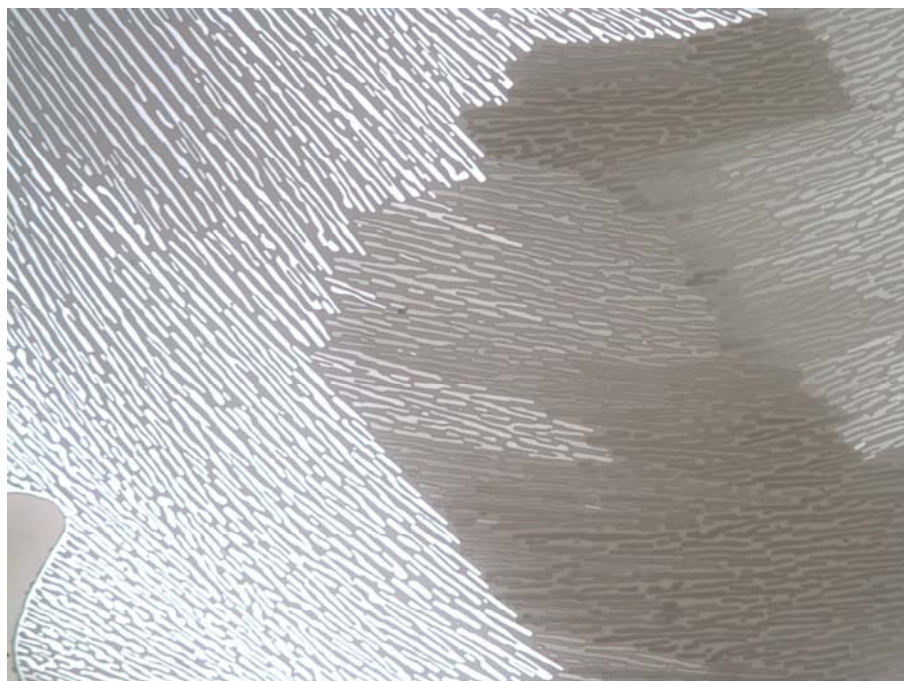
(d)
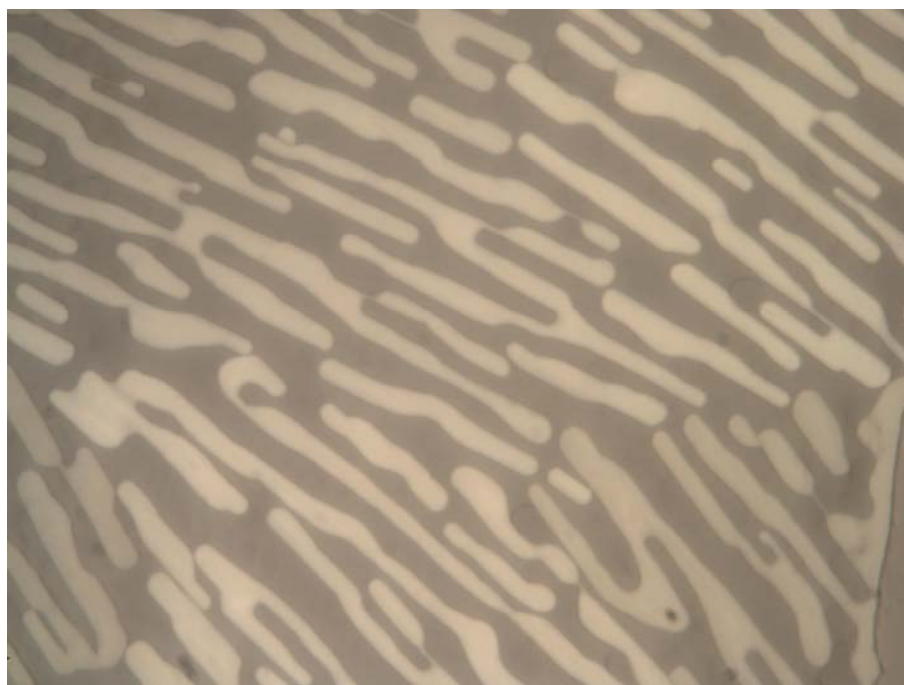
Figure 2.38 The cholesteric textures of the LC$_6$ bulk polymer observed by polarized light microscopy **(a), (b).** in the second heating cycle **(a)** at 97.5°C (the original magnification calibration 10x10) **(b)** at 98.7°C (the original magnification calibration 10x20); **(c), (d)** in the third heating cycle **(c)** at 97.7°C (the original magnification calibration 10x20) **(d)** at 99.1°C (the original magnification calibration 10x50).

The LC phase of the bulk polymer was explicitly defined by textural observation by optical microscope. On heating from the crystalline form, the cholesteric phase transitions are observed at 97.5°C and 98.7°C. The spherulitic cholesteric domains appear in Figure 2.38 (a) as a full-wave retardation plate with an original magnification of 100x. Different colors correspond to different twist states of the cholesteric liquid crystalline polymer. The image presents the spherulitic cholesteric domains as birefringent spheres with blue and orange interference colors. On the other hand, Figure 2.38 (b) represents the oily streak texture for which the original magnification is 200x. Whereas, in the third heating cycle, the most well-known cholesteric transition, Fingerprint, is screened for Figure 2.38(c), (d) with different magnification calibrations.

Using the sample preparation technique discussed in the experimental part, we have measured the X-ray diffraction (XRD) data of PolyLC$_6$, rapidly quenched by liquid nitrogen from its liquid crystalline state.
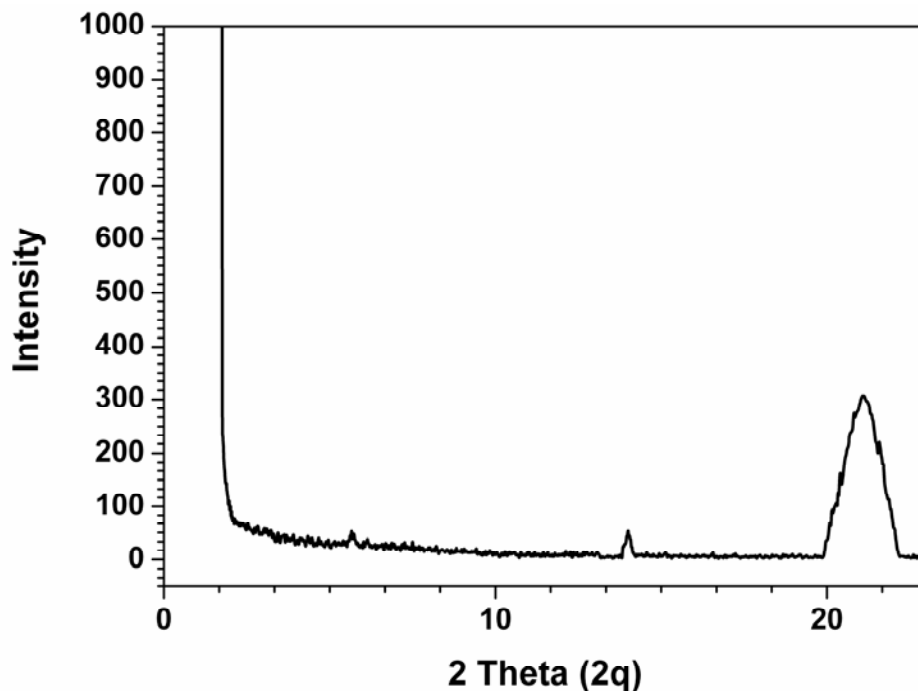
Figure 2.39 The X-ray measurement for the copolymer at room temperature.

In general, a sharp and a strong peak at low angle ($1° < 2\theta < 4°$), associated with lateral packing curves at wide angles, can be observed for smectic structures, whereas, only wide angle X-ray diffraction curves are detected for cholesteric structures. Since no reflection is observed at low angles in the diffractogram in Figure 2.39, it can be said that no layer ordering within the mesophase is present and that is why, the polymeric mesophase is considered out of the smectic classification. Hence, the broad peak centered at $2\theta = 21.12°$ representative of cholesteric mesomorphic structure. By using Bragg's Law ($2d \sin\theta = n\lambda$), the d-pacing of this reflection is derived as 4.20 Å. Lengthening the spacer unit in the side chains has shown itself as a broadened peak. As it is known, the appearance of a broad or sharp peak furnishes a qualitative indication of the degree of order. Explicitly, the sharp peak at high angle region for $PolyLC_0$ implies a better ordered side chain structure in comparison to the $PolyLC_6$.

On the other hand, the copolymer shows additionally two mid–angle reflections in the X-ray diffraction pattern. These mid-angle reflections at about $2\theta = 5.62°$ and $2\theta = 14°$ are characteristic peaks of the copolymer which are observed in the crystalline form as well and correspond to the average intermolecular distance about 15.71 Å and 6.32 Å respectively. Compared to the one for LC_0 copolymer, reductions in the intensities of these reflections are observed. This is reasonable due to the weakened crystallinity of the LC_6 copolymer as a consequence of the increased spacer length.

The phase assignment was conducted by optical polarizing microscopic observation and X-ray diffraction measurement. The results correlate with each other and the coexistence of a cholesteric structure was verified.
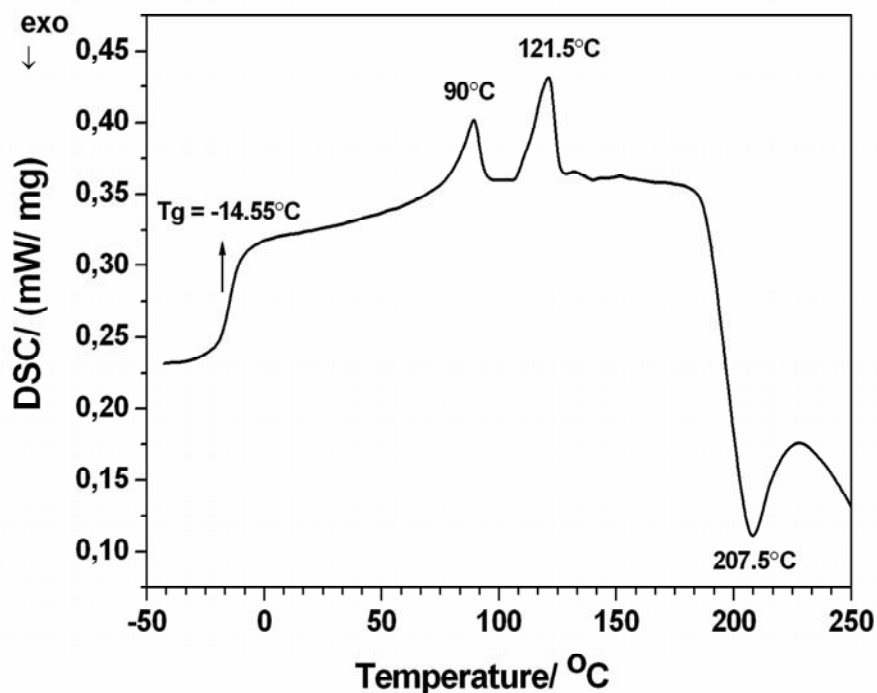
Figure 2.40 The DSC thermogram of the copolymer from LC_6 monomer in the second heating cycle with a heating rate of 10°/C.

Coming to the thermal characterization of the $PolyLC_6$, an obvious Tg curve is detected at -14.55 °C. In comparison with the LC_0 analogue, the decrease in the Tg value for this polymer is very probable by increasing the spacer length of the mesogenic unit. This is due to the enhancement on the free motions of the side chains and hence presenting a plasticizing effect on the polymeric backbone. The decomposition of the polymeric material is observed at 207.5°C, very close to its LC_0 analogue. Unlikely to $polyLC_0$, no exothermic peak is monitored as representative of the crystalline to crystalline transition ($k \rightarrow k^{'}$ transition). One possible explanation comes with the notification of the highly crystalline structure of the obtained LC_0 monomer. The monomer without a spacer unit actually is in a highly crystalline form unlikely to the obtained waxy LC_6 monomer. Additionally, the crystalline to liquid crystalline transition prolongs more during optical investigation for the LC_0 polymer than its LC_6 analogue and thus, presenting more time for transformation to a better ordered crystalline subphase.

Actually, two more transitions can be read from the thermogram, the one at 90°C involves a crystal-to-cholesteric transition and the one at 121.5°C is responsible for the cholesteric-to-isotropic transition. Polarized optical microscopy observation is in great agreement with these transitions as well.

As mentioned above, the glass transition temperature decreases slightly with increasing spacer length, probably due to a plasticizing effect of the side chain on the backbone, in agreement with common findings for side-chain liquid crystalline polymers [106]. As can be clearly seen from Table 2.3, the polymer containing six spacer unit, shows far higher isotropization (or clearing) temperature than that of its homologue without spacer unit. Dubois *et al.* [102] have also reported a similar thermal behaviour: the acrylic analogue with 3 spacer unit exhibited lower clearing temperatures than the one with six sapcer unit. Consequently, the copolymer obtained from LC_6 monomer, presents an enlarged mesomorphic temperature range ($\Delta T= Ti-Tg$) in comparison to the LC_0 copolymer and its acrylic analogues. Hence, these materials are exhibiting another practical benefit in terms of liquid crystallinity. The trends in glass transition and isotropization temperatures for $polyLC_0$ and its acylic analogues with 3 and 6 spacer unit, as a function of the methylene carbon atoms in the spacer, are presented in Table 2.3.

Table 2.3 Comparison of the Tg and Ti values of homologue and analogue polymers.

Reactants	Spacer Unit	Tg (°C)	Ti (°C)
PolyLC$_0$	N= 0	-3.3	90.1
PolyLC$_6$	N=6	-14.5	121.5
Acryloyl chloride and 4-cyano-4$^{'}$-hydroxybiphenyl	N=3	68	97
Acryloyl chloride and 4-cyano-4$^{'}$-hydroxybiphenyl	N=6	45.5	124

2.5   CONCLUSION

2.5.1   Conclusions on the copolymerization mechanism

By using an environmentally benign approach, synthesis of a mesogenic epoxides and their copolymerization with CO_2 has yielded optically active SCLCPs in a single-step reaction.

The presence of a chiral center in the main chain is beneficial since it provides information about the magnitude of decoupling between the mesogenic unit and the backbone. As demonstrated with the chiral nematic (cholesteric) phase transitions on the optical microscopy textures, a transfer of chirality from the macromolecular backbone to the mesophase become feasible for both copolymers. Being consistent with the ^{13}C-NMR spectrum, the appearance of a sharp peak at high angle regions in the X-ray diffraction patterns implies an ordered side chain structure between the main chains.

Additionally, the carbonate group in the backbone can provide enough flexibility to the mesogenic unit to introduce liquid crystallinity, and the ether moieties in the backbone further enhance flexibility. Therefore, a SCLCP with a flexible backbone was prepared for the possibility of obtaining better electro-optical properties than those of their non-flexible analogues.

Finally, our copolymers present extended mesomorphic temperature ranges compared to those of its acrylic analogues. This can be a good basis in the materials design for preparing the practical materials suitable for device applications. Attributable to the flexible backbone, polymers that are synthesized in $scCO_2$ media, may lead to different thermal applications.

We describe the advantages of polymerization in $scCO_2$ media, in terms of liquid crystallinity and the stereoregularity of the obtained polymers. Starting from the fact that copolymerization mechanism in $scCO_2$ media does not alter the arrangement of the enantiopure monomer, one can easily obtain a highly stereoregular polymers by a purposeful design of a chiral monomer or catalyst.

2.5.2 Conclusions on the Effect of Spacer Length

To get more information about the copolymerization mechanism in $scCO_2$ media, and to investigate the tail length effect on the arrangement of the monomers in the backbone, we have synthesized enantiopure LC_6 monomer additional to LC_0 monomer.

It is still possible to acquire the magnitude of decoupling between the mesogenic unit and the backbone, even if the spacer unit length is increased to six. Furthermore, starting from these enantiopure monomers and achiral catalyst system, highly stereoregular (isotactic) polymers are obtained. It is demonstrated that, copolymerization mechanism in $scCO_2$ media does not alter the arrangement of the monomer even if the tail length is increased. Namely, the bulky group in LC_6 monomer could not manage to change the arrangement and eventually the isotacticity of the copolymer. On the other hand, LC_6 copolymer presents a practical benefit in terms of thermal applications. Compared to its LC_0 homologue and its acrylic analogues, LC_6 copolymer provides an extended mesomorphic temperature range. And thus, presents superiority in the materials design for preparing practical materials suitable for device applications. It is now possible to synthesize different spacer-length LCPs in $scCO_2$ media, which are precursor for a great variety of different liquid crystalline applications.

3   CHAPTER 3

A   DETAILED INVESTIGATION ON MICRO AND MACRO STRUCTURES OF POLYCABONATES FROM DIFFERENT EPOXY MONOMERS

3.1   Introduction

In order to elucidate the copolymerization mechanism with the synthesized catalyst and shed light on the microstructure and macrostructure of the obtained copolymers under the defined conditions, a detailed study on the ^{13}C-NMR spectroscopy has been conducted in this chapter.

A considerable attention have been directed to investigate the macrostructures of the polymers because the stereochemistry of a polymer determines both the mechanical and physical properties, as well as their rates of chemical and biological degradation [1]. Furthermore, synthesis of new microstructures may lead to new applications for the copolymers obtained from various epoxy monomers. With the microstructure investigation also the mechanisim of the catalysis reaction is understood.

In the following the background studies in the literature, related with the microstructure and macrostructure investigations are presented in turn.

3.1.1   Macrostructure Investigations

Stereochemical information of polymers is conveniently collected by ^{13}C-NMR spectroscopy, because signals of ^{13}C-NMR spectra of polymers split clearly reflecting configurational sequences. Assignment of the peaks to the corresponding sequences is

commonly based on spectroscopic analyses of oligomers with well defined stereochemical identity [107]. For example, Sato et al. assigned signals of methylene and ipso carbons in polystyrene, referring to signal assignment of all diastereomers of styrene pentamer [108]. Zambelli and Bovey assigned the stereochemistry of methyl carbons in polypropylene through synthesis of model compounds [109].

Moreover, as previously mentioned alternating copolymerization of epoxy ring and carbon dioxide has received great interest in recent years because of utilization of carbon dioxide as a raw material [84, 110]. In addition to the above mentioned structural investigations, in 1994 Kuran et al. [111]. demonstrated that ^{13}C-NMR spectroscopy could be applicable to determination of the stereochemistry of the copolymer of cyclohexene oxide. They observed two main signals at 153.7 and 153.1 ppm in a carbonate region and attributed them to syndiotactic diad (-*SSRR*-) and isotactic diad (-*SS-SS-* or -*RR-RR*-), in analogy to 2,2-oxydicyclohexanol, syndiotactic and isotactic dimeric diol models having an ethereal linkage in place of a carbonate functionality. Recently, Nakano et al [112] and Coates et al. [113] have independently succeeded in the asymmetric alternating copolymerization of cyclohexene oxide and carbon dioxide. As a result of this asymmetric synthesis, the resulting optically active copolymers are easily hydrolyzed into *trans*-1,2- cyclohexenediol and CO2 by alkali treatment, which enable unambiguous determination of the degree of asymmetric induction. However, depending on the enantiomeric excess, they had contradiction with the study of Kuran and this prompted them to reexamine the ^{13}C-NMR assignment. In their report Nakano et al., present the final configurational assignment of the copolymer as: the signal at 153.7 ppm includes isotactic diads, and the ones at 153.3-153.1 ppm include syndiotactic diads. In the scheme below, the isotactic and syndiotactic diads are demonstrated.
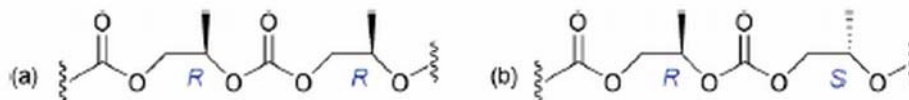
Scheme 3.1 The representation of **(a)** isotactic and **(b)** syndiotactic diad of a polymer [114].

Figure 3.1 illustrates a close-up look for the carbonate region and points up the two main signals of a poly (cyclohexene carbonate) as Kuran et al. asserted priviously.

97
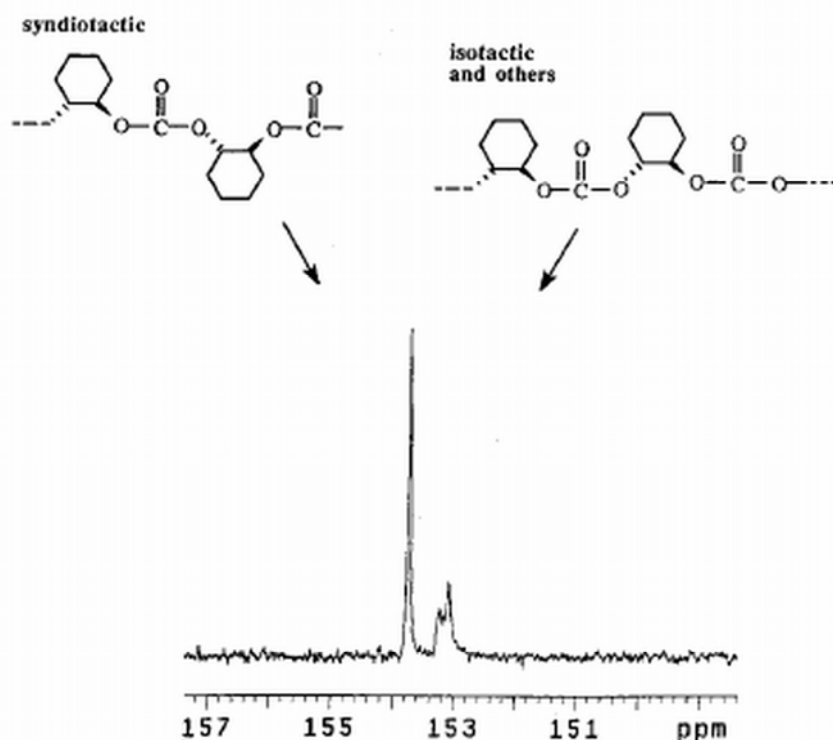
Figure 3.1 ^{13}C NMR spectrum of poly (cyclohexene carbonate) obtained with a zinc complex as catalyst. Recorded in CDCl$_3$ at ambient temperature.

With the rationale that tacticity is directly related to the side group orientation, its influence should be observed most clearly in the side groups. For this reason, a consideable attention should be given to the methine (-CH) and the methylene (-CH$_2$) carbons of the polymers. The methylene group assignment is more difficult due to partial overlap of the CH$_2$ groups in backbone and spacer with one another and with the first CH$_2$ group of the alkoxy tail. Consequently, in the course of our study the methine carbon of the epoxy ring in ^{13}C-NMR spectrum will be concentrated on.

During the last couple of years, such studies, to elucidate the tacticity of the polycarbonates that are obtained with various catalyst systems have been aroused in the literature. For instance, Chisholm et al. [85] work with the polymers that are obtained from lactides and propylene oxides in correspondence with several catalyst systems. Similarly, in another study of Chisholm et al. [93], a zinc glutarate catalyst is employed and the tacticity was investigated in the methine carbon region for both racemic and enantiomerically pure propylene oxide monomers.
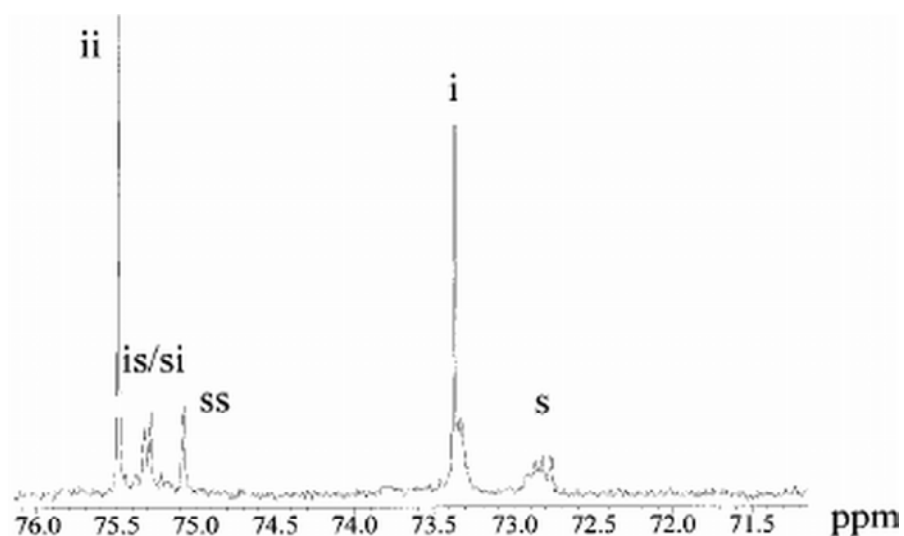
Figure 3.2 The expanded ^{13}C-NMR spectrum in the methine and methylene carbon region of copolymer from PO prepared with zinc glutarate catalyst [93].

Also in another report Antelmann et al. [115] not only give close-up ^{13}C-NMR spectra both for the polymers from racemic and the S enantiomer of propylene oxide (S-PO) but also give very comprehensive results of DEPT (distortionless enhancement by polarization transfer) spectra of them. These DEPT spectra distinguish the methine and the methylene carbon signals and also present information on the microstructure regions in depth. Figure 3.3. shows the DEPT spectra, given in the study of Antelmann, of polypropylene oxide both from racemic and S-enantiomer of propylene oxide in the methine and methylene region.

(a)
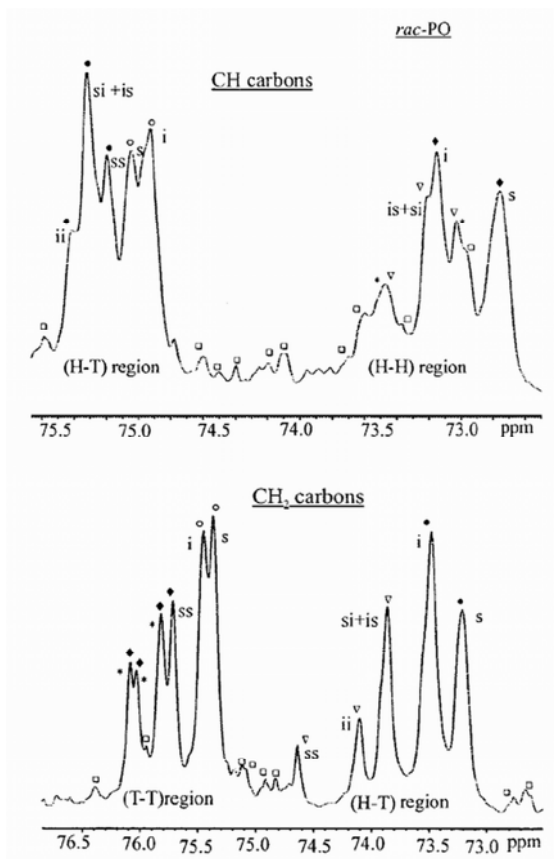
(b)
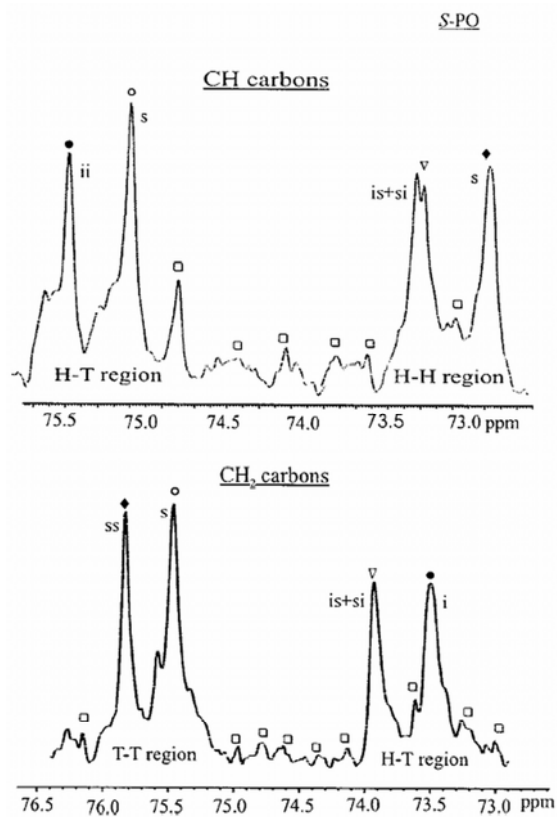
Figure 3.3 The DEPT NMR spectra showing the methine and methylene carbons for the polymers from **(a)** racemic PO (rac-PO) and **(b)** S-PO [115].

3.1.2   Microstructure Investigations

The elucidation of a microstructure of the obtained copolymer is another fundamental matter and is directly related with the properties of the product. On the other hand, very few previous literature reports have dealt with the microstructure of aliphatic polycarbonate (PC), and focus were on the carbonate carbon [93, 116]. Three regions in the ^{13}C -NMR spectrum of the carbonate carbon were assigned as head to tail (HT), tail to tail (TT), and head to head (HH) for a polypropylene carbonate as shown in Figure 3.4 and these junctions are shown in Scheme 3.2. Even if the Polypropylene carbonate chain was formed from *rac*-propylene oxide, each stereosequence can be further broken down to **i** (isotactic) or **s** (syndiotactic) stereosequences instead representing a single peak. As is evident from an inspection of Figure 3.4, there are more than two resonances in the HT and HH regions, and this implies that the carbonate carbon must be sensitive to more than its adjacent PO units.

Splitting of the carbonate peak was found by Lednor and Rol [117] by high resolution ^{13}C-NMR spectroscopy of poly(propylene carbonate) and by Darensbourg et al. [84] for poly(propylene carbonate-*co*-cyclohexylenecarbonate). The differences in the chemical shift in the polymer of Lednor and Rol (153.5–154.5 ppm) were, however, much higher than in the present polymers, and they ascribed it to the presence of head-to-head (HH), head-to-tail (HT) and tail-to-tail (TT) groups.
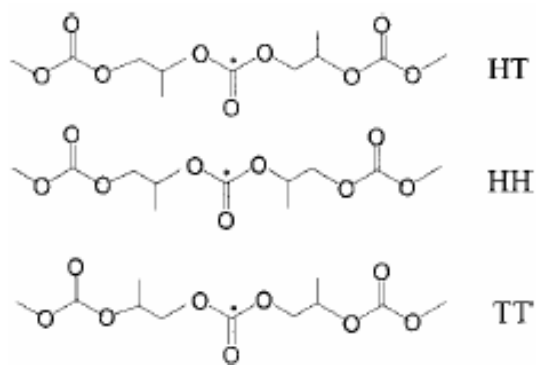
Scheme 3.2 Three Possible Regiosequences of Polypropylene carbonate at the Diad Level When Looking at the Central Carbonate Carbon
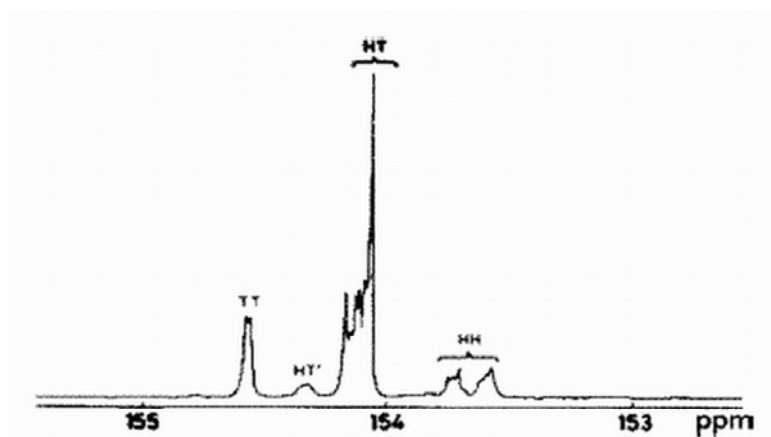
Figure 3.4 ^{13}C -NMR spectrum of the C=O region of PPC reported in ref [93].

3.2   Motivation

It is becoming increasingly clear that, the 'greener' route for polycarbonate synthesis is the polymerization in supercritical carbon dioxide media. And therefore, this technique has the potential to supplement current processes for the production of polycarbonates, which involve the condensation polymerization of highly toxic diols and phosgenes [7, 118].

Moreover, synthesis of copolymers with well-defined structure is a subject of fundamental as well as practical importance. In this respect, control of structural sequence as well as molecular weight of the polymer is desirable.

Over the last half decade, impressive advances in living copolymerization reaction in scCO₂, (supercritical carbon dioxide) using different catalysts have been achieved. In the recent literature, several ground-breaking reports have appeared concerning living polymerization [84, 119, 120]. Upon exploring these systems for ring opening polymerization we are intended to synthesize different functional grouped polycarbonates with a narrow distribution and well molecular weight. It is noteworthy to state here that, polymers with controlled parameter (Mn) and low polydispersity have been formed as a result of ring opening polymerization of these epoxides. For these ring opening copolymerization reactions, not only some commercial monomers but also the purposefully synthesized monomers have been used. Additionally, in this study to investigate the effect of chirality to the macro and micro structures of the obtained polymers, some chiral monomers have been utilized.

The outcomes of these asymmetric syntheses are optically active polymers and have great importance. It is well known that, almost all naturally occurring polymers are chira1 [121]. Historically, interest in chiral synthetic polymers has focused on modeling natural polymers, interpreting the conformational properties of macromolecules in solution [122] and investigating the mechanism of polymerization reaction [123]. Optically active polymers have also been utilized as chromatographic supports [124] polymeric reagents, and catalysts. More recently, the proposal that chirality can be used as a means of influencing the two- or three-dimensional order of macromolecules [125] has focused efforts on the application of chiral macromolecules for piezoelectric, ferroelectric, and nonlinear optical application [126].

As previously mentioned, in this study some chiral monomers are employed for the synthesis of optically active polymers. Such polymers can be synthesized by using either chiral monomers or chiral catalysts. The polymerization of a chiral monomer is probably the most widely used method of synthesizing an optically active polymer. Nature takes advantage of the readily available chiral monomers such as amino acids and sugars to construct proteins, nucleic acids, and polysaccharides. As an example, Endo and his coworkers developed novel optically active polycarbonates, applicable to biocompatible materials, by anionic ring opening polymerization of naturally chiral monomers. Since then, for synthetic macromolecules, the strategy of polymerizing chiral monomers has enjoyed considerable success [127].

Such a polymerization is interesting not only because optically active polymers can be obtained, but also because the monomer activity can affect polymer tacticity. Tacticity is directly related to the side group orientation, and therefore its influence should be observed most clearly in the side groups. Up to now, there have been many studies on the stereocontrol and mechanism of the ring opening polymerization of carbon dioxide with cyclohexene oxide and lactide. For instance, the polymerization of optically active (*R,R*)-lactide yields isotactic PLA [127], while polymerization of *meso*-lactide using an optically active initiator can produce syndiotactic PLA [128]. Polymerization of *rac*-lactide typically produces amorphous, atactic polymers. [129].

However, prior to work in our laboratory, a very limited numbers of studies have been reported on the microstructure and macrostructure of the polymers from epoxy rings. Nevertheless, in none of these studies the effect of functional group on the obtained structure have been investigated. Starting from this fact, we have synthesized several different functional grouped polycarbonates from either racemic or chiral epoxy monomers. Accordingly, by these examinations we aimed to say more about the modes of the ring opening of epoxides in $scCO_2$ media in coordination with the used catalyst as well as the tacticity and the microstructure of the resultant polymers. In addition to these, some detailed investigations on the thermal behavior of the obtained copolymers have been conducted during this study.

3.3   Experimental

3.3.1   Reagents

3.3.1.1   Materials

Zinc oxide (ZnO, MW = 81.37 g/mol, purity > 99.99%), (±)-Epichlorohydrin (C_3H_5ClO, MW = 92.53 g/mol, purity > 99%), (S)-(+)-Epichlorohydrin (C_3H_5ClO, MW = 92.53 g/mol, purity > 98%), and Glycidyl methacrylate ($C_7H_{10}O_3$, MW = 142 g/mol, purity > 97%), were all supplied from Aldrich Chemicals, Germany. On the other hand,

Phthalic Anhydride ($C_8H_4O_3$, 148.12, purity >99%), (S)-(+)-Glycidyl Nosylate ($C_9H_9NO_6S$, MW = 259.23 g/mol, purity > 98%), Potassium Carbonate (K_2CO_3, MW = 138.21g/mol, anhydrous), were purchased from Acros Organics. The fluoro monomer (1H,1H-perfluoropenthyl)oxirane ($C_7F_9H_5O$, MW = 276 g/mol, purity > 98%) was purchased SIA, Russia. The other perfluoroalkyl chemicals (EA600 and EA612), Perfluoroalkyl Ethanol ($CF_3(CF_2)_5CH_2CH_2OH$, MW = 370g/mol, purity > 97.5%) and its analogue with 12 spacer unit were supplied from Clariant GmbH, Frankfurt, Germany. All the materials were used as received.

3.3.1.2 Solvents and Drying Agents

The Dichloromethane (CH_2Cl_2, 84.9 g/mol, analytical grade) and the Ethyl acetate (EtOAc) ($C_4H_8O_2$, 88.11 g/mol, analysis grade) were supplied from Labkim Corporation, Turkey. N,N-Dimethylformamid (DMF) (C_3H_7NO, MW = 73.1 g/mol, anhydrous) and Ethanol (C_2H_6O, MW = 46.07 g/mol, 99% grade and denaturized with 1% MEK) were obtained from Aldrich Chemicals Company and used under an inert atmosphere. Other solvents, Hexane (C_6H_{14}, MW= 86 g/mol, analytical grade), Tetrahydrofuran (THF) (C_4H_8O, 72.11 g/mol, analytical grade) and Hydrochloric acid (HCl) (36.46 11 g/mol, 37% extra pure), were purchased from Riedel-de Haen Chemicals and used as they received.

3.3.2 Characterization

3.3.2.1 Methods

Characterizations of the catalyst monomer and polymer were performed using ATR method by Fourier transform infrared spectroscopy (FT-IR) recorded on Equinox 55/S Fourier transform (Bruker). ^{1}H-NMR and ^{13}C-NMR were recorded on Unity Inova 500 MHz nuclear magnetic resonance (Varian AG, Switzerland). DSC thermal analyses were run at N_2/N_2 atmosphere with a heating rate of 10ºC/min. using Netzsch Phoenix differential scanning calorimeter 204 (Selb, Germany). The number-

average molecular weights (M_n) and polydispersity index (M_w/M_n) were measured with gel permeation chromatography (GPC) on a Agilent Model 1100 instrument containing a pump, a refractive index detector and four Waters Styragel columns HR 5E, HR 4E, HR 3, HR 2; and THF was used as eluent at a flow rate of 0.3 mL/min at 30°C. Data analysis was performed with PL Caliber software. The system was calibrated with narrow polystyrene standards (Polymer Laboratories).

Polymerizations held in scCO$_2$ were performed by P-50 High Pressure Pump Contrivance (Thar) in a 100mL high-pressure stainless-steel vessel. Heating was achieved with a heating band and temperature was controlled by a thermocouple adapted to the vessel.

3.3.2.2 Characterization of the Commercially Obtained Material

Epichlorohydrin: 'H-NMR (CDCl$_3$): δ 2.68 (dd, 1H), 2.88 (dd, 1H), 3.23 (m, 1H), 3.55 (dd, 1H), 3.64 (dd, 1H); ^{13}C-NMR (CDCl$_3$): 51.33, 46.90, 45.32; IR (ATR): 3002, 1480, 1432, 1397, 1266, 1254, 1136, 1091, 960, 925, 905, 852, 759, 720, 695cm^{-1}.

(S)-glycidyl 3-nitrobenzenesulfonate (Nosylate): 'H-NMR (CDCl$_3$): δ 2.77 (dd, H), 2.92 (dd, 1H), 3.37 (m, 1H), 3.98 (dd, 1H), 4.28 (dd, 1H), 7.82 (d, a-CH~)), 8.25 (d, (a-CH~)), 8.53 (d, (a-CH~)), 8.56 (d, (a-CH~)); ^{13}C-NMR (CDCl$_3$): δ 148.12, 137.92, 133.35, 130.85, 128.42, 123.17, 71.78, 48.70, 44.48 IR (ATR): 3087.47, 1671.86, 1608.00, 1532.73, 1430.44, 1255.16, 1131.86, 1076.19, 951.22, 911.35, 881.69, 811.30, 754.75, 732 cm^{-1}

(Perfluoropentyl) oximase: 'H-NMR (CDCl$_3$): δ 2.34 (m, 2H), 2.58 (dd, 1H), 2.87 (t, 1H), 3.22 (m, 1H); ^{13}C-NMR (CDCl$_3$): δ 110.14, 109.6, 73.4, 51.7, 50.5, 43, 41.5; (IR):1421, 1347, 1218, 1129, 1090, 1057, 1021, 935, 880, 867, 811, 750, 732, 708, 689 cm^{-1}.

Glycidyl methacrylate: 'H-NMR (CDCl$_3$): δ 1.94 (t, 3H), 2.65 (dd, 1H), 2.84 (dd, 1H), 3.23, (m, 1H), 3.99 (dd, 1H), 4.46 (dd, 1H), 5.58 (m, 1H), 6.14 (m, 1H); ^{13}C-NMR (CDCl$_3$): 166.93, 135.82, 127.33, 125.45,65.17, 49.38, 44.59 , 21.79 (IR): 2956, 1727, 1636, 1452, 1379, 1348, 1315, 1294, 1254, 1016, 942, 907, 841, 814, 760, 654cm^{-1}.

3.3.3 Synthesis Methods

3.3.3.1 Synthesis of the Catalyst

The preparation of the catalyst from zinc oxide and phthalic anhydride in the presence of an alcohol is explained in detailed in Chapter 2. Its characteristic peaks are also given in the previous chapter.

3.3.3.2 Synthesis of the racemic and optically active polycarbonates from Epichlorohydrin; (Poly (epoxycarbonate) (PEC))

In a typical reaction to obtain the PECH copolymer, 2.4 g catalyst (5% of the monomer by mole percentage) and 6 g of the racemic epichlorohydrin were added into a 100 ml stainless steel reactor which was previously flashed with 99% purity argon gas. Small amount of dichloromethane (2 ml) was used as co-solvent in the system. The schematic representation of the supercritical set-up is given in Figure 1.1. The reaction mixture was then pressurized by carbon dioxide and several different conditions were used. After a definite time, the volatile fractions were removed from the reaction mixture at R.T. under reduced pressure and the residue was obtained [25]. The same synthesis route is followed for to obtain its chiral analogue from optically active epichlorohydrin. The following characterization data is obtained from polymer synthesized from chiral epichlorohydrin; 'H-NMR (CDCl$_3$): δ 3.67 (m, 2H), 4.39 (m, 2H), 4.56 (m, 1H); ^{13}C-NMR (CDCl$_3$): 43,48, 45,28, 66,98, 69.50, 75.50, 154.10; IR (ATR) 3312, 1740, 1603, 1535, 1496, 1446, 1427, 1404, 1282, 1123, 1074, 1039, 885, 851, 831, 746, 711, 702, 655, 613 cm^{-1}; GPC: Mn= 719034, Polydispersity (Mw/Mn)= 1.17.

3.3.3.3 Synthesis of the polycarbonate from Glycidyl Nosylate; (Poly(nosylcarbonate) (PNC))

The corresponding poly (nosylcarbonate) (PNC) was synthesized according to the same procedure with poly (epoxycarbonate) (PEC), as reported above. For this polymer, the following data can be obtained; 'H-NMR (CDCl$_3$): δ 4.06 (dd, 2H), 4.21 (m, 2H), 4.49 (dd, 1H), 7.82 (d, a-CH~)), 8.25 (d, a-CH~)), 8.53 (d, a-CH~)), 8.56 (d, a-CH~)); ^{13}C-NMR (CDCl$_3$): δ 48.94, 72.86, 74.38, 123.52, 131.00, 133.59, 149.06, 151.00, 165.40 ; IR (ATR): 3446, 3091, 1799, 1743, 1607, 1434, 1280, 1073, 954, 881, 812, 754 cm^{-1}; GPC: Mn= 478674, Polydispersity (Mw/Mn)= 1.588.

3.3.3.4 Synthesis of the polycarbonate from (Perfluoropentyl) oximase; (Poly ((Perfluoropentyl) oximase) Carbonate (PPFOC))

The same copolymerization procedure with the PEC is used to obtain this copolymer. The characterization values can be given as the following; 'H-NMR (CDCl$_3$): δ 2.03 (m, 2H), 3.53 (d, 1H), 4.06 (d, 1H), 4.24 (m, 1H); ^{13}C-NMR (CDCl$_3$): δ 43.05, 50.61, 61.04, 73.93, 74.95, 75.41, 112.08, 151.01, 151.82, 154.09; (IR): 3448, 2961, 1798, 1746, 1560, 1491, 1402, 1289, 1241, 1195, 1126, 1080.18, 1033.40, 748.69, 710.88, 653 cm^{-1}; GPC: Two different peaks are observed, for which the Mn values are 83649 and 535732 and the polydispersities are 1.041 and 1.171 respectively.

3.3.3.5 Synthesis of the polycarbonate from glycidyl methacrylate; (Poly (glycidyl methacryl) carbonate (PGMC)

The same copolymerization procedure is utilized for to synthesize the PGMC copolymer. The characterization of the polymer is as follows; 'H-NMR (CDCl$_3$): δ 1.94 (m, 3H), 3.73 (m, 2H), 4.05 (m, 2H), 4.25, (m, 1H), 4.96 (d, 1H), 5.28 (d, 1H); ^{13}C-NMR (CDCl$_3$): δ 17.69, 18.28, 29.55, 30.93, 49.41, 62.58, 65.16, 70.27, 74.70, 126.43, 137.73, 150.85, 153.09, 155.18, 165.08; (IR): 2930, 1742, 1564, 1451, 1399, 1259, 1133, 1006, 978, 917, 813, 746, 706, 652 cm^{-1}; GPC: Mn= 107199, Polydispersity (Mw/Mn)= 2.487.

3.3.3.6 Synthesis of perfluoroalkyl epoxides

Generally, perfluoroalkyl alcohols are not used often in organic synthesis because of their weak acidic character, resulting in poor reactivity towards polyaddition and polycondensation reactions. Consequently, their reaction with epichlorohydrin is rather difficult. To achieve this reaction we utilize different nucleophiles to activate perfluoroalkyl alcohols as is mentioned in the results and discussion section. Again, several different conditions are employed to obtain the synthesis route with the best yield. The optimum conditions for the synthesis of perfluoroalkyl epoxides are found as follow; Tetrabutyl ammonium hydroxide (TBAOH) as a phase transfer agent, epichlorohydrin as an epoxy specious, a reaction time of 3 days and a reaction temperature of 25°C. The attempts to optimize the reaction procedure are given in detailed in the results and discussion section.

'H-NMR (CDCl$_3$): δ 2.35 (m, 2H), 2.66 (dd, 1H), 2.86 (t, 1H), 3.21, (m, 1H), 3.54 (m, 2H), 3.93 (dd, 1H); ^{13}C-NMR (DMSO): δ 12.14, 35.49, 49.31, 60.20, 106.69, 109.19, 110.87; (IR): 2930, 1742, 1564, 1451, 1399, 1259, 1133, 1006, 978, 917, 813, 746, 706, 652 cm^{-1}.

3.3.3.7 Synthesis of polycarbonate from perfluoroalkyl epoxides (Poly (perfluoroalkyl) carbonate (PFAC))

The copolymerization procedure utilized is as the synthetic procedure for PEC. The characteristic peaks of the obtained polymer can be given as in the following;

'H-NMR (CDCl$_3$): δ 2.35 (m, 2H), 3.58 (m, 1H), 3.91m, 2H), 4.32, (m, 1H); ^{13}C-NMR (DMSO): δ10.68, 13.17, 41.38, 42.69, 45.91, 49.38, 50.93,74.22, 74.49, 75,36, 108.29, 110.12, 111.95, 153.08, 155.41, 156.35, 156.45, 159.23; (IR): 2930, 1742, 1564, 1451, 1399, 1259, 1133, 1006, 978, 917, 813, 746, 706, 652 cm^{-1}.

3.4   Results and Discussion

3.4.1   Synthesis and characterization of the racemic and optically active polycarbonates obtained from Epichlorohydrin (PEC)

Both racemic and enantiomerically pure epichlorohydrin are used to elucidate the effect of optical activity on the micro and macro structures of the obtained copolymers. The following scheme illustrates the copolymerization reaction of epichlorohydrin in $scCO_2$ media.
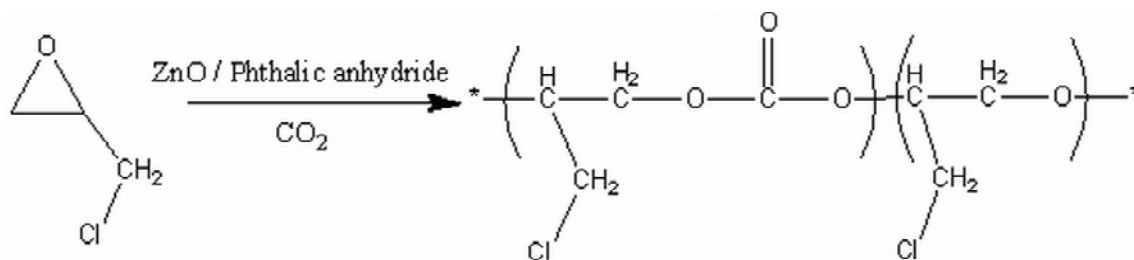
Scheme 3.3 The representation of the copolymerization reaction of epichlorohydrin in $scCO_2$ media.
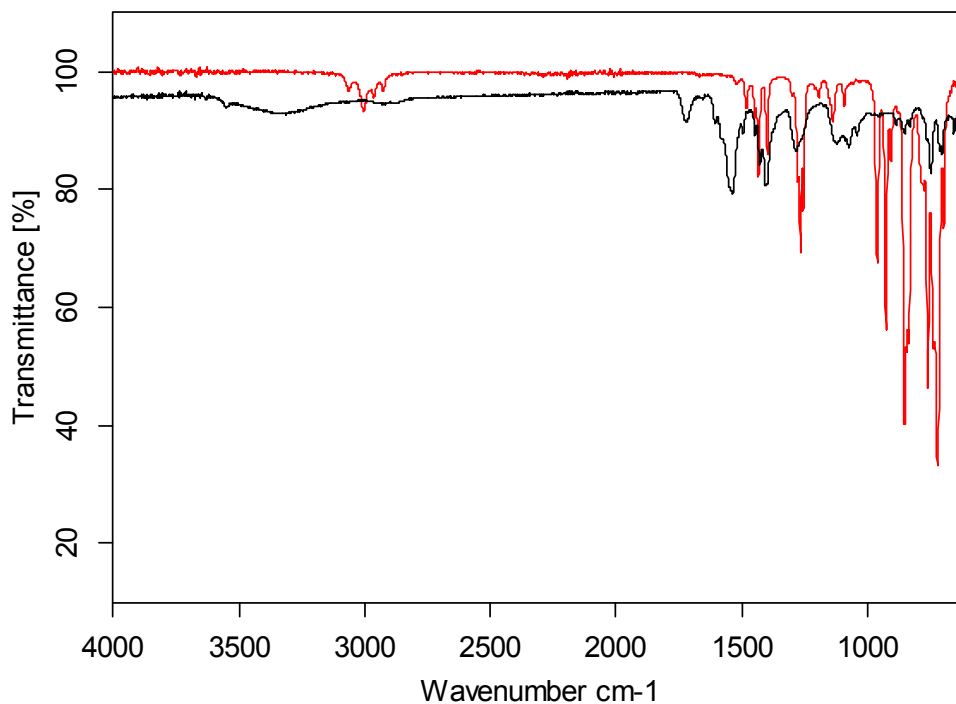
Figure 3.5 The FTIR spectrum of the synthesized copolymer from epichlorohydrin.

Figure 3.5 compares the spectrum data obtained for the epichlorohydrin and it's copolymer with CO_2 and is represented as red and black in color respectively. In the FTIR spectra the three membered ring compounds of epoxides usually give three bands, and for our epoxy ring, the following values are observed; a medium intensity symmetric stretching vibration at 1266 cm^{-1}, an asymmetric vibration at 851 cm^{-1}, and a strong absorption at 720 cm^{-1}. Considering the absence of the three membered ring compounds of the epichlorohydrin and appearance of the absorption band attributable to linear polycarbonate linkage (1740cm^{-1}) in the final product, these results confirm that copolymerization of carbon dioxide and epichlorohydrin has been achieved.

A selected region for the ^{1}H-NMR of several copolymers obtained from different polymerization trials are illustrated in Figure 3.6. The curve at 1.6 ppm occurs when there is water in the media and it is denoted by the star sign on it. The polymerization conversions are calculated depending on the comparison of the unreacted epoxide's methine peak and the methyl peak of the catalyst in ^{1}H-NMR. Since molar feed ratio of catalyst to monomer is 0.2 (N_{cat} / N_{mon} = 1/5) for all of the polymerization trials, one can formulate the polymerization conversion rule as follows;

$$(5 \times I_C/3) = I_{MT} \text{ (Total monomer intensity)}$$

$$100 \times [(I_{MT} - I_{UM}) / (I_{MT})] = \% \text{ Reaction Conversion}$$

I_{MT}, I_{UM} and I_C represent the total monomer intensity, unreacted monomer intensity and catalyst intensity in ^{1}H-NMR respectively.
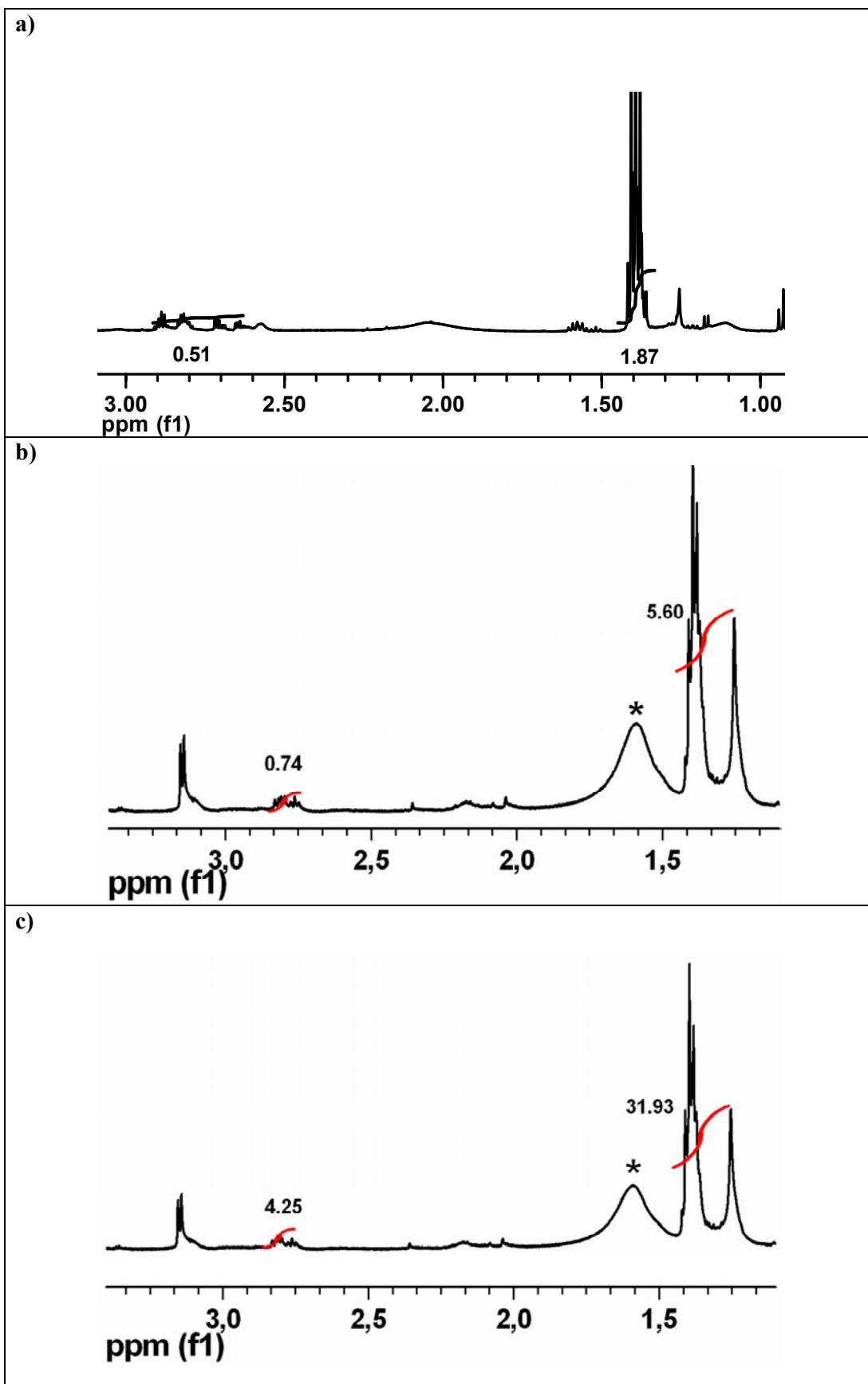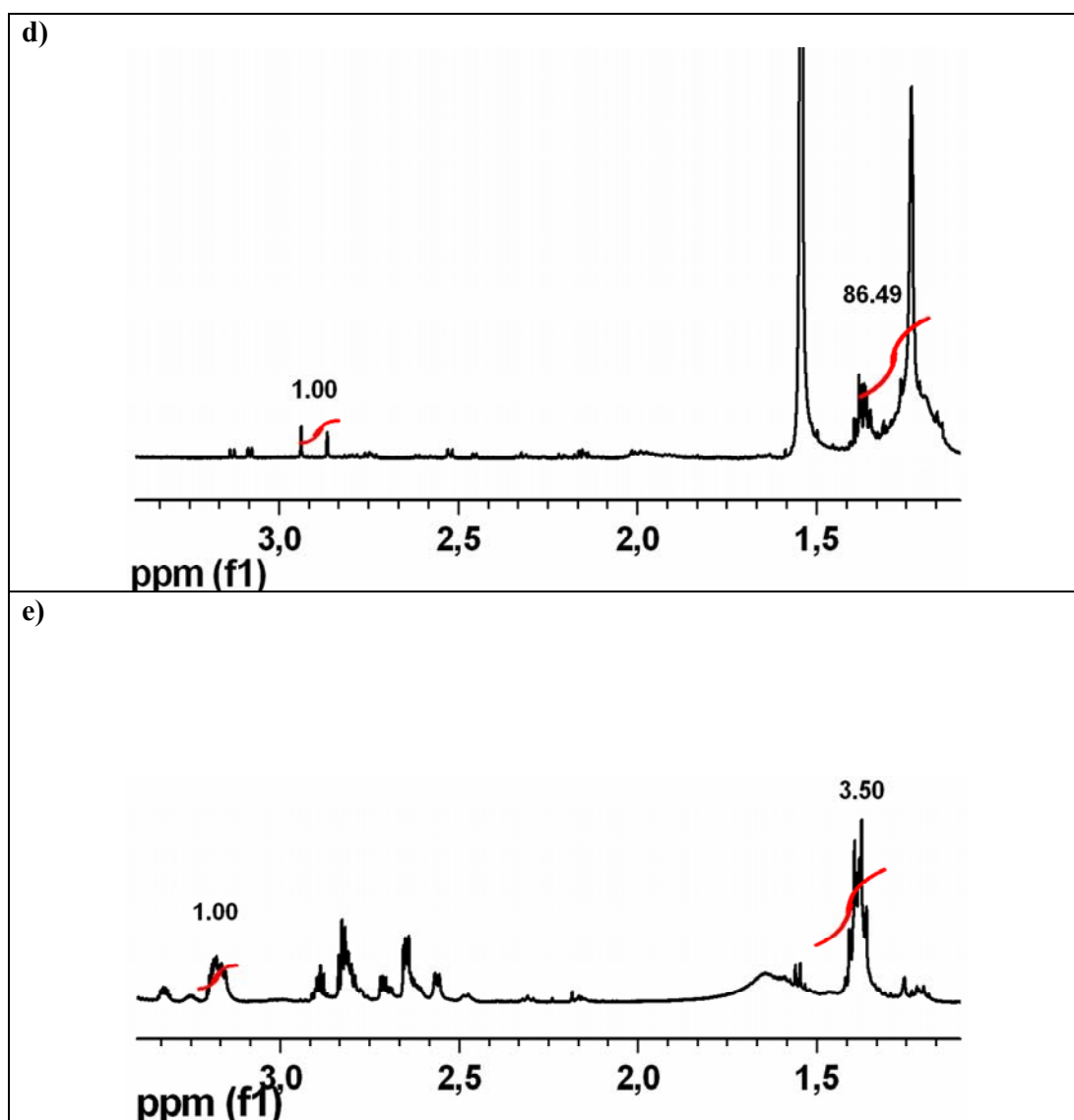
Figure 3.6 Comparison of the polymerization conversion corresponding to different polymerization conditions. Spectra **(a), (b), (c), (d)** represent polymers produced from racemic monomer with %91.82, %96.03, and % 96.1, % 99.93 polymerization conversions respectively. Spectrum **(e)** represents polymer produced from chiral monomer with a polymerization conversion of % 83.

In order to characterize the obtained polymer, the expanded form of spectrum in Figure 3.6.d is given below. Due to the existence of carbonate group in the polymer, we observe the shift of the ring's methine and methylene peak more to the spacer methylene peak. The sharp peak at 3.67 and 4.39 ppm are due to the methylene units in the polymer. Additionally the peak at about 4.56 ppm accounts for the methine hydrogen in the backbone. Other peaks correspond to the catalyst hydrogens.
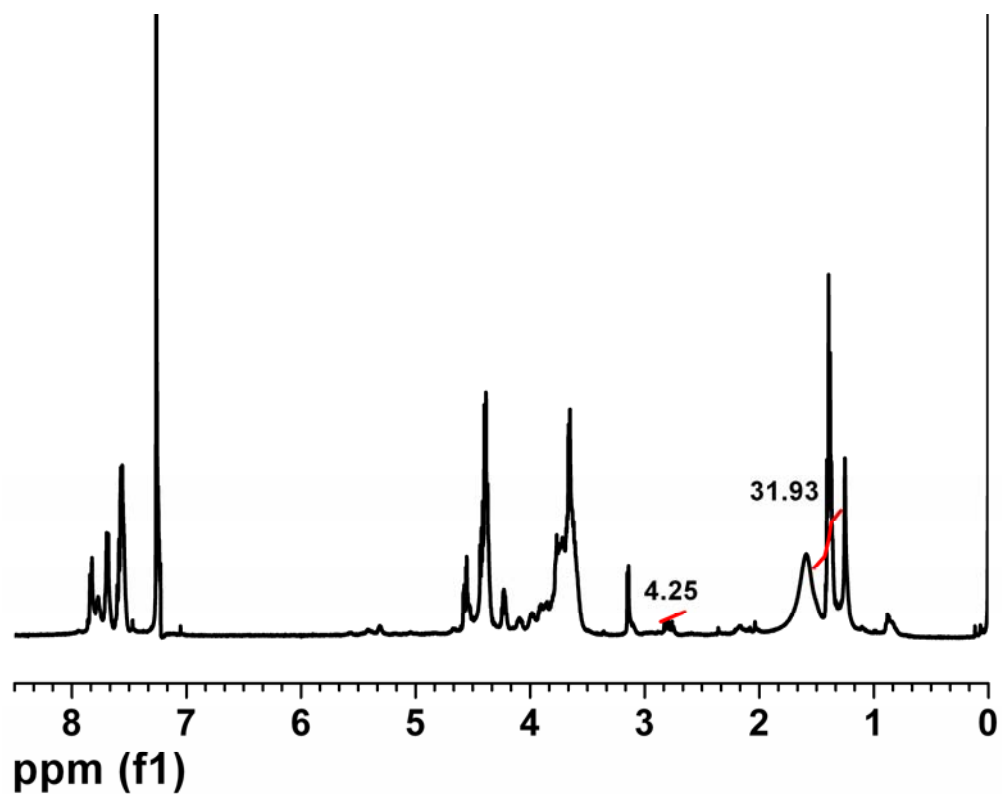
Figure 3.7 The expanded ^{1}H-NMR spectrum of the copolymer obtained from epichlorohydrin

Table 3.1 Polymerization conversions of Epichlorohydrin to their corresponding reaction conditions

Polymer	Polymerization Conditions	Polymerization Conversions	Mn Value	Polydispersity
P-1 racemic	T=90°C, P=2000 psig, t = 5 h	%91.82	_	_
P-2 racemic	T=90°C, P= 2000 psig, t = 20 h,	%96.03	12800	1.08
P-3 racemic	T=90°C, P= 3000 psig, t = 20 h	%96.1	_	_
P-4 racemic	T=90°C, P= 3000 psig, t = 24 h	%99.93	719034	1.171
P-5 chiral	T=90°C, P= 3000 psig, t = 24 h	% 83	_	_

To obtain the copolymer of racemic epichlorohydrin and CO_2 we followed the well-documented procedure [25]. In order to understand the effect of pressure and the reaction time, several copolymerization trials have been conducted. In all of the polymerization trials the reaction temperature is not altered since the minimum temperature needed to open the epoxy ring is reported as 90°C in the literature and further heating of the system may not only cause back biting of the aliphatic carbonate and form a cyclic polycarbonate, but may also decompose the obtained polymer [26]. For all of the trials, the molar feed ratio of catalyst to monomer is taken as 0.2 as stated in the literature [25]. Depending on the above table, to be used with the epichlorohydrin, no pronounced increase in the polymerization conversion is noted as the pressure of the system elevated. On the other hand, longer reaction times give higher polymerization conversions. However, much longer reaction times are excluded since cyclic polycarbonate is observed as a byproduct.

Gel-permeation chromatography (GPC, versus polystyrene standards) revealed high Mn values and a low molecular weight distributions (MWD) as illustrated in the table. This narrow polydispersity, high Mn value and percent conversion are indicative of a well-defined polymer structure and is a subject of fundamental as well as practical importance [27].

Similar to the procedure in the literature, two different epichlorohydrin have been employed to copolimerize with a zinc-phythalate catalyst to clarify the effect of optical activity to the structures of the resultant copolymers .The two different samples of PEC were those derived from *rac*-PE and 99% *S*-PE.

The following spectra show the carbonyl region of the ^{13}C-NMR of the polymers produced from copolymerization of CO_2 with racemic epichlorohydrin and 99% S-epichlorohydrin respectively. The splitting of the carbonate peaks were investigated by high resolution ^{13}C-NMR spectroscopy. The differences in the chemical shifts in the copolymers both obtained from racemic and optically active epichlorohydrin, have been ascribed to the head-to-head (HH), head-to-tail (HT) and tail-to-tail (TT) groups as reported in the literature. The natural abundance ^{13}C-NMR spectrum of the copolymer from racemic epichlorohydrin shows the ratio of the TT: HT: HH junctions, in the order of 36: 50: 14. Thus the preference is mostly in the favor of HT junctions for racemic

PEC. The simplest of the spectra shown in the figure arises from the copolymerization of *S*-PO and CO_2. For racemic epichlorohydrin different carbonate carbon signals refering to all possible juctions is obtained whereas, the one for S-epichlorohydrin signals mainly prefer to HT formation are achieved. The ratio of the TT: HT: HH junctions for the polymer obtained from S-epichlorohydrin, is in the order of 3:93:4. This much regularity in the microstructure is coherent since an enantiomerically pure monomer is used.

As a consequence of the obtained data The homopolymerization of PO with similar zinc catalyst (in the absence of CO_2) gives regioregular PPO (HT) as stated in the literature [93]. In the case of PEC formation, a transition state for ring-opening is anticipated involving backside attack on a zinc bound epoxy ring by a neighboring alkoxide group which in turn is bound to a zinc(II) center (Scheme 3.4).
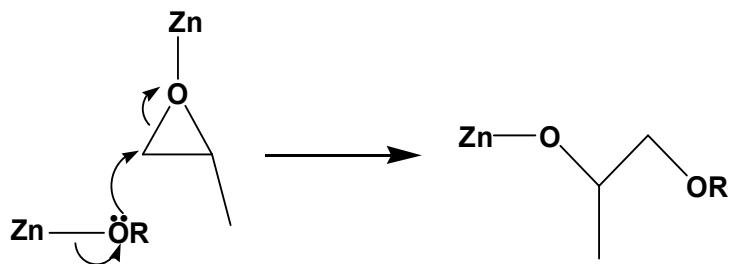
Scheme 3.4 The proposed ring opening mechanism of the epoxy

Several observations support this proposal in the literature: First, when the copolymer produced from *cis* cyclohexene oxide and CO2 was hydrolyzed, the resulting 1,2-cyclohexanediol was found to have the *trans* configuration.[21]. The inversion of one of the C-O bonds in the epoxide indicates that the ring-opening results from backside attack. Second, studies with optically active epoxides established that the carbon atom which is favored for nucleophilic attack showed an inversion of configuration, again suggesting a nucleophilic mechanism.[22,23]. In this way the head to tail PPC is formed, and in coordinate catalysis this has been seen to favor the formation of isotactic junctions when the epichlorohydrin monomer is racemic [24].

116

In the case of ring-opening of PO in PPC formation, a carbonate oxygen is the nucleophile. This is less sterically demanding and apparently less discriminating in its attack on a PO carbon. Similar to the polymer produced from propylene oxide, the head to tail junction is favored and natural abundance of the isotactic triads are much more than the other configurations as illustrated in Figure 3.8 (b). From these results, it has been understood that our catalyst system works with the same principle of previously discussed PO copolymerization mechanism.[104]. The same transition state with a backside attack is again expected for our copolymerization system. Similarly, we can rationalize the mechanism of copolymerization of our catalyst as in follows.
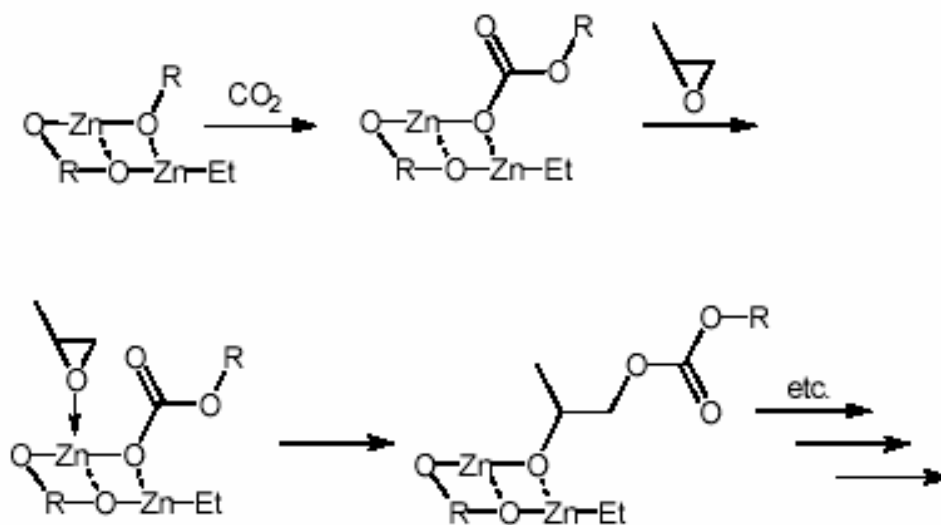
Scheme 3.5 The proposed mechanism of the ring opening copolymerization in correspondence with zinc oxide catalyst system.

117

(a)

TT　　　　　　　HT　　　　　HH

154.60　154.50　154.40　154.30　154.20　154.10　154.00　153.90　153.80
ppm (t1)

(b)

HT

TT

HH

154.67　　154.50　　154.33　　154.17　　154.00　　153.83　　153.67
ppm (t1)
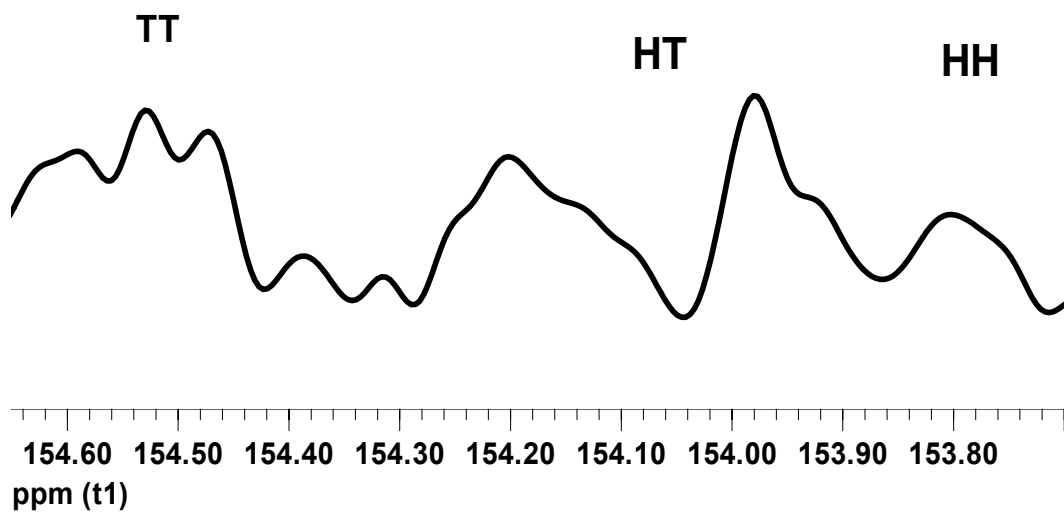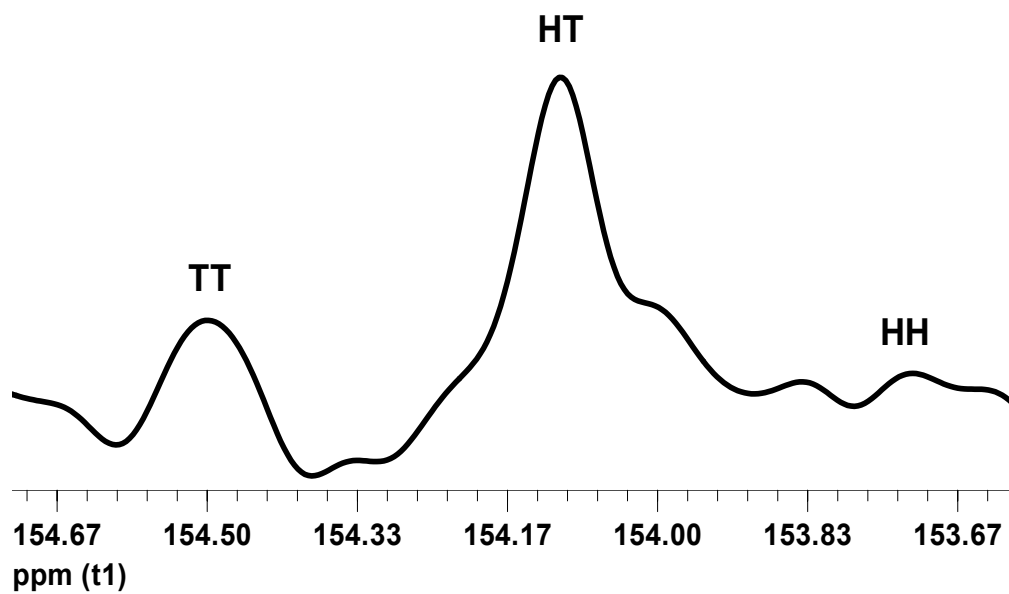
Figure 3.8   The close-up ^{13}C-NMR spectra of the copolymers obtained from **(a)** Racemic epichlorohydrin **(b)** S-Epichlorohydrin in the carbonyl region

Being aware of the direct relation between the tacticity and side group orientation, to observe the influence of the side group, we close up to the carbon region of the side group as is given in Figure.3.9. The assignments of the carbon signals derived from epichlorohydrin's methine and methylene are complementary to those of the carbonate carbon. However, the methylene group assignment is more difficult due to partial overlap of the CH_2 groups in backbone and spacer with one another and with the first CH_2 group of the alkoxy tail. Consequently, we concentrate on the methine region of the polymer. There are there main signals refering to differnt diads;

i) The isotactic triads (ii) with both neighbors having the same configuration,

ii) The syndiotactic triads (ss) with both neighbors having the opposite configuration, iii) The hetero(iso- and syndio-)tactic triads (is+si) with two oppositely configured neighbors.

Three different configurations for the racemic PE are obtained and assigned as did for PPO in the report of Antelman et al.[12] .On the other hand, in the spectrum for S-PE only one signal is obtained representing a single chiral environment [28].

(a)

(b)

ii

H-T region

76.00
ppm (t1)

75.50

75.00

74.50
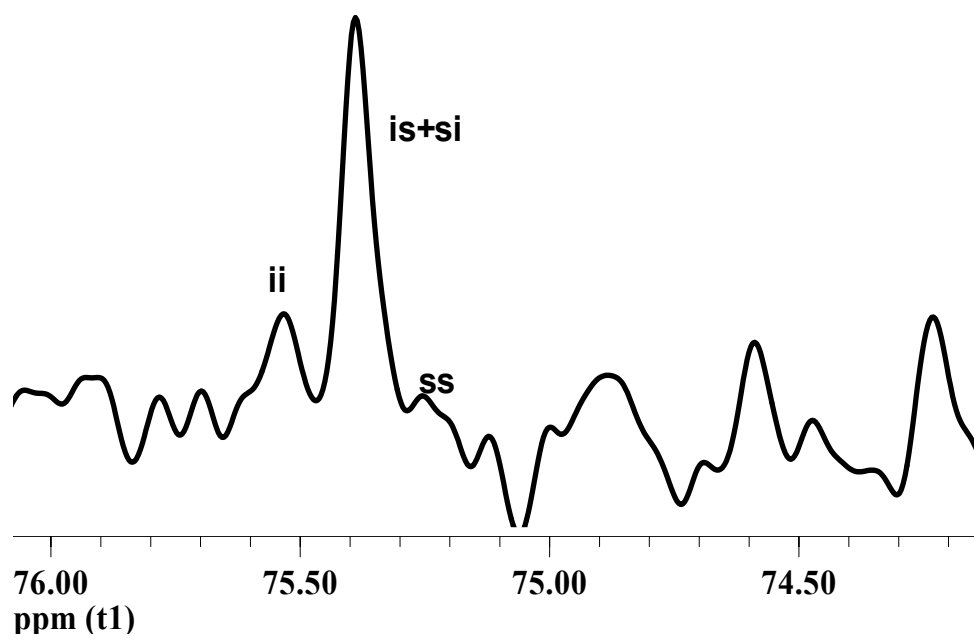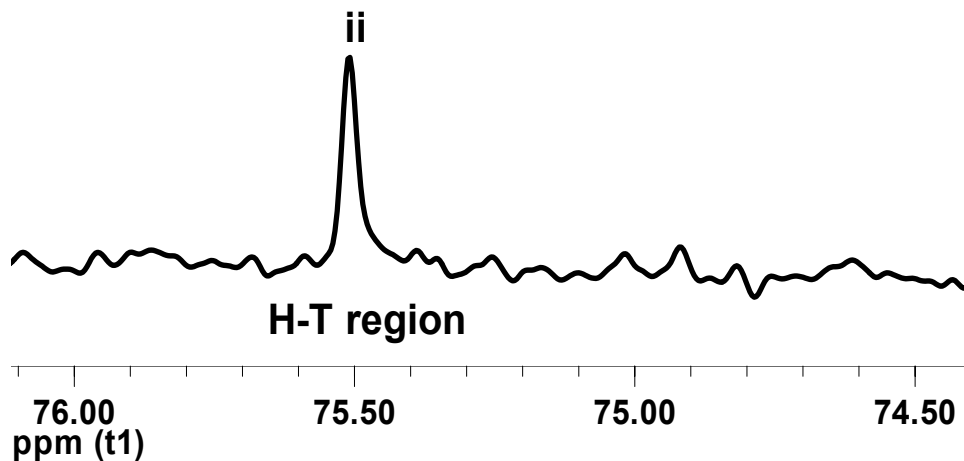
Figure 3.9 The close-up ^{13}C-NMR spectra of the copolymers obtained from **(a)** Racemic epichlorohydrin **(b)** S-Epichlorohydrin in the methine carbon region
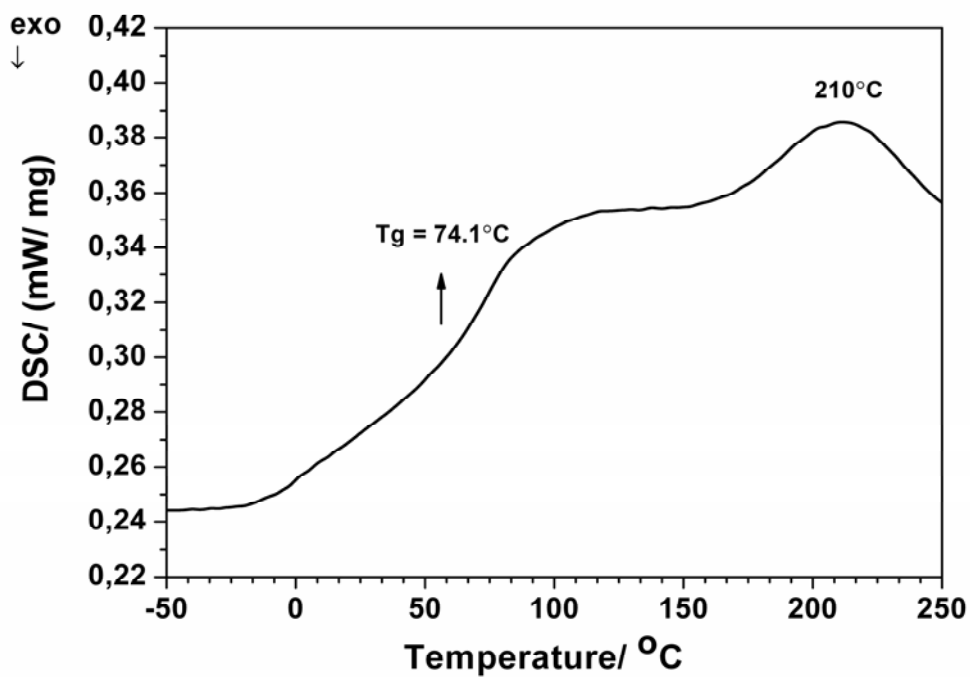
Figure 3.10 The DSC thermogram of the copolymer from epichlorohydrin in the second heating cycle with a heating rate of 10°C/min.

121

To explain the thermal behavior of the copolymer, the DSC analysis has been carried out. Depending on the DSC analysis of the copolymer a Tg (glass transition temperature) value of 74.1°C and a Tm (melting temperature) of 210°C is detected. The Tm value for the polycarbonate homopolymer on the other hand, is reported as 220°C [130]. The Tg value of our poly (ether-carbonate) copolymer is in this temperature range as it is supposed to be.

3.4.2 Synthesis and Characterization of the Polycarbonate obtained from Nosylate (PNC)

To conclude on the effect of optical activity another copolymerization reaction is conducted with enantiomerically pure glycidyl nosylate. In the following scheme the copolymerization of (S)-glycidyl nosylate in $scCO_2$ media is illustrated.
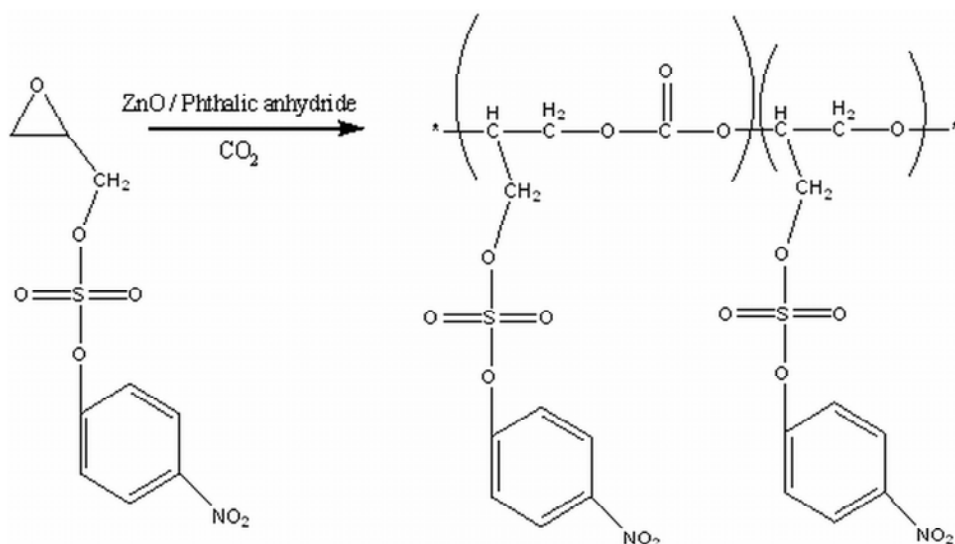
Scheme 3.6 The representation of the copolymerization reaction of (S)-glycidyl nosylate in $scCO_2$ media.
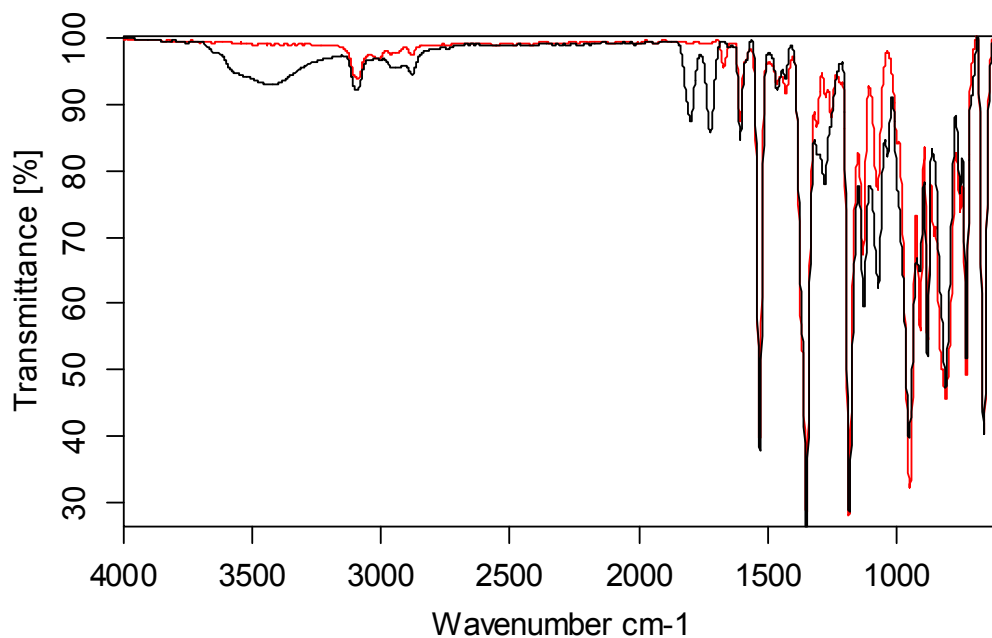
Figure 3.11 The FTIR spectrum of the synthesized copolymer from glycidyl nosylate.

The illustration of the absorption data of both glycidyl nosylate and its copolymer with CO_2 is given in the figure above. The identification of the cyclic and aliphatic polycarbonate is made with the medium intensity absorptions occur at 1799 and 1743 cm^{-1} respectively. The disappearance of the mentioned vibrations of epoxy ring, also support the idea of the polymer formation. The intense asymmetric C-O-C stretching vibration is also observed in the spectrum range of open-chain ethers (at 1280 cm^{-1}). The stretch which is to the downfield of 3000 cm^{-1} and the absorptions occurring in pairs at 1607 cm^{-1} and 1434 cm^{-1} on the other hand are indicative of the aromatic rings.
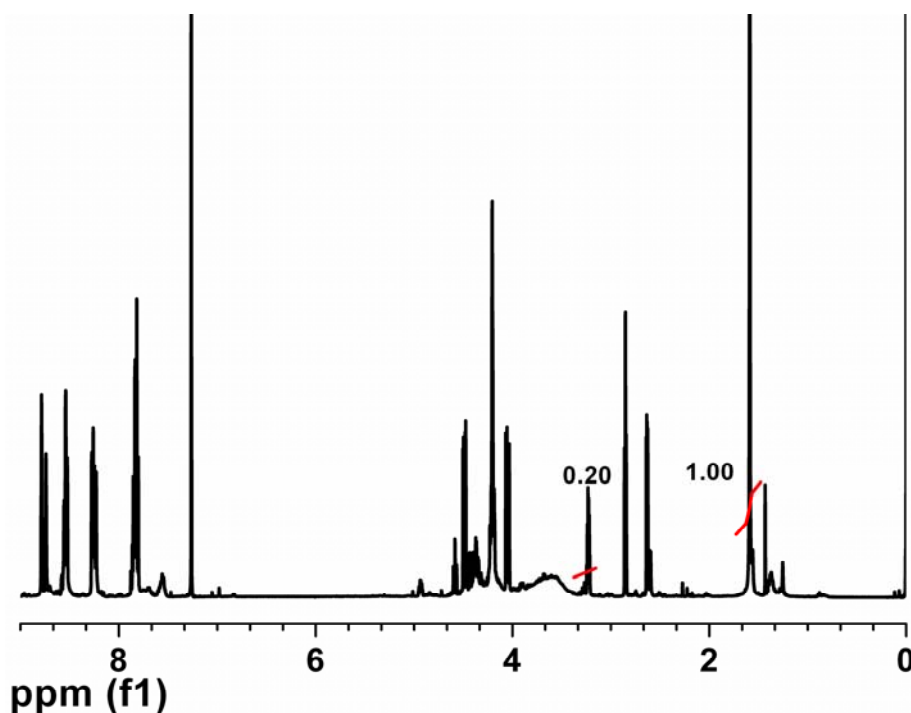
Figure 3.12 The 1H-NMR spectrum of the synthesized copolymer from glycidyl nosylate.

In the ^{1}H-NMR spectrum above, the shift to lower fields is observed for the nosylate ring protons with the strong deshielding effect of the carbonate group in comparison with the monomeric epoxy group. The methylene and the methine protons are shifted to 4.21 ppm and 4.49 ppm, respectively. Additionally, the methylene units in the spacer groups give a broad band at 4.06 ppm. The polymerization conversions are calculated depending on the comparison of the unreacted nosylate's methine peak and the methyl peak of the catalyst with the same rule as in epichlorohydrin in ^{1}H-NMR. The integration intensities are illustrated on Figure 3.12.

Table 3.2 The polymerization conversion of (S)- glycidyl nosylate to its corresponding reaction conditions

Polymer	Polymerization Conditions	Polymerization Conversions	Mn Value	Polydispersity
P-1 chiral	T=90°C, P=3500 psig, t = 24 h	%91.82	478674	1.588

(a)

124
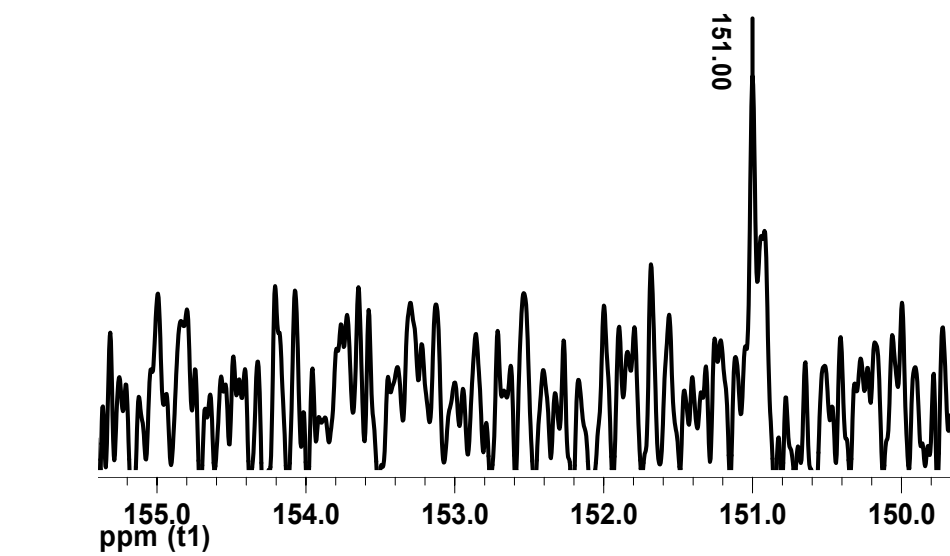
(b)
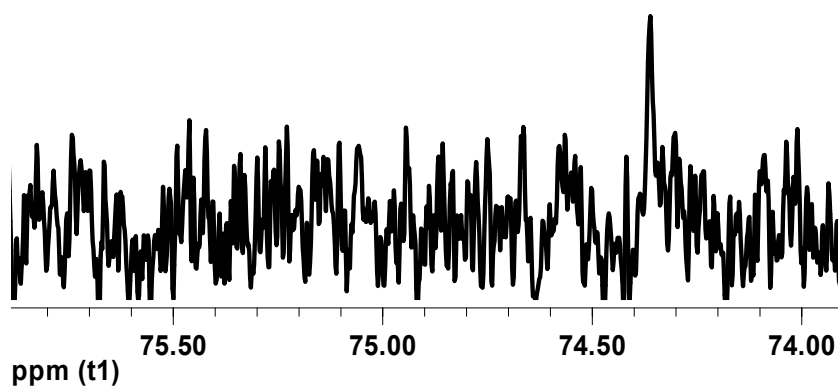
Figure 3.13 The close-up ¹³C-NMR spectra of the copolymer obtained from (S)-Glycidyl Nosylate in the region of **(a)** carbonyl **(b)** methine carbons

Above, the close –up to the most interesting parts of the ¹³C-NMR spectrum (in CDCl₃) of the polymer produced from 98% S-Glycidyl Nosylate are given. In agreement with the carbonyl carbon, the methine carbon gives also a single signal which represents a single chiral environment. Since we use an enantiomerically pure monomer we can rationalize this tacticity as isotactic depending on the literature report [29] and the copolymerization mechanism we have proposed.

3.4.3 Synthesis and Characterization of the Polycarbonate obtained from Glycidyl methacrylate (PGMC)

Several copolymerization trials with glycidyl methacrylate have been conducted to provide evidence for the conclusion. In the following scheme the copolymerization of glycidyl methacrylate in $scCO_2$ media is illustrated.
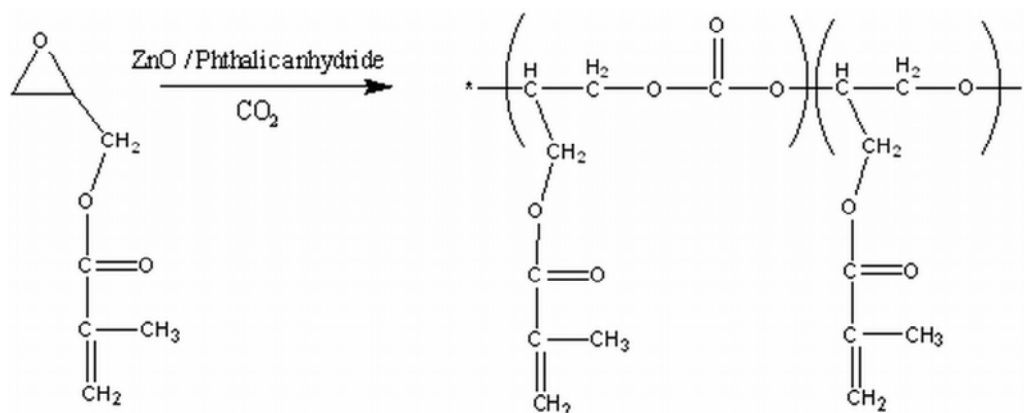
Scheme 3.7 The representation of the copolymerization reaction of glycidyl methacrylate in $scCO_2$ media.
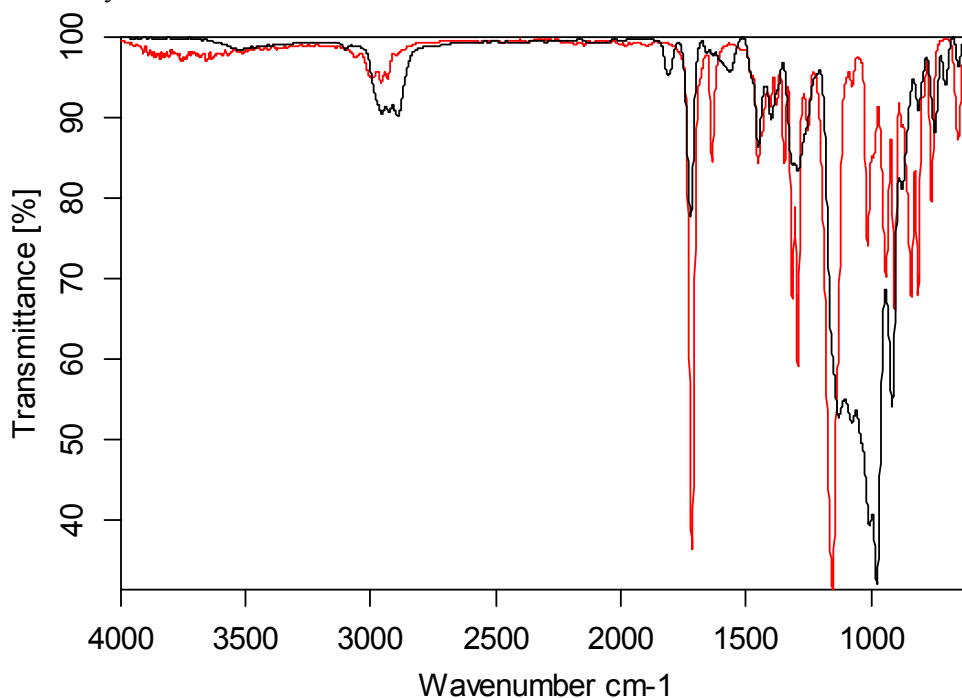
Figure 3.14 The FTIR spectrum of the synthesized copolymer from glycidyl methacrylate
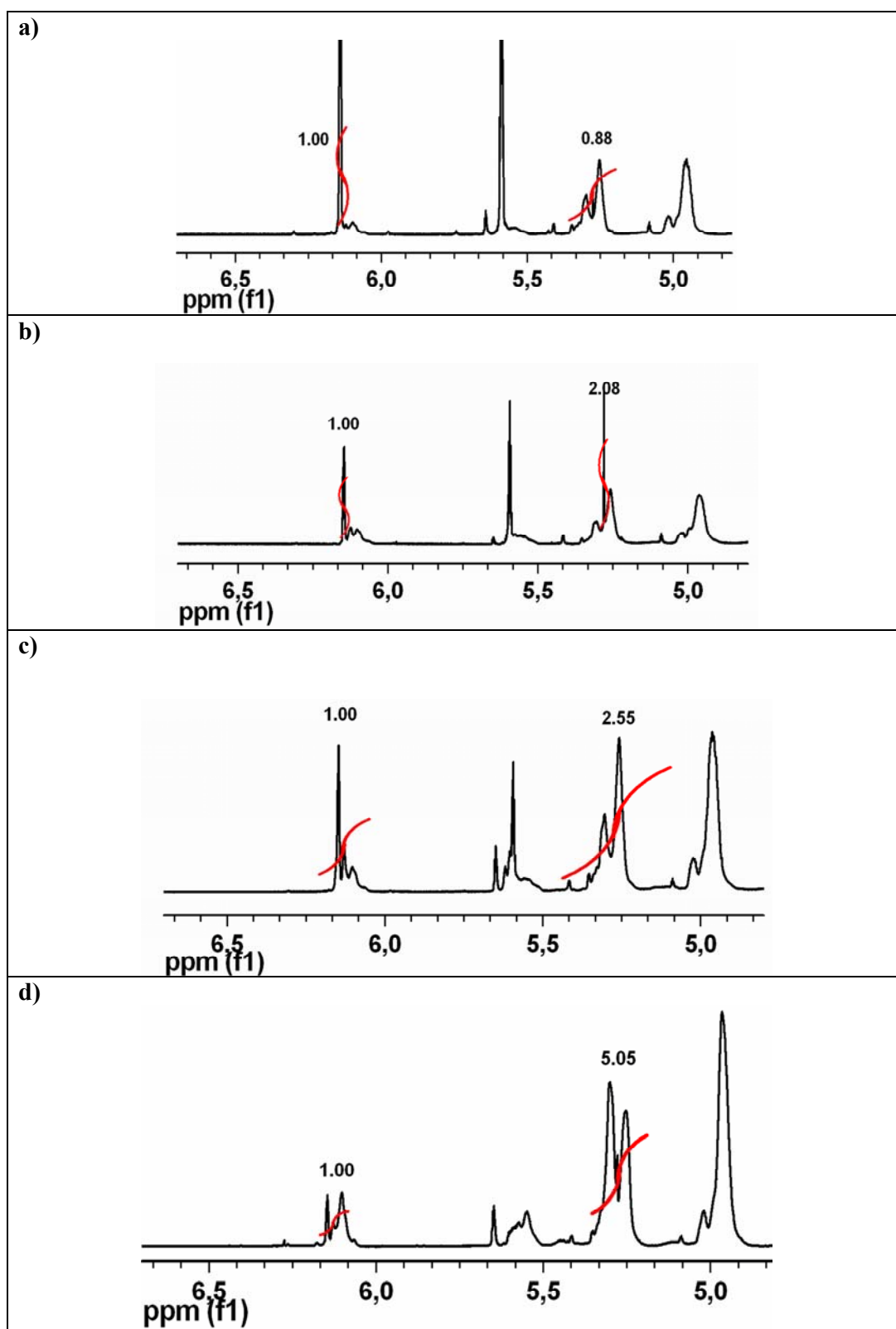
Figure 3.15 Comparison of the polymerization conversion corresponding to different polymerization conditions. Spectrums **a), b), c),** and **d)** represent %46.81, %67.53, %71.83, and %83.47polymerization conversions respectively.
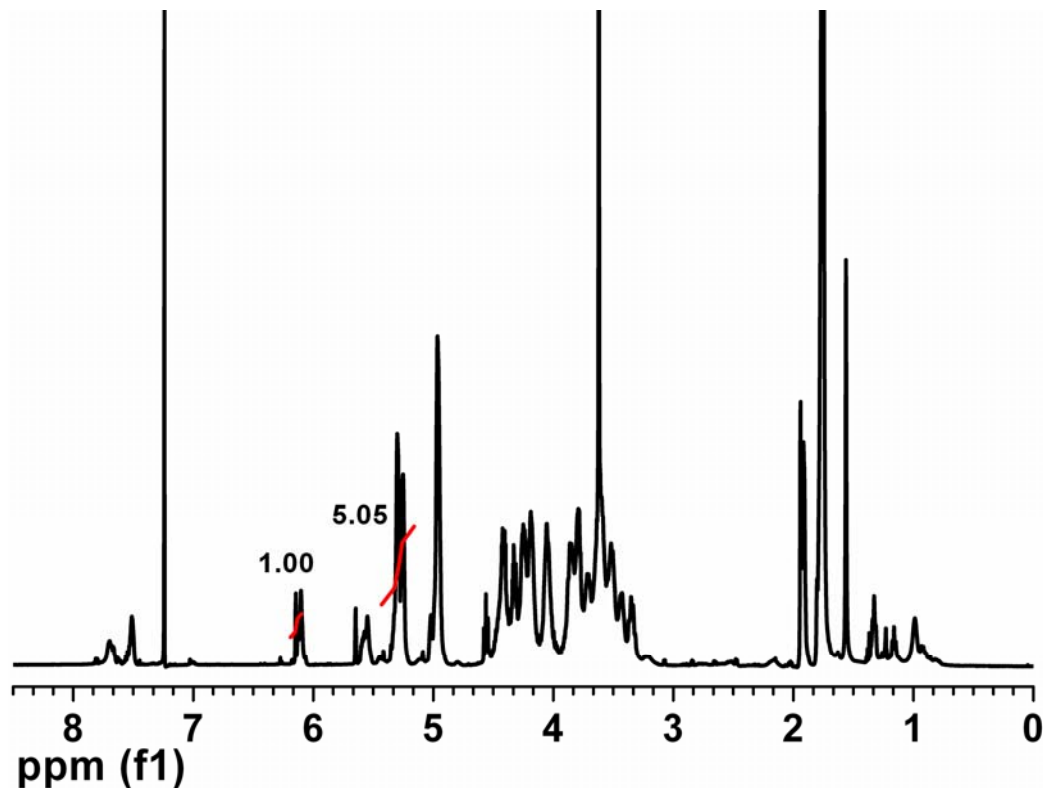
Figure 3.16 The expanded ^{1}H-NMR spectrum of the copolymer obtained from glycidyl methacrylate.

In order to characterize the copolymer completely, an expanded ^{1}H-NMR of Figure 3.15d is given above. Due to the strong deshielding effect of the carbonate group in the polymer, we observe the shift of the ring's methine and methylene peak more to the spacer methylene peak. The broad band at the range of 3.3 to 4.8 ppm represents the methylene and methine units in the polymer. Additionally the peak at 1.94 is due to the methyl unit of the polymer. Peaks at 4.96 and 5.28 ppm can be assigned to the vinyl hydrogens. The intense peak at 3.6 ppm on the other hand, corresponds to the fluorosurfactant. The polymerization conversions are calculated depending on the comparison of the polymer's unreacted and reacted vinyl methine peak in ^{1}H-NMR. The integration intensities are illustrated on Figure and the polymerization conversion rule is as follows;

$$(I_M + I_{UM}) = I_{MT} \text{ (Total monomer intensity)}$$

$$100 \times [I_M / I_{MT}] = \% \text{ Reaction Conversion}$$

128

I_{MT}, I_{UM} represent the total monomer intensity, unreacted monomer intensity and catalyst intensity in ^{1}H-NMR respectively.

Table 3.3 Polymerization conversions glycidyl methacrylate to their corresponding reaction conditions

| Polymer	Polymerization Conditions	Polymerization Conversions	Mn Value	Polydispersity
P-1 racemic	T=90°C, P=2000 psig, t = 5 h	%46.81	_	_
P-2 racemic	T=90°C, P= 2000 psig, t = 20 h,	%67.53	_	_
P-3 racemic	T=90°C, P= 3000 psig, t = 22 h	%71.83	_	_
P-4 racemic	T=90°C, P= 3000 psig, t = 27 h, fluorosurfactant	%83.47	104153	2.588
P-5 racemic	T=90°C, P= 3000 psig, t = 27 h	%86.68	107199	2.487

Concerning the information drawn from Table 3.3, as the reaction time increases polymerization conversion increases, and hence this copolymerization reaction displays a similar behavior with the one for epichlorohydrin. Again much longer reaction times above 60 hours are excluded with the same reason previously mentioned. On the other hand, in comparison with epichlorohydrin, the time needed to reach a 99% conversion for glycidyl methacrylate is longer. In addition, to elucidate the effect of surfactant, a separate polymerization trial has been conducted. Accordingly, not a profound improvement on the conversion is observed. Also in such fundamental properties of a polymer like molecular and polydispersity a slight drop off is noted.

(a)
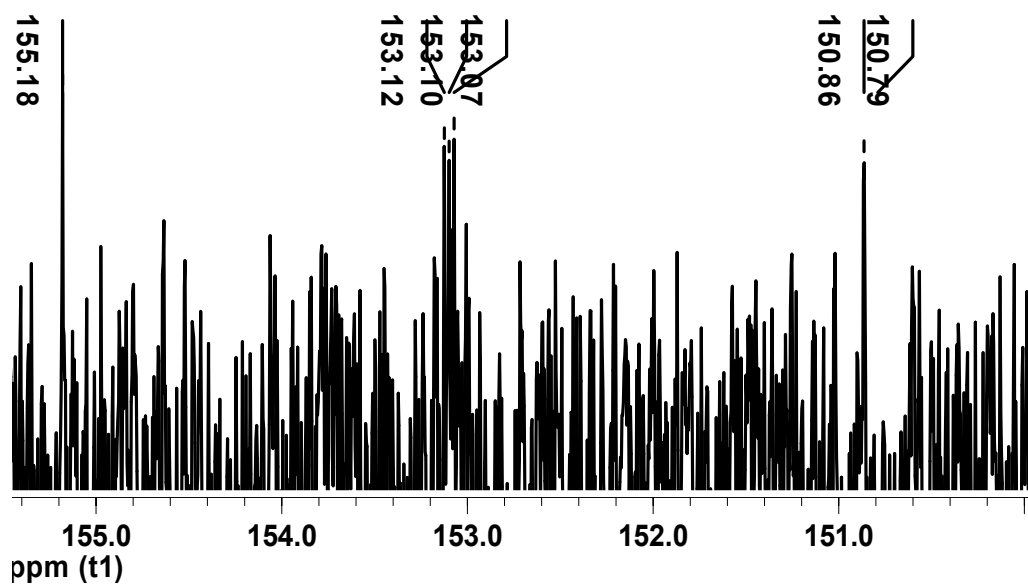
(b)
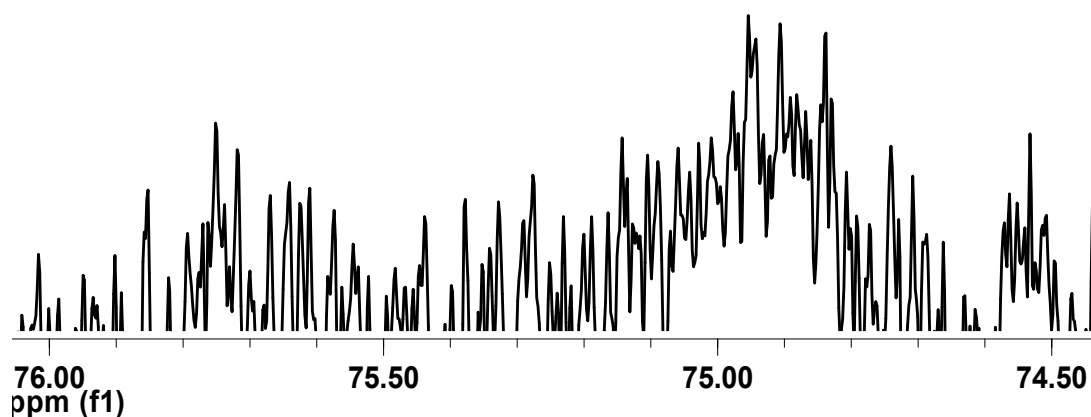
Figure 3.17 The close-up ¹³C-NMR spectra of the copolymer obtained from 1H, 1H-(per-fluoropenthyl) oximase in the region of **(a)** carbonyl **(b)** methine carbons

In Figure 3.17 the carbonyl and the methine carbon region are expanded. The same analogy is established between the spectrum of previously reported polypropylene oxide (PPO) and this spectrum and we attribute the most downfield shift as TT, the

most upfield shift to HH and the one in between to HT signal. The ratio of the TT: HT: HH junctions for the polymer obtained from racemic glycidyl methacrylate, is on the order of 6: 87: 7. The HT junctions are favored over their statistical occurrence and this indicates that the ring opening of glycidyl methacrylate occurs with a regiospecifity in the formation of poly (glycidyl methacrylate) carbonate (PGMC).

In contrast to the stereoregular poly(epichlorohydrin) carbonate (PEC) and poly(nosylate) carbonate (PNC) synthesized from enantiomerically pure monomers, the racemic glycidyl methacrylate give a highly stereoirregular polymer as shown Figure 3.17 (b). The irregularity in the structure indicates that the ring opening of glycidyl methacrylate occurs without a stereospecifity in the formation of PGM. As many signals in the methine region are observed, the tacticity of the polymer is concluded as heterotactic. The irregularity in tacticity is attributed to the inefficient sequencing due to the steric hinderance of the side group.
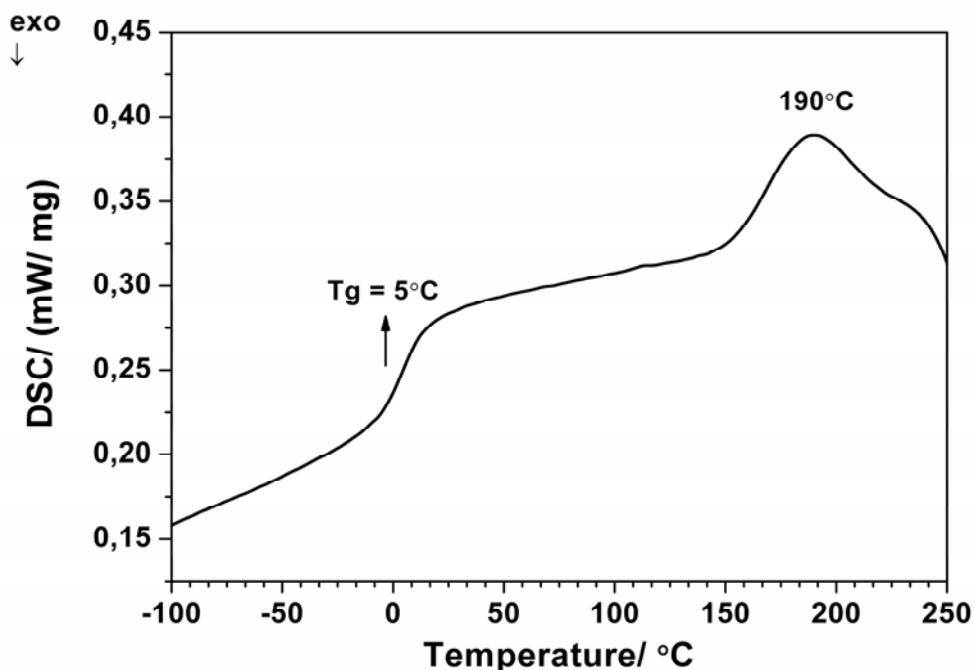
Figure 3.18 The DSC thermogram of the copolymer from glycidyl methacrylate in the second heating cycle with a heating rate of 10°C/min.

The increase in the tail length or incorporation of more stericly hindered groups in these side chain polymers shows its effect as a drop off in the Tg value. In comparison to

its analogue from epichlorohydrin, composed of a bigger side group, the copolymer from glycidyl methacrylate gives lower Tg value at 5°C. Whereas, not much decrease in the Tm value is observed. In consequence of these, the copolymer from glycidyl methacrylate offers an enlarged processing temperature range in comparison to its analogue synthesized from epichlorohydrin and potentially provides different applications.

3.4.4   The Design of Polycarbonates from Fluorinated Epoxides

The use of organofluorine compounds has generated much research effort. The replacement of one or several hydrogen atoms by fluorine confers to the resulting material unusual and peculiar properties which allow their use as good precursors with many applications: surface coating, fire retardants, biomedicine and much research has contributed to increase the knowledge of these compounds within the field of molecular organized systems.

Moreover, fluorine is used in organic materials in order to give them particular properties as compared to their hydrocarbon homologues. On introduction of fluorine atoms into organic compounds molecules, as a rule, their photo-, chemo- and thermo-stability are increased, and therefore the synthesis of fluorinated materials and the study their properties are of interest in terms of the science and practice [131, 132].

Concerning the above facts, this part of the research has been carried out on the synthesis of polyfluorinated compounds. Again, in this part the micro and macro structures of the obtained fluoro-copolymers will be dicussed.

3.4.4.1   Synthesis and Characterization of Polycarbonates Obtained from (Perfluoropentyl) oximase (PPFOC)

In the following scheme the copolymerization of (perfluoropentyl) oximase in scCO$_2$ media is shown.
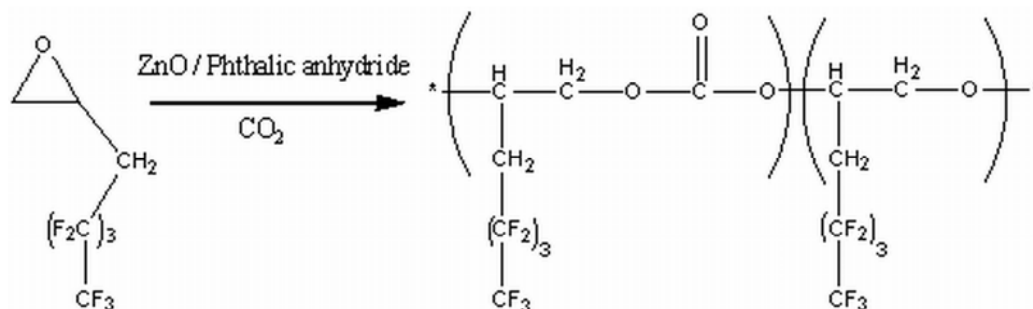
Scheme 3.8 The representation of the copolymerization reaction of 1H, 1H-(perfluoropenthyl) oximase in scCO$_2$ media.
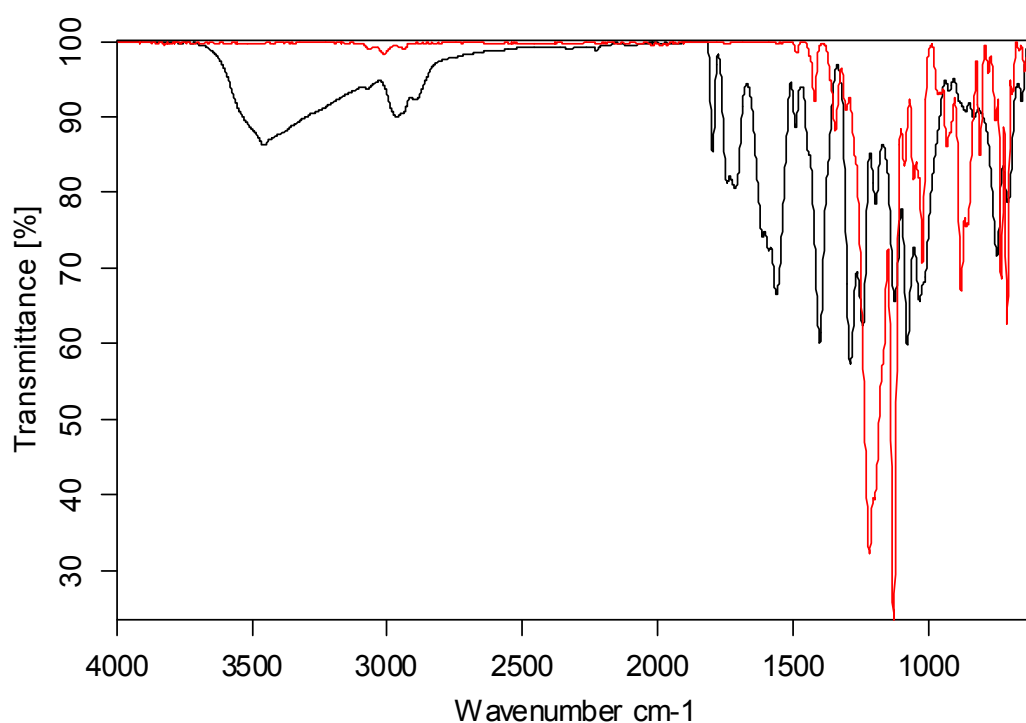
Figure 3.19 The FTIR spectrum of the synthesized copolymer from (perfluoropenthyl) oximase

Figure 3.19 illustrates the comparison of IR spectra of the obtained polymer with the raw material (Perfluoropentyl) oximase Carbonate. The red curve represents the monomer whereas; the black one represents the copolymer. Appearance of the carboxylate signals at 1798.23 and 1746.509 cm^{-1}, which can be attributed to the cyclic carbonate and aliphatic carbonate respectively, indicate the conversion to polycarbonate. With the rational that fluorinated materials have better miscibility with scCO$_2$ media than epoxy rings, there is no need to apply hard reaction conditions. It is already affirmed in the literature that, longer reaction times tend to decrease the weight

of the synthesized polymer. This decrease in the molecular weight, is due to the relatively slow initiation and rapid propagation reaction, while the cyclic carbonate is formed in a simultaneous side reaction and by depolymerization of the already formed polymers [32]. So, for not to witness a cyclic carbonate formation as a byproduct, the reaction time for this monomer should be less than the ones given in Table 3.3.

The consumption of the epoxy ring in the ring opening reaction is evidenced by the disappearance of the ring signals that are downfield of 3000 cm^{-1} and the three membered ring compounds of the epoxide in the range of 1300 and 700 cm^{-1}. Moreover, the increased intensity of the aliphatic CH- and CH$_2$- stretching at frequencies of 2900 indicate the formation of an aliphatic polycarbonate. The identification of the fluoro content is made by strong absorptions at 1100 and 1200 cm^{-1} for both of the materials.
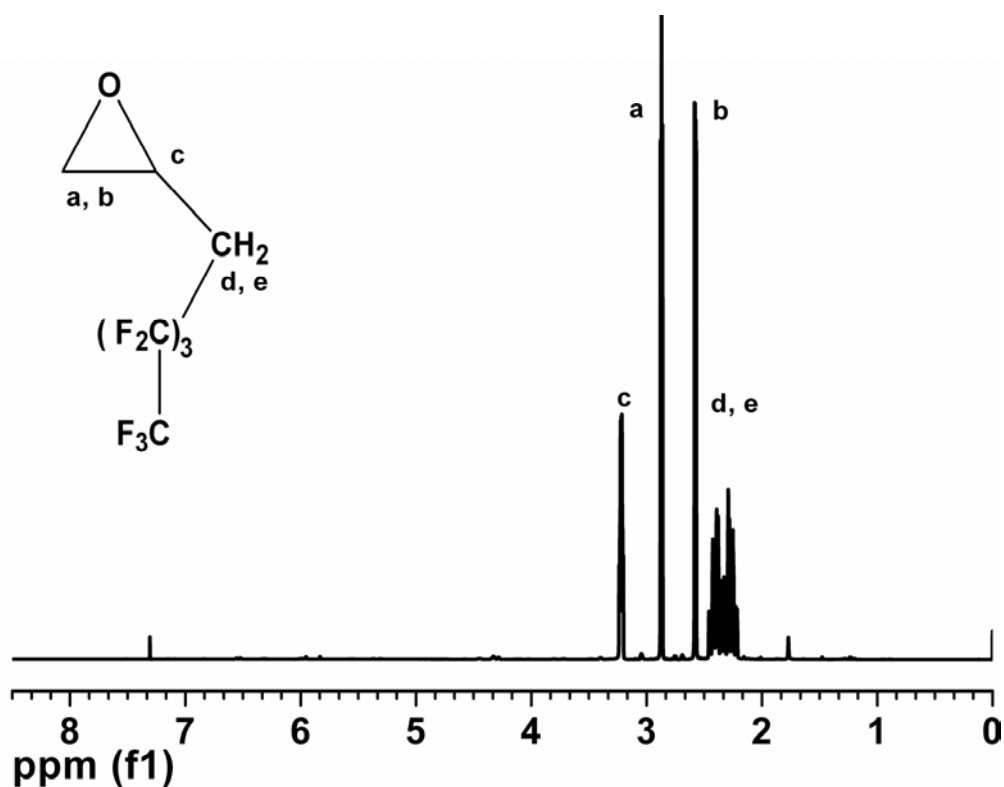
Figure 3.20 The ^{1}H-NMR spectrum of 1H, 1H-(perfluoropenthyl) oximase

134

Table 3.4 The polymerization of (Perfluoropenthyl) oximase conversion to its corresponding reaction conditions

Polymer	Polymerization Condition	Polymerization Conversion	Mn Value	Polydispersity
P-1 racemic	T=90°C, P=3000 psig, t = 24 h	%91.82	83649	1.041
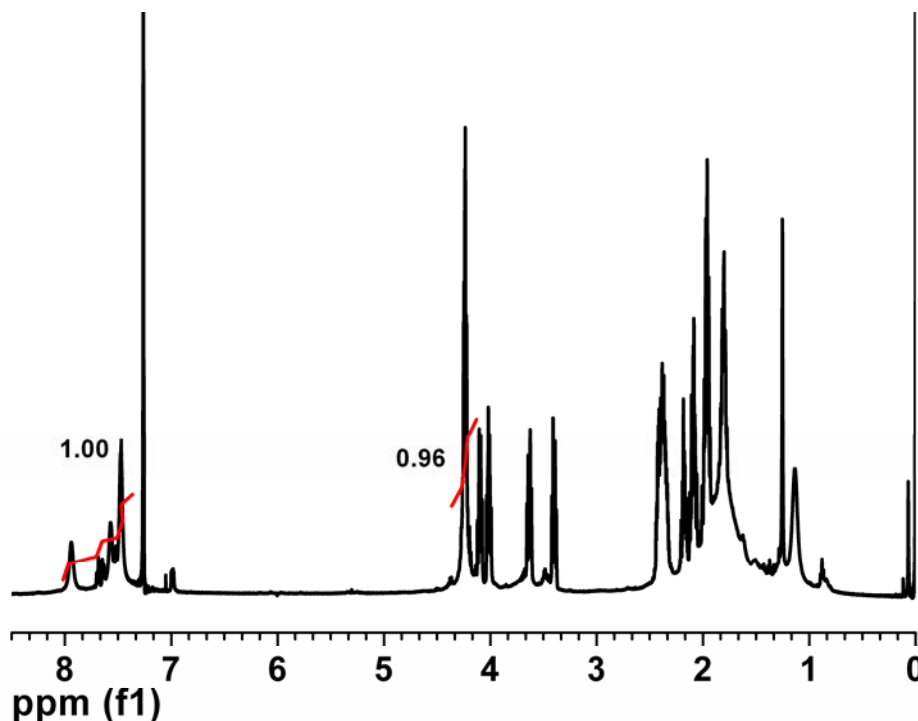
Figure 3.21 The ^{1}H-NMR spectrum of the copolymer from 1H, 1H-(perfluoropenthyl) oximase

Figure 3.21 represents the ^{1}H-NMR spectrum of the fluoropolymer, the shift to lower fields for the ring protons is obvious on going from the monomer to the polymer. The methine protons of the ring are shifted to 4.24 ppm from 3.22 ppm and the doublet methylene protons are shifted to 4.05 and 3.45 ppm from 2.87 and 2.58 ppm. On the other hand, the methylene units in the spacer group give a broad band and do not shifted much, since the chemical environment does not change significantly in comparison with the monomer. The polymerization conversions are calculated depending on the comparison of the polymer methine peak and the aromatic hydrogen peaks of the catalyst in ^{1}H-NMR. The four hydrogen peaks of the catalyst and their respective integration intensities are illustrated in Figure 1.13. The molar feed ratio of catalyst to

monomer is adjusted as 0.2 (N_{cat} / N_{mon} = 1/5) for the polymerization, and considering this fact one can formulate the polymerization conversion rule as follows;

$$(5 \times I_C/4) = I_{MT} \text{ (Total monomer intensity)}$$
$$100 \times [(I_M) / (I_{MT})] = \% \text{ Reaction Conversion}$$

I_{MT}, I_M and I_C represent the total monomer intensity, reacted monomer intensity and catalyst intensity in ^{1}H-NMR respectively.

(a)
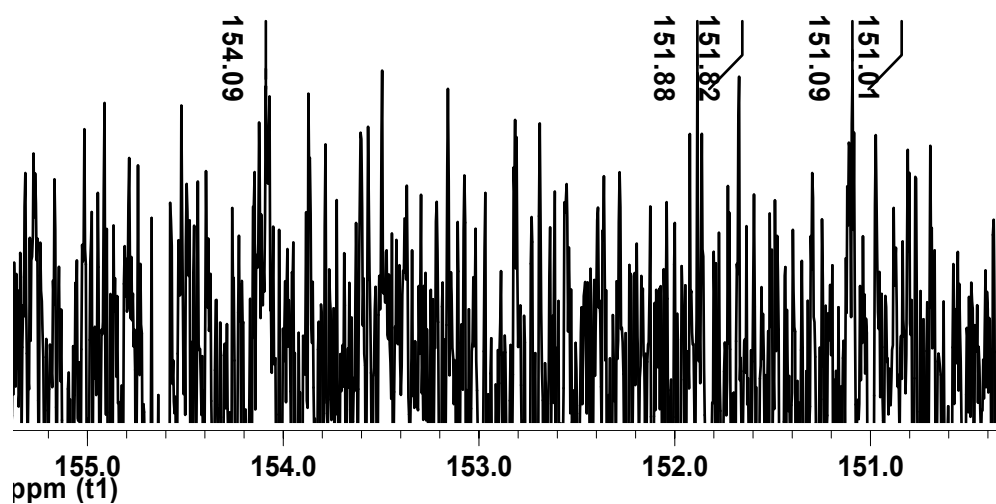
(b)
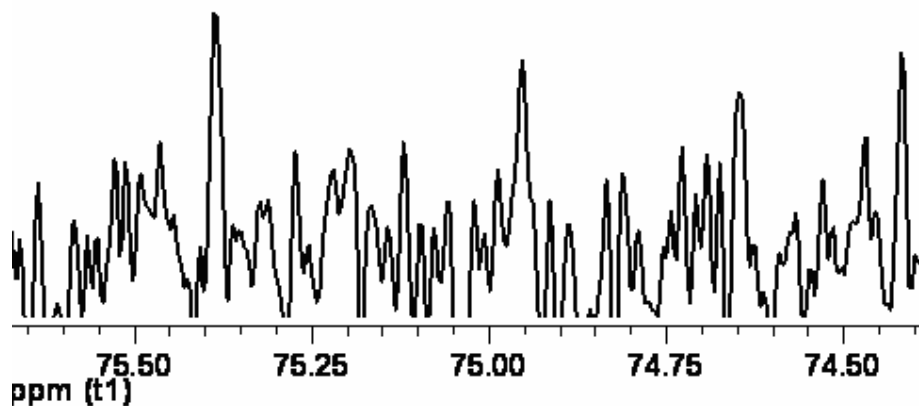
Figure 3.22 The close-up ^{13}C-NMR spectra of the copolymer obtained from 1H, 1H-(perfluoropenthyl) oximase in the region of **(a)** carbonyl **(b)** methine carbons

In Figure 3.22 (a) and (b), the expanded regions of the carbonyl and the methine carbon are given. If an analogy is established between the spectrum of previously reported polypropylene oxide (PPO) and this spectrum, we can easily attribute the most downfield shift as TT, the most upfield shift to HH and the one in between to HT signal. The HT junctions are favored over their statistical occurrence and this indicates that the ring opening of epichlorohydrin occurs with a regiospecifity in the formation of PPFOC. Additionally, in contrast to the stereoregular poly(epichlorohydrin carbonate) (PEC) and poly(nosyl carbonate) (PNC) synthesized from enantiomerically pure monomers, the racemic perfluorooximase carbonate (PPFOC) yields a highly stereoirregular polymer as shown Figure 3.22 (b).

It is noteworthy to state here that, the natural abundance of ^{13}C-NMR spectrum of the racemic perfluorooximase has no pronounced preference to any of the sequence, whereas, the polymer of racemic epichlorohydrin favors HT junction. This result can be attributed to the steric hinderance of the bulky fluoro groups in the side chain.
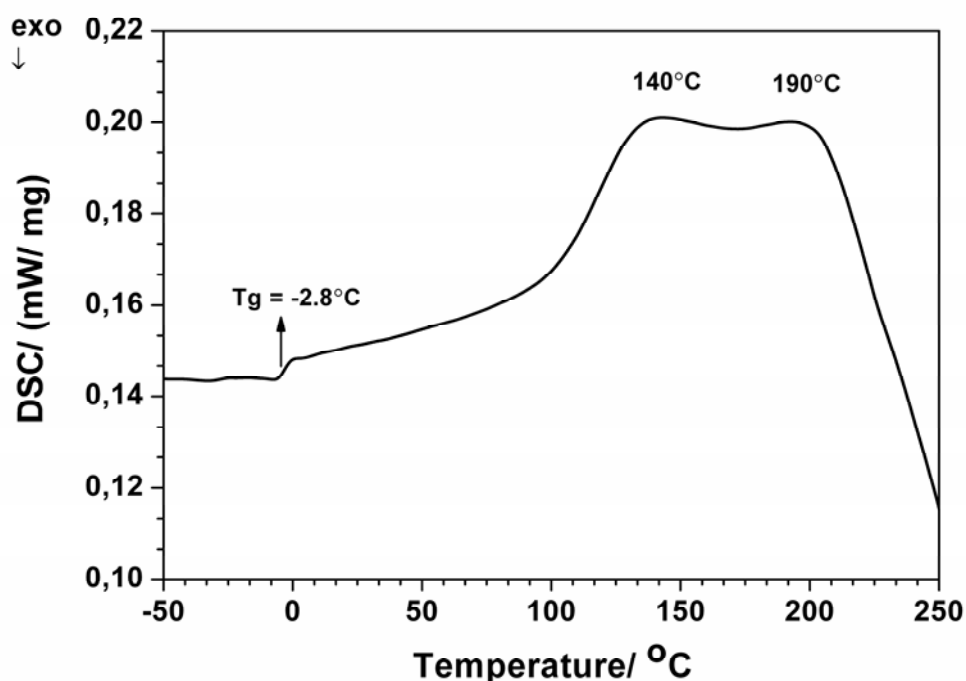
Figure 3.23 The DSC thermogram of the copolymer from 1H, 1H-(perfluoropenthyl) oximase in the second heating cycle with a heating rate of 10ºC/min.

Furthermore, the thermal analysis of the copolymer furnishes a Tg value of -2.8°C and two different melting points at 140°C and 190°C. These two different melting points are as a result of two different molecular weight polymers. This result is supported by the GPC analysis of the polymer with two peaks representing different molecular weight chains. Also, the additional decrease in the Tg value in comparison to the copolymer obtained from epichlorohydrin, is coherent due to the fluoro content incorporated into the structure.

3.4.5 Synthesis and Characterization of Polycarbonates from Perfluoroalkyl Oxiranes (PFAC)

3.4.5.1 Characterization and Optimization of the Synthesis for Perfluoroalkyl Epoxides as Monomer

In order to obtain different substituted polycarbonates and investigate their material characteristics as well as their structural orders, several different epoxides are synthesized. For this purpose, two alternative lengthened perfluoroalkyl alcohols (n= 6, 12) are chosen for the reaction with epoxy ring. We firstly describe the strategy for synthesis of highly fluorinated epoxides from perfluoroalkyl alcohols having the general formula of $HOCH_2CH_2(CF_2)_nF$ and then react them with carbon dioxide in $scCO_2$ media.

Interestingly, perfluoroalkyl alcohols are not used often in organic synthesis because of their weak acidic character, resulting in poor reactivity towards polyaddition and polycondensation reactions. As a consequence, their reaction with epichlorohydrin is rather difficult. To achieve this reaction we utilize different nucleophiles to activate perfluoroalkyl alcohols. For this purpose, we used several different nucleophiles in 1A Group in the periodic table (Sodium metal, sodium tertier butoxide, potassium tertier butoxide and finally Cs_2CO_3). Sodium and potassium tertier butoxide are chosen purposefully to achieve the nucleophilic substitution of the alcohol's hydroxyl proton and the nucleophile by Sn_2 reaction mechanism. As it is expected, better efficiency is obtained in substitution reactions by increasing the nucleophilic power (Na< K< Cs).

This reaction was also tried by creating a surface that is able to do the ionic transition between the surfaces of the reactants. So, alternative to the nucleophiles mentioned above TBAOH .5H_2O (tetrabutyl amonium hydroxyl pentahydride) is assigned as phase transfer catalyst. The hydroxyl part should react with the attribute alcohol and the tetrabutyl amonium part should react with the chlorine of the epichlorohydrin. After this sophisticated monomer synthesis, the resultant monomer directly substituted into a scCO$_2$ media. In the scheme below the monomer reaction trials have been summarized.
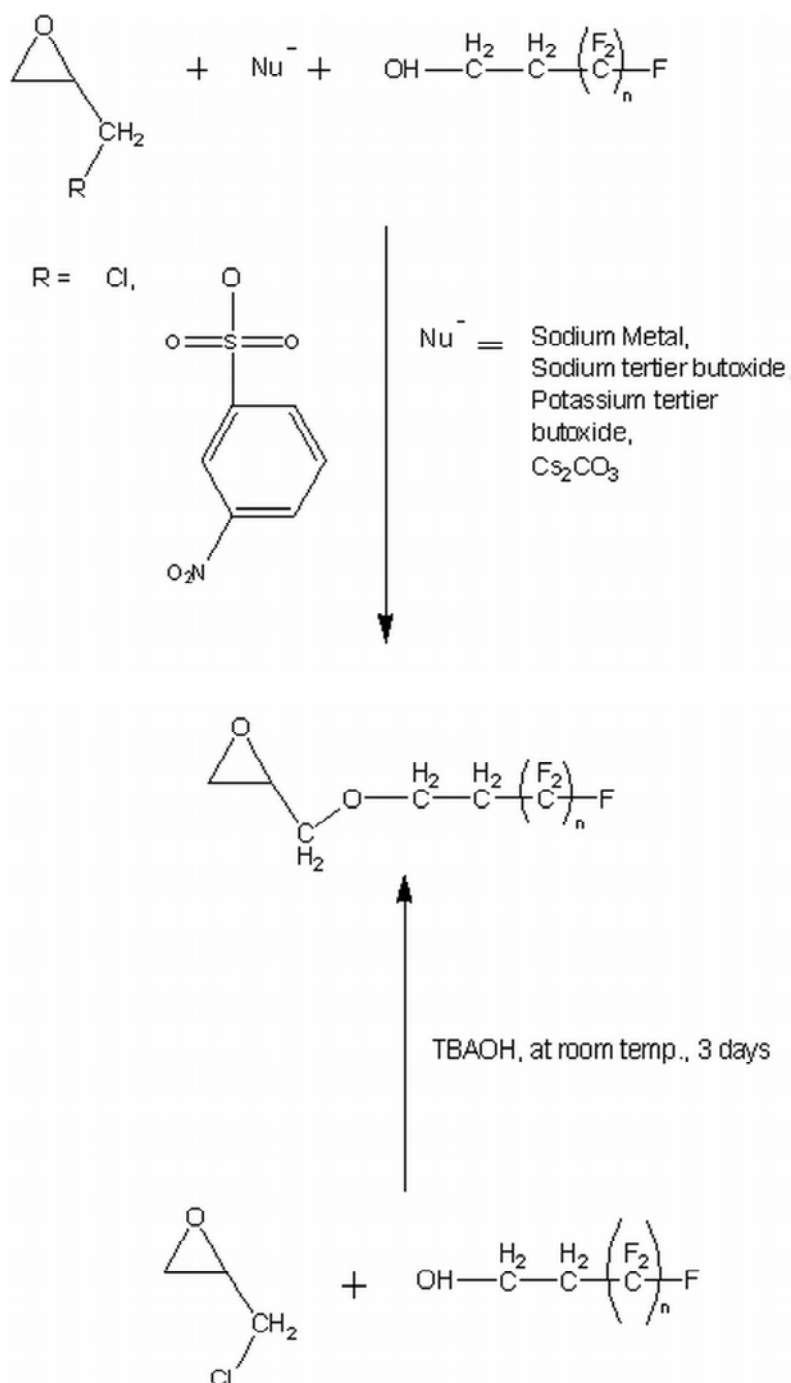
Scheme 3.9 The representation of the monomer synthesis reactions from perfluoroalkyl alcohols.

Table 3.5 Reaction conversions to their corresponding conditions

Trial no	Reactant	Nucleophile	Epoxy	Rxn Condition	Rxn Conversion
1	E612	Metallic sodium	Epichlorohydrin	THF	9%
2	E612	Sodium Tertier Butoxide	Epichlorohydrin	THF	Very low rxn conv.
3	E600	Sodium Metal	Nosylate	DMF	16%
4	E600	Sodium Tertier Butoxide	Nosylate	DMF	33%
5	E600	Sodium Tertier Butoxide	Epichlorohydrin	DMF	39%
6	E600	Potassium Tertier Butoxide	Epichlorohydrin	THF+ a drop of pyridine	40%
7	E612	Potassium Tertier Butoxide	Epichlorohydrin	THF	45%
8	E612	Cs_2CO_3	Epichlorohydrin	DMF	51%
9	E612	Cs_2CO_3	Epichlorohydrin	1:1 water/ DMF mixture	80%
10	E612	TBAOH	Epichlorohydrin	No solvent	97%

As it is mentioned above, the unwilligness of perfluoroalkyl alcohols for most of the reactions has converted us to utilize different type of nucleophiles to achive and consequently enhance the conversion of these reactions. Prior to the reaction with epoxides, perfluoroalkyl alcohols are activated with the mentioned nucleophiles (Metallic sodium, sodium tertier butoxide, potassium tertier butoxide Cs_2CO_3) and finally with the phase transfer catalyst (TBAOH).

Table 3.5 clearly elucidates that, the strength of the nucleophile is important to ease the reaction and enhance the reaction conversion. Thus, the stronger nucleophile the better yields we get. Other than, it should be mentioned that the purity and the isolation ease of the resultant product is a fundamental matter. More complicated reaction yields were obtained with the tertier butoxide salts of sodium and potassium and isolation of them were difficult. For the sake of purity of the product, metallic sodium or Cs_2CO_3 should be chosen as the nucleophile.

Due to the high viscosity of perfluoroalkyl alcohols, it is better to work with a solvent as viscosity diluent which accordingly increases the probability of better miscibility. Solvents which are miscible both with water and organic phase are chosen as reaction media to obtain better mixtures of the nucleophile and perfluoroalkyl alcohols. Although, DMF is a better chose for miscibility with these alcohols in some of the trials THF have been preferred owing to the hard isolation of DMF. The alcohol having 12 ethylene units (E612) is more viscous than the one with 6 ethylene units (E600) but in most of the trials E612 is chosen on account of its higher purity.
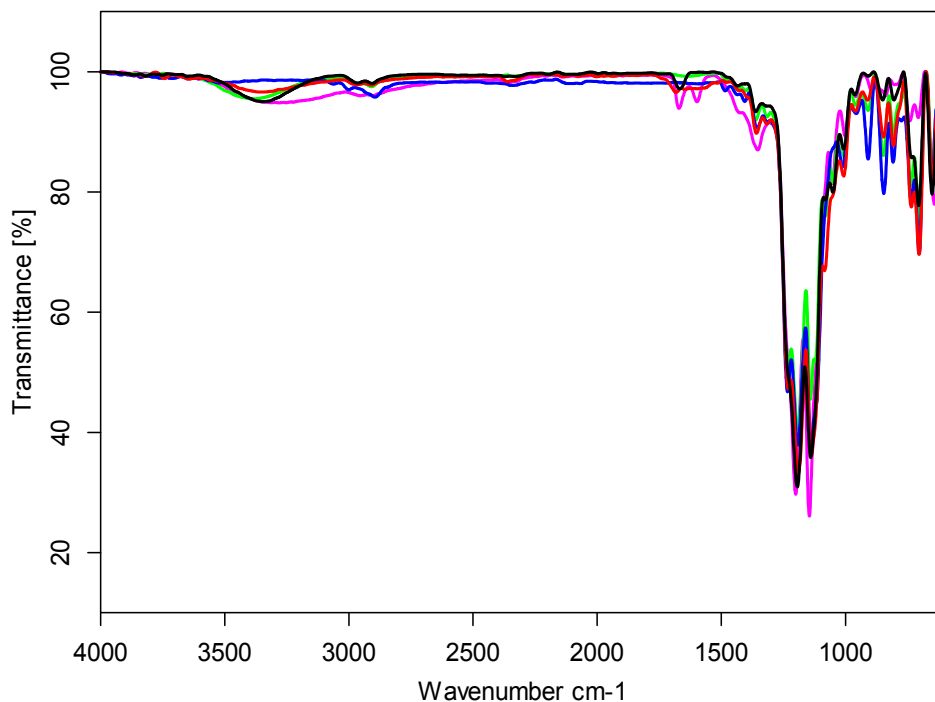
Figure 3.24 The FTIR Spectrum of **(a)** Alcohol (indicated in black color), **(b)** Reaction of alcohol and epichlorohydrin in the presence of phase transfer catalyst (indicated in blue color) **(c)** Reaction of alcohol and epichlorohydrin in the presence of Pottassium tertier butoxide (indicated in red color) **(d)** Reaction of alcohol and epichlorohydrin in the presence of Cs2CO3 (indicated in pink color) **(e)** Reaction of alcohol and epichlorohydrin in the presence of sodium metal (indicated in green color)
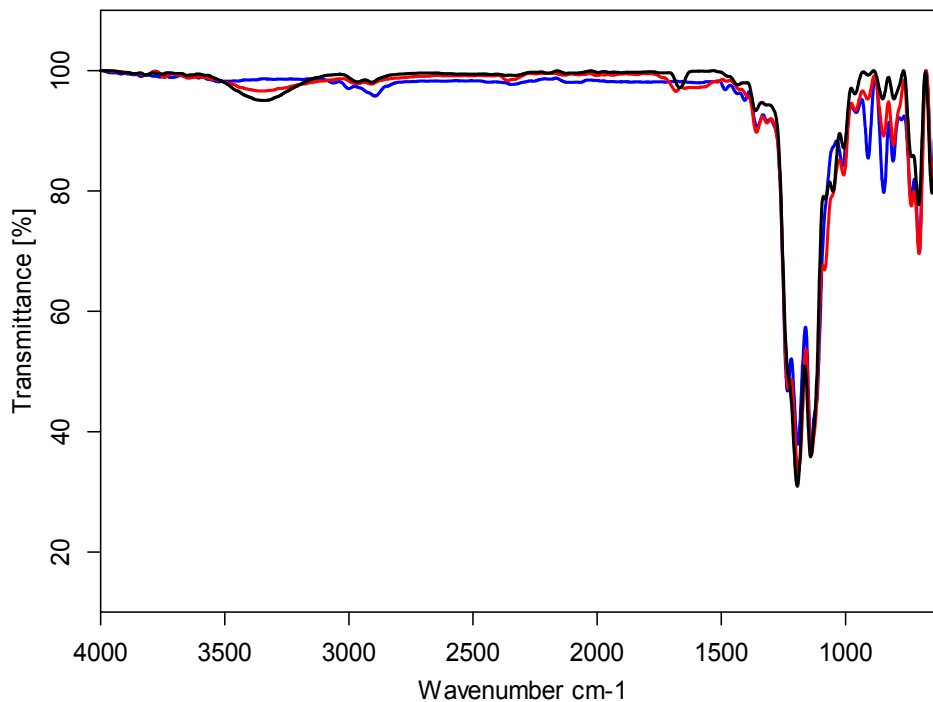
Figure 3.25 The FTIR Spectrum of **(a)** Alcohol (indicated in black color), **(b)** Reaction of alcohol and epichlorohydrin in the presence of phase transfer catalyst (indicated in blue color) **(c)** Reaction of alcohol and epichlorohydrin in the presence of pottassium tertier butoxide (indicated in red color)

The Figure 3.24 represents the reaction of the activated perfluoroalkyl alcohols with epichlorohydrin. The activation of the fluoro alcohols have been achieved by various nucleophiles and the phase transfer catalyst and all of them are denoted in a different color as indicated in the figure caption.

The decrease in the intensity of the OH peak, on the other hand, is indicative of the successive nucleophilic substitution reaction. Since, more noticeable decrease in the hydroxyl absorption peak can be observed in Figure 3.25, it presents more conclusive data on the success of the monomer synthesis reaction. In this figure the monomers are activated by pottassium tertier butoxide and the TBAOH phase catalyst. Different colors indicate different reactive specious as indicated in the figure caption. The other distinguishable absorption bands in both of the figures, observed at 1200 cm^{-1} and 1144 cm^{-1}, characterize the fluoro content of the alcohols.

143
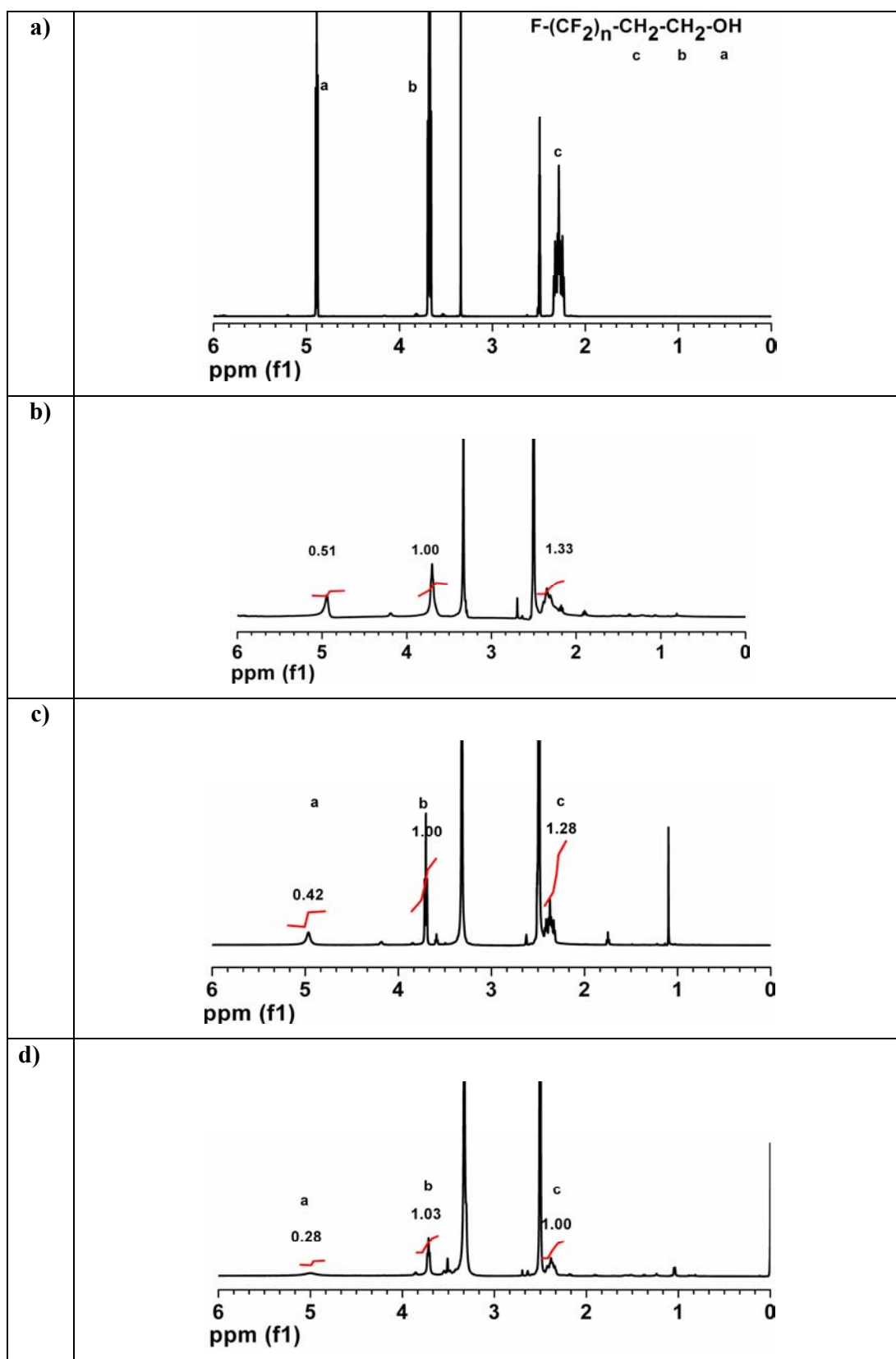
Figure 3.26 ^{1}H-NMR of **(a)** Perfluoroalkyl alcohol; E612 (in CDCl$_3$) **(b)** Sodium salt of alcohol (in DMSO) **(c)** Pottasium salt of alcohol (in DMSO) **(d)** Cessium salt of alcohol (in DMSO)

After several trials on optimization of monomer synthesis reaction, it is safe to conclude that better efficiency is obtained with a stronger nucleophile in the activation step of perfluoroalkyl alcohol. Depending on the comparison of integration values "**a**" and "**b**" (pointed up on the NMR spectra), Cs_2CO_3 increases the amount of activated alcohol as illustrated in Figure 3.26 (d). Further, studies on these systems affirmed that enhanced conversion is achieved with TBAOH phase transfer catalyst. By using this system, the probability of gathering the water soluble activated alcohol with the organic soluble epichlorohydrin is increased. Below the ^{1}H-NMR of the synthesized monomer is given. The exact assignement is done on the spectrum.
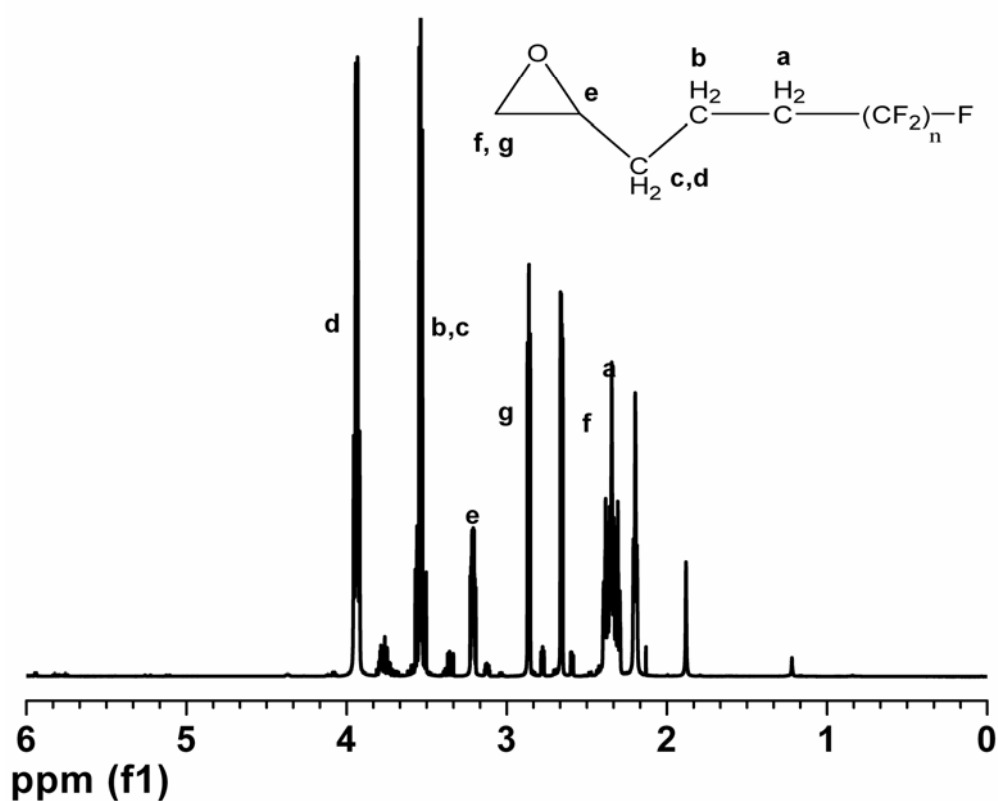
Figure 3.27 ^{1}H-NMR of perfluoroalkyl alcohol (E612) and epichlorohydrin in the presence of phase transfer catalyst

For the subsequent step, the synthesized monomer is polymerized in a $scCO_2$ environment as schematically illustrated in Scheme 3.10.

3.4.5.2 Synthesis and Characterization of the Polymer
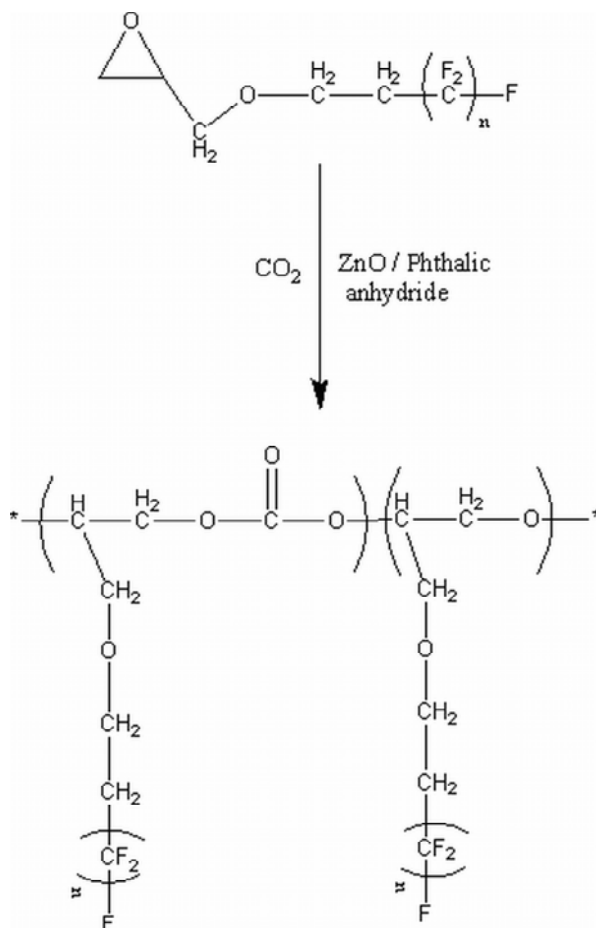
Scheme 3.10 The representation of the copolymerization reaction of perfluoroalkyl oxiranes in $scCO_2$ media.

There different polymerization conditions are applied to obtain the best yield. In the following spectra, polymerization conversions are calculated depending on the integration values of unreacted methine peak for epichlorohydrin and the methine peak of the carbonate group in H-NMR. The integration intensities are illustrated on Figure and the polymerization conversion rule is as follows;

$$(I_M + I_{UM}) = I_{MT} \text{ (Total monomer intensity)}$$

$$100 \times [I_M / I_{MT}] = \% \text{ Reaction Conversion}$$

I_{MT}, I_{UM} represent the total monomer intensity, unreacted monomer intensity and catalyst intensity in ^{1}H-NMR respectively
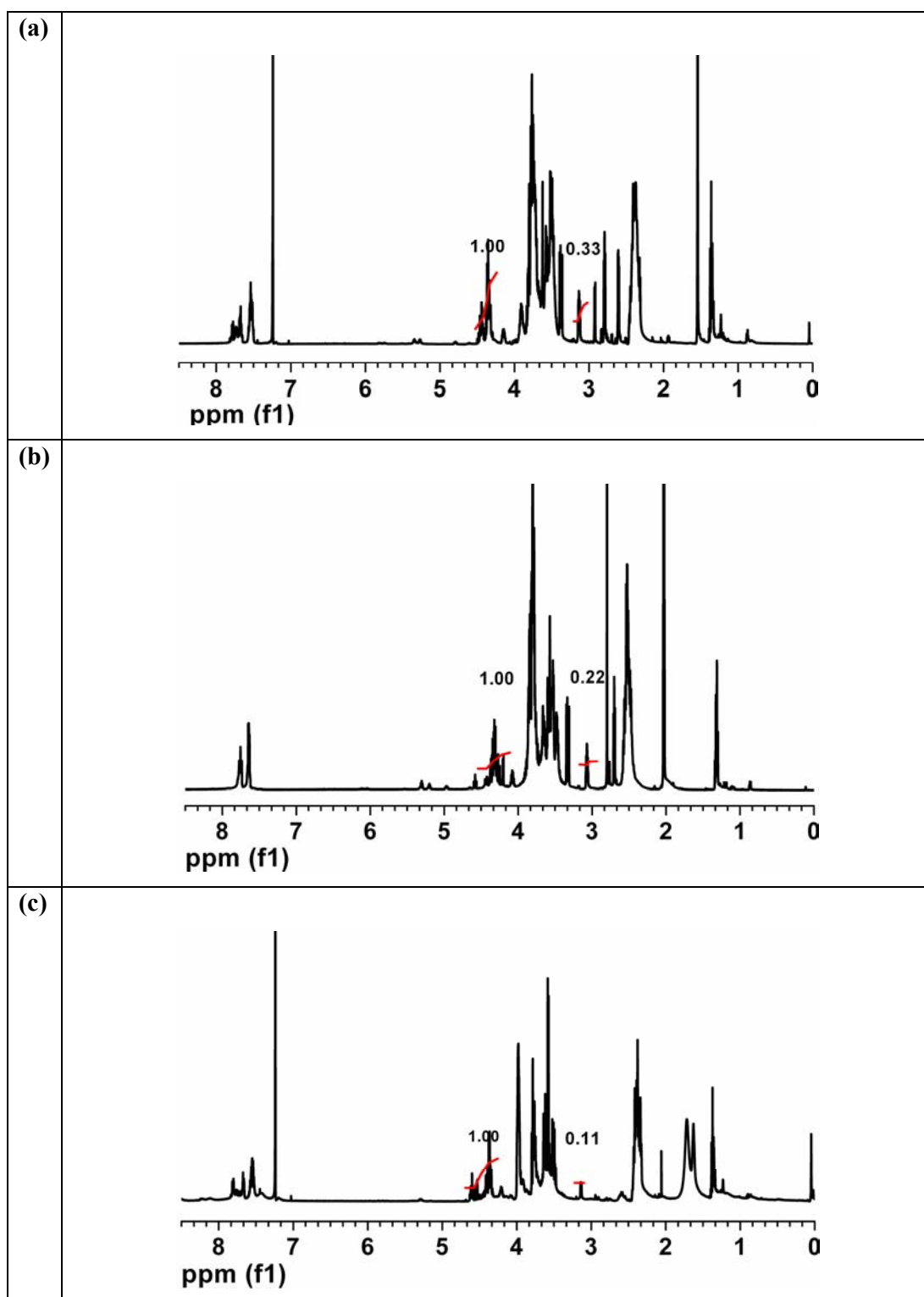
Figure 3.28 Comparison of the polymerization conversion corresponding to different polymerization conditions. Spectra **(a), (b), (c)** represent polymers produced from perfluoroalkyl epoxide monomer with %75.19, %81.97, and %88.5 polymerization conversions respectively.

Furthermore, the micro and macro structure investigations reveal that a regioirregular and stereoirregular polymers are synthesized as a result of the synthesis these perfluoroalkyl oxiranes. This result is rational since the sterichinderance of the bulky fluoro groups in the side chains restricts the regular arrangement in the polymer.

(a)
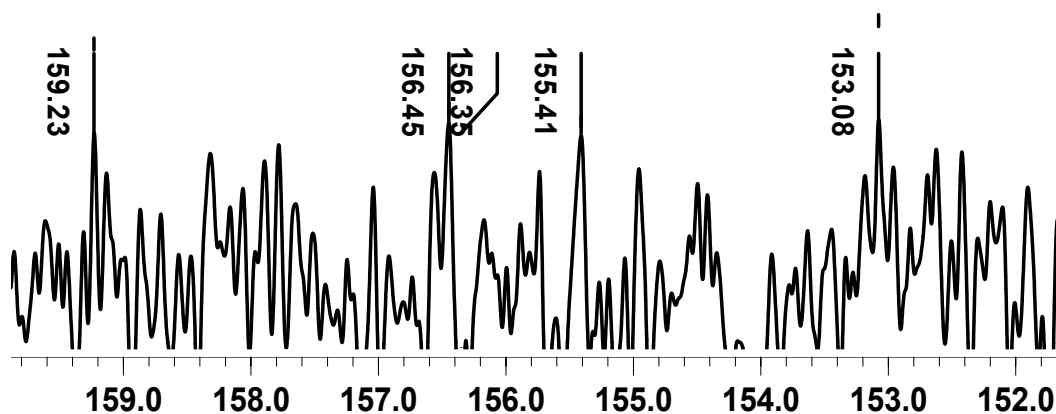
(b)
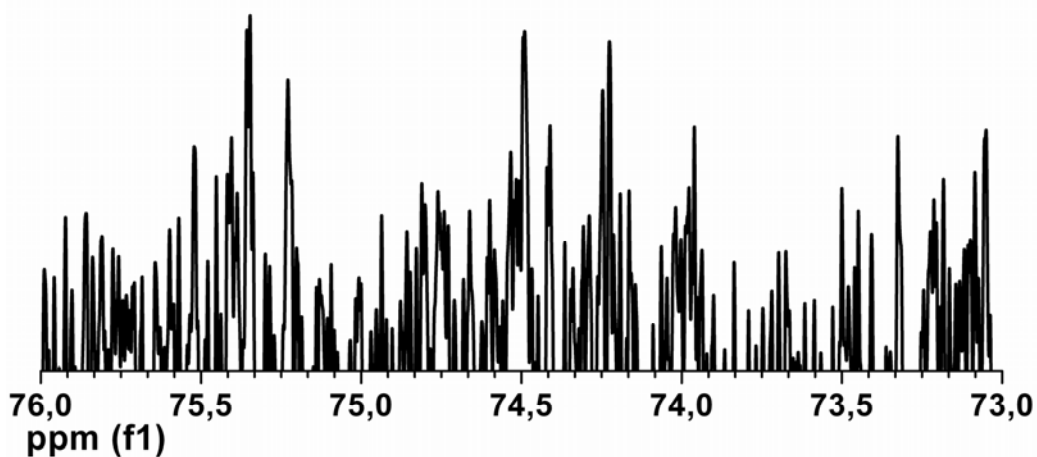
Figure 3.29 The close-up ^{13}C-NMR spectra of the copolymer obtained from perfluoroalkyl oxiranes in the region of **(a)** carbonyl **(b)** methine carbons.
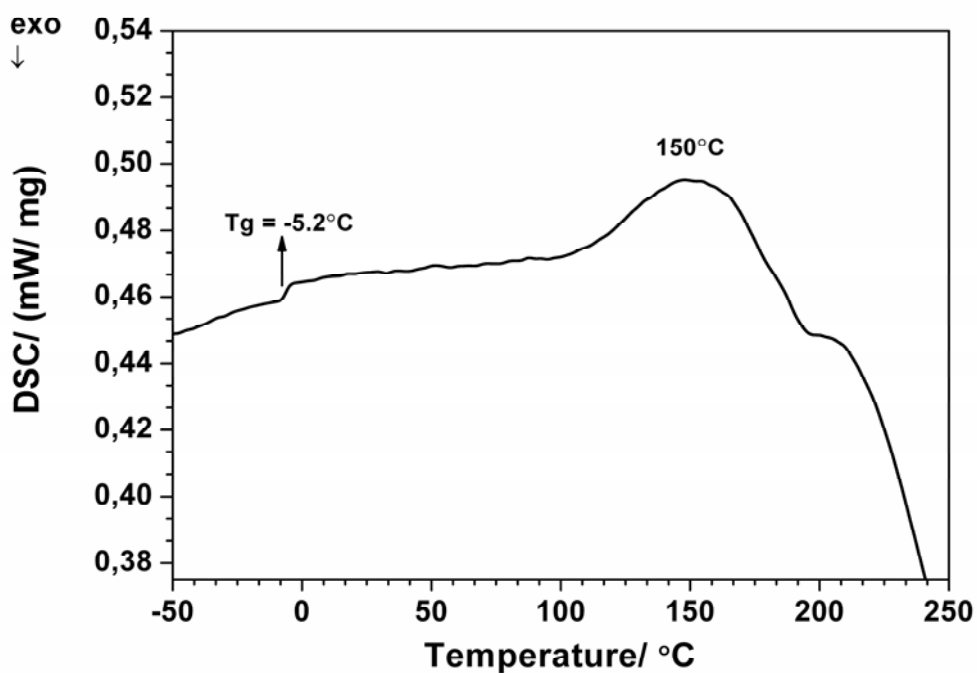
Figure 3.30 The DSC thermogram of the copolymer from perfluoroalkyl alcohol of six spacer unit, in the second heating cycle with a heating rate of 10ºC/min.

As illustrated in the DSC thermogram of the copolymer, a Tg value of -5.2 and a Tm value of 150 are obtained. The further decrease in the Tg and Tm values are again due to the integrated fluoro content into the polymeric structure. Yet, the decrease in the Tm value does not disturb the enlarged processing window obtained with this catalyst system.

3.5   Conclusion of Chapter 3
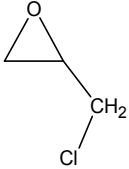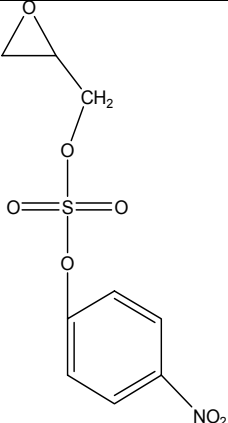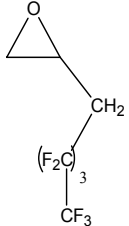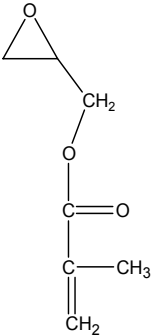
By using different set of conditions, the optimum polymerization conversion is obtained for the synthesis of copolymers with well-defined structures. In this respect, control of sequence (microstructure), tacticity as well as the molecular weight of polymer is investigated. Consequently, polymers with controlled parameter (high Mn and low polydispersity) have been formed as a result of ring opening of different functional group epoxides, yielding practical applications. The obtained narrow polydispersity is in linear correlation with the experimentally determined Mn value and
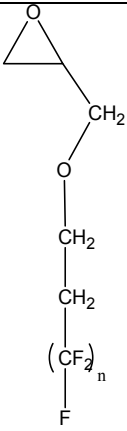
percent conversion. In terms of reaction conversions, short reaction times yield a low polymerization conversion whereas, longer reaction times tend to decrease the weight of the synthesized polymer. This decrease in the molecular weight, is due to the relatively slow initiation and rapid propagation reaction, while the cyclic carbonate is formed in a simultaneous side reaction and by depolymerization of the already formed polymers. On the other hand, no pronounced increase in the polymerization conversion is noted as the pressure of the system is elevated. For this reason, in order to generalize, the optimum reaction conditions to be used with these epoxy monomers appear to be a temperature of 90°C, a pressure of 4500 psi, and a reaction time of 24 hours. Except, owing to better miscibility of fluorinated monomers with scCO$_2$ media, applying hard reaction conditions for these systems are not necessary. Hence less reaction time for these polymerizations are enough to a reach high molecular weights.[6]

The summary of the obtained data from copolymerization of different epoxy monomers are given in the below table. Correspondingly, the data obtained from copolymerization of racemic epichlorohydrin and glycidyl methacrylate show that the preference of the microstructure is mostly in the favor of head to tail (HT) junctions. As a consequence of these results, the working principle of the catalyst system we utilized is concluded. Concerning this, a transition state for ring opening is expected involving a backside attack on zinc bound epoxy ring by a neighboring alkoxide group which in turn is bound to a zinc (II) center. Whereas, for the racemic monomers consisting of fluoro content the preference of HT junction is an exception and do not prove this rule. This is attributed to the steric hinderance of the bulky fluoro groups in the side chains. Further more, the enantiomeric purity has an influence on the microstructure of the obtained polymer by enhancing the head to tail junction and leads to more regioregular structures.

Table 3.6 The summary of the structural properties for the utilized monomers.

150

Monomer	Optical Activity	Regioregularity	Stereoregularity
(epoxide with CH_2Cl substituent)	Racemic	Main formation: HT (TT:HT:HH/36:50:14)	Main formation: isotactic Stereoirregular (-)
	Chiral (S-enantiomer)	Main formation: HT Regioregular	Main formation: isotactic Stereoregular (+)
(epoxide with CH_2–O–SO_2–O–phenyl–NO_2 substituent)	Chiral (S-enantiomer)	Main formation: HT Regioregular	Main formation: isotactic Stereoregular (+)
(epoxide with CH_2–$(F_2C)_3$–CF_3 substituent)	Racemic	Regioirregular (-)	Stereoirregular (-)
(epoxide with CH_2–O–C(=O)–C(–CH_3)=CH_2 substituent)	Racemic	Main formation: HT (TT:HT:HH/6:87:7)	Stereoirregular (-)

	Racemic	Regioirregular (-)	Stereoirregular (-)

On the other hand the enantiomeric purity is more effective than steric hinderance on determining the tacticity of the polymers. Because a chiral and highly stericaly hindered nosylate group favors the isotactic structure whereas, the ones with racemic and stericly hindered groups result heterotactic polymers. Being consistent with the reports on different catalyst systems in the literature, by using this achiral catalyst, we obtain stereoregular polymers from chiral monomers. Some heterotactic polymers are produced from racemic monomers.

In terms of thermal investigations, the copolymerization with the synthesized catalyst system in scCO$_2$ media, presents us very low Tg values and high Tm values in correspondence with its analogues. Since, polycarbonates are known as biocompatible materials, the obtained polymers, offering an enlarged processing window, allow one to study for various applications in this area.

REFERENCES

1.   Lomborg, B., The Skeptical Environmentalist; Measuring the Real State of the World. **2001**, Cambridge: Cambridge University Press.

2.   Afonso, C.A.M. and Crespo, J.G., *Green separation processes : fundamentals and applications*. **2005**, Weinheim ; Chichester: Wiley. p.363

3.   *World Commission on the Environment and Development (WCED)*, in *Our common future*. 1987, Oxford University Press: Oxford:. p. 320.

4.   (NEIC), N.E.I.C. *Greenhouse Gases, Climate Change, and Energy*.   [cited 2006; Available from: http://www.eia.doe.gov/environment.html.

5.   Kendall, J.L., Canelas, D.A., Young, J.L., and DeSimone, J.M., Polymerizations in Supercritical Carbon Dioxide. *Chem Rev,* **1999**. *99* (2),543-564.

6.   Beckmann, E., Supercritical and near-critical CO2 in green chemical synthesis and processing. *Coordination Chemistry Reviews,* **2004**. *28* (2-3), 121-191.

7.   Gross S. M., Roberts G. W. , Kiserow D. J., and M., D.J., Crystallization and Solid-State Polymerization of Poly(bisphenol A carbonate) Facilitated by Supercritical CO2. *Macromolecules* **2000**. *33*, 40-45.

8.   Maury, E.E., *Heterogeneous Free Radical Polymerizations in Supercritical Carbon Dioxide*. **1995**, University of North Carolina.

9.   DeSimone, J.M., Maury E.E., Menceloglu Y.Z., McClain J.N., Romack T.J., and J.R. Combes. , Dispersion Polymerizations in Supercritical Carbon Dioxide. *Science,* **1994**. *265*, 356-359.

10.   Jung, J.H., Ree, M., Chang, T., Copolymerization of Carbon Dioxide and Propylene Oxide Using An Aluminum Porphyrin System and Its Components. *Journal of Polymer Science: Part A: Polymer Chemistry,* **1999**. *37*, 3329–3336

11.   Jessop, G.P. and Leitner, W., Phase Behavior and Solubility. *In Chemical Synthesis Using Supercritical Fluids*, ed. P.G. Jessop and W. Leitner. **1999**, Weinheim: WILEY-VHC. 37-53.

12.   Jessop, G.P. and W., L., Basic Physical Properties of Supercritical Fluids. Philip G. Jessop and Walter Leitner ed. *In Chemical Synthesis Using Supercritical Fluids*. **1999**, Weinheim: WILEY-VHC. 38.

13.   Jessop, G.P. and W., L., Temperature and Pressure Effects. *In Chemical Synthesis Using Supercritical Fluids*, ed. P.G.J.a.W. Leitner. **1999,** Weinheim: WILEY-VHC. 51-53.

14.   McHugh, M.A. and Krukonis, V.J., Supercritical Fluid Extraction, ed. M.A. McHugh and V.J. Krukonis. **1994**, Boston: Butterworth-Heinemann.

15.   Menceloğlu, Y.Z., *Processing in Supercritical Carbon Dioxide. Report Presentation*. **2002**, Sabancı University: Tuzla.

16. Kiran, E., Debenedetti, P.G., and P., C.J., Polymer Prosessing. *In Supercritical Fluids/Fundamentals and Applications*, ed. P.G.D.a.C.J.P. Erdogan Kiran. **1989**, Dordrecht: NATO Science Series. p. 27.

17. Jessop, G.P. and W., L., Supercritical Fluids as a Media for Chemical Reactions. *In Chemical Synthesis Using Supercritical Fluids*, ed. P.G.J.a.W. Leitner. **1999**, Weinheim: WILEY-VHC. p. 6.

18. Kirmizialtin, S., Menceloglu Y. Z., and C., B., New Surfactants Design for CO2 Applications: Molecular Dynamics Simulations of Fluorocarbon-Hydrocarbon Oligomers. *Journal of Chemistry and Physics,* **2003**. *36*, 1132-1137.

19. Sarbu, T., Styranec, T., and Beckman, E.J., Non-fluorous polymers with very high solubility in supercritical CO2 down to low pressures. *Nature,* **2000**. *405* (6783), 165-8.

20. Kumar, A. and Gupta, R.K. *Fundamentals of Polymers,* **1998**, New York: McGraw-Hill.

21. Wooda, D.C., Cooperb, A.I., and DeSimone, J.M., Green synthesis of polymers using supercritical carbon dioxide. *Current Opinion in Solid State and Materials Science,* **2004**. *8* (5), 325-331.

22. Ehrlich, P. and Mortimer, G.A., Fundamentals of the Free-. Radical Polymerization of Ethylene. *Adv Polym Sci.,* **1970**. *7*, 386.

23. Kirby, C.F., McHugh, M.A., and . Phase Behavior of Polymers in Supercritical Fluid Solvents, *Chem. Rev.,* **1999**. *99* (2), 565-602.

24. Allada S.R., Solubility parameters of supercritical fluids. *Ind Eng Chem Proc Des Dev 23*, 344-348.

25. Mcfann, G.J., Johnston, K.P., and Howdle, S.M., Solubilization in. Nonionic Reverse Micelles in Carbon Dioxide. *AIChE J.,* **1994**. *40*, 543-555.

26. Harris, T.V., Irani, C.A., and Pretzer, W.R., *US Patent No.5,045,220*. **1991**, Sept. 3.

27. Consani, K.A. and Smith, R.D., Observations on the solubility of surfactants and related molecules in carbon dioxide at 50°C *J. Supercrit. Fluids,* **1990**. *3* (2), 51-65.

28. DeSimone, J.M., Guan, Z., and Elsbernd, C.S., Synthesis of fluoropolymers in supercritical carbon dioxide *Science,* **1992**. *257*, 945-947

29. McClain, J.B., . Betts, D.E.C., D.A., Samulski, E.T., DeSimone, J.M., Londono, J.D., Cochran, H.D., Wignall, G.D., ChilluraMartino, D., Triolo, R., and . Design of Nonionic Surfactants for Supercritical Carbon Dioxide. *Science* **1996**. *274* (5295), 2049.

30. Dardin, A., Cain, J.B., DeSimone, J.M., Johnson, C.S., Jr.; , and Samulski, E.T., High-Pressure NMR of Polymers Dissolved in Supercritical Carbon Dioxide. *Macromolecules,* **1997**. *30* (12), 3593-3599.

31. Diep, P., Jordan, K.D., Johnson, J.K., and Beckman, E.J., CO2-Fluorocarbon and CO2-Hydrocarbon Interactions from First-Principles Calculations. *J. Phys. Chem. A,* **1998**. *102* (12) ,2231-2236.

32. McHugh, M.A., Park, I.-H., Reisinger, J.J., Ren, Y., Lodge, T.P., and Hillmyer, M.A., Solubility of CF2-Modified Polybutadiene and Polyisoprene in Supercritical Carbon Dioxide *Macromolecules,* **2002**. *35* (12), 4653-4657.

33. Kazarian, S.G., Vincent, M.F., Bright, F.V., Liotta, C., and Eckert, C.A., Specific Intermolecular Interaction of Carbon Dioxide with Polymers *J. Am. Chem. Soc.,* **1996**. *118* (7), 1729-1736.

34. O'Neill, M.L., Cao, Q., Fang, M., Johnston, K.P., Wilkinson, S.P., Smith, C.D., Kerschner, J.L., and Jureller, S.H., Solubility of Homopolymers and Copolymers in Carbon Dioxide *Ind. Eng. Chem. Res,* **1998**. *37* (8), 3067-3079.

35. Bilgin, N., *Synthesis of fluorinated segment containing oligomers for supercritical carbon dioxide applications* in *Material Science and Engineering.* 2003, MS thesis, Sabanci University.

36. Sarbu, T., Styranec, T.J., and Beckman, E.J., Design and Synthesis of Low Cost, Sustainable CO2-philes *Ind. Eng. Chem. Res,* **2000**. *39* (12), 4678-4683.

37. Odian, G. *Principles of Polymerization.* **1991**, New York: third ed, Wiley and Sons.

38. Odell, P.G. and Hamer, G.K., Polycarbonates via melt transesterification in supercritical carbon dioxide. *Polym Prepr,* **1997**. *38,* 470 - 471.

39. Inoue, S., Koinuma, H., and Tsuruta, T., Copolymerization of Carbon Dioxide and Epoxide with Organometallic Compounds, *Makromol. Chem.,* **1969**. *130,* 210-216.

40. Kuran, W., Coordination polymerization of heterocyclic and heterounsaturated monomers *Prog Polym Sci* **1998**. *23* (6), 919-992.

41. Super, M., Berluche, E., Costello, C., and Beckman, E., Copolymerization of 1,2-Epoxycyclohexane and Carbon Dioxide Using Carbon Dioxide as Both Reactant and Solvent, *Macromolecules,* **1997**. *30* (3), 368-372.

42. Cheng, M., Moore, D.R., Reczek, J.J., Chamberlain, B.M., Lobkovsky, E.B., and Coates, G.W., Single-Site -Diiminate Zinc Catalysts for the Alternating Copolymerization of CO2 and Epoxides: Catalyst Synthesis and Unprecedented Polymerization Activity *J. Am. Chem. Soc.,* **2001**. *123* (36), 8738-8749.

43. Buzdugan, E. and Beckman, E.J. *CO2 Utilization*. in *Presentation at the Sixth International Conference on CO2 Utilization*. September 10-14, 2001. Breckenridge.

44. Tomasko, D.L., Li, H., Liu, D., Han, X., Wingert, M.J., Le, L.J., Koelling, K.W., and A Review of CO2 Applications in the Processing of Polymer, *Ind. Eng. Chem. Res.,* **2003**. *42*, 6431-6456.

45. Wood , C.D., Cooper, A.I., and DeSimone, J.M., Green synthesis of polymers using supercritical carbon dioxide, *Current Opinion in Solid State and Materials Science,* **2004**. *8*, 325-331.

46. Aida, T. and Inoue, S., Activation of carbon dioxide with aluminum porphyrin and reaction with epoxide. Studies on (tetraphenylporphinato)aluminum alkoxide having a long oxyalkylene chain as the alkoxide group, *J. Am. Chem. Soc.,* **1983**. *105* (5), 1304-1309.

47. Darensbourg, D.J., Rainey, P., and Yarbrough, J., Bis-Salicylaldiminato Complexes of Zinc. Examination of the Catalyzed Epoxide/CO2 Copolymerization, *Inorg. Chem.,* **2001**. *40* (5), 986-993.

48. Sun, H.-N., in *U.S. Patent No: 4,783,445*. 1988, November 8, Arco Chemical Company.

49. Aida, T., Ishikawa, M., and Inoue, S., Alternating copolymerization of carbon dioxide and epoxide catalyzed by the aluminum porphyrin-quaternary organic salt or -triphenylphosphine system. Synthesis of polycarbonate with well-controlled molecular weight, *Macromolecules,* **1986**. *19* (1) 8-13.

50. Aida, T. and Inoue, S., Synthesis of polyether-polycarbonate block copolymer from carbon dioxide and epoxide using a metalloporphyrin catalyst system *Macromolecules,* **1982**. *15* (2), 682-684.

51. Odell, P.G., in *US Patent No. 5,698,665*. 1997, Dec. 16.

52. Kim, K.-S., Danishevsky, S., Peterson, C.B., and *US Patent No.6,100,372,.* 2000, Aug. 8.

53. Chandrasekhar, S. *in Liquid Crystals, 2nd edition,*ed. S. Chandrasekhar. **1992**, Cambridge, New York, NY, USA Cambridge University Press.

54. Collings, P.J. and Hird, M. *Introduction to Liquid Crystals Chemistry and Physics*, ed. P.J.C.a.M. Hird. **1997**: Taylor and Francis.

55. Sahin, Y.M., Diele, S., and Kresse, H., Liquid crystalline hydrogen-bonded ionic associates*. Liquid Crystals,* **1998**. *25* (2), 175-178.

56. Kato, T. and Frechet, J.M.J., A new approach to mesophase stabilization through hydrogen bonding molecular interactions in binary mixtures, *J. Am. Chem. Soc.,* **1989**. *111* (22), 8533-8534.

57.   Mohanty, S. (2003, November) Liquid Crystals – The 'Fourth' Phase of Matter [electronic resource]. *RESONANCE* 52-70.

58.   WikimediaCommons. *Liquid Crystal*. Wikipedia   2004, October 2006, May [cited;   Available   from: http://en.wikipedia.org/wiki/Liquid_crystal#Thermotropic_liquid_crystals.

59.   Collings, P.J. *Title Liquid crystals : nature's delicate phase of matter. 2nd ed*. **2002**, Princeton: Princeton University Press.

60.   Marder, M.P. *Condensed matter physics*. **2000**, New York: John Wiley. 107-108

61.   DoITPoMS, D.o.M.S.a.M., University of Cambridge. *Liquid crystals*.   [cited 2006,   April;   Available   from: http://www.doitpoms.ac.uk/tlplib/anisotropy/liquidcrystals.php.

62.   Aitken, R.A. and Kilenyi, S.N., Chirality. *in Asymmetric Synthesis*, ed. R.A. Aitken and S.N. Kilenyi. **1992**, London, Glasgow, New York, Tokyo, Melbourne, Madras: Blackie Academic and Professional.

63.   *Chirality (chemistry)*. Art History Reference Guide.2005, June [cited 2006, April];   Available   from: http://www.arthistoryclub.com/art_history/Chirality_%28chemistry%29.

64.   Marder, M.P., Condensed matter physics, ed. M.P. Marder. **2000** New York John Wiley. p. 38.

65.   *What are Liquid Crystals?* Last updated 12 February 1998 [cited; Available from: http//:www.mc2.chalmers.se/mc2/pl/lc.

66.   Ciardelli, F. and Pieroni, O. *in Chiroptical Molecular Switches*, ed. B.L. Feringa. **2001**, Weinheim: Wiley-VCH. Chapter 13, 399-441.

67.   Wang, X.-J. and Zhou, Q.-F. *Liquid crystalline polymers [electronic resource] Sabanci University*. 23-02-2006. [cited.

68.   *Introduction*. Polymer Liquid Crystals   [cited 2006, March; Available from: http://plc.cwru.edu/tutorial/enhanced/files/plc/intro.htm.

69.   Montornés, J.M., Reina, J.A., and Ronda, J.C., High-molecular-weight side-chain liquid-crystalline polyethers based on 4-cyanobiphenyl-4-oxy mesogenic groups, *Journal of Polymer Science Part A: Polymer Chemistry,* **2004**. *42* (12), 3002-3012.

70.   *Side-Chain Liquid Crystalline Polymers (SCLCPs)*. Polymer Liquid Crystals [cited   2006,   April;   Available   from: http://www-personal.umich.edu/~akiste/sclcp.html.

71. Chen, H.P., Katsis, D., Mastrangelo, J.C., Chen, S.H., Jacobs, S.D., and Hood, P.J., Glassy Liquid-Crystal Films with Opposite Chirality as High-Performance Optical Notch Filters and Reflectors, *Adv Mater,* **2000**. *12* (17), 1283-1286.

72. Goto, H. and Akagi, K., Asymmetric Electrochemical Polymerization: Preparation of Polybithiophene in a Chiral Nematic Liquid Crystal Field and Optically Active Electrochromism. *Macromolecules,* **2005**. *38* (4), 1091-1098.

73. Schadt, M. and Helfrich, W., Voltage-Dependent optical activity of a nematic liquid crystal *Appl. Phys. Lett.,* **1971**. *18*, 127-128.

74. Goto, H., Dai, X., Ueoka, T., and Akagi, K., Synthesis and Properties of Polymers from Monosubstituted Acetylene Derivatives Bearing Ferroelectric Liquid Crystalline Groups, *Macromolecules,* **2004**. *37* (13), 4783-4793.

75. Vlahakis, J.Z., Wand, M.D., and Lemieux, R.P., Photoswitching of Ferroelectric Liquid Crystals Using Unsymmetrical Chiral Thioindigo Dopants: Photoinduced Inversion of the Sign of Spontaneous Polarization, *Adv Func Mater*, **2004**. *14* (7), 637-642.

76. Cowie, J.M.G. and Duncan, D.M., Short wavelength light reflecting films from side-chain liquid crystal homopolymers with chiral spacer, *Polym Adv Technol,* **2001**. *12* (9), 506-514.

77. Mehl, G.H., Valvo, F., Lacey, D., Goodby, J.W., and Das-Gupta, D.K., Properties of side chain liquid crystal polyesters containing chiral groups in the main chain, *Polym Eng Sci,* **1996**. *36* (24), 2921-2931.

78. Taton, D., Le Borgne, A., Chen, J., and Shum, W., Synthesis of racemic and optically active glycidic ethers, precursors of liquid crystalline polyethers, *Chirality,* **1998**. *10* (9), 779-785.

79. Fisch, R.M., in *Title Liquid crystals, laptops and life [electronic resource], Sabanci University*. 2004, New Jersey ; London : World Scientific Publishing Company, .

80. Tibell, G. Linné on Line 2006, February [cited 2006, March]; Available from: http://www.linnaeus.uu.se/online/phy/microcosmos/liquid_crystals.html.

81. *History and Properties of Liquid Crystals*.   [cited 2006, April]; Available from: http://nobelprize.org/physics/educational/liquid_crystals/history/index.html.

82. Kong, X. and Tang, B.Z., Synthesis and Novel Mesomorphic Properties of the Side-Chain Liquid Crystalline Polyacetylenes Containing Phenyl Benzoate Mesogens with Cyano and Methoxy Tails *Chem. Mater,* **1998**. *10* (11), 3352-3363.

83. Kitaori, K., Furukawa, Y., Yoshimoto, H., and Otera, J., CsF in Organic Synthesis. Regioselective Nucleophilic Reactions of Phenols with Oxiranes Leading to Enantiopure Beta-Blockers, *Tetrahedron* **I 999**. *55*, 1438 I-14390.

84. Darensbourg, D.J., Holtcamp, M.W., Struck, G.E., Zimmer, M.S., Niezgoda, S.A., Rainey, P., Robertson, J.B., . Draper, J.D., and Reibenspies, J.H., Catalytic Activity of a Series of Zn(II) Phenoxides for the Copolymerization of Epoxides and Carbon Dioxide, *J. Am. Chem. Soc.,* **1999**. *121*, 107-116.

85. Chisholm, M.H. and Navarro-Llobet, D., A Comparative Study in the Ring-Opening Polymerization of Lactides and Propylene Oxide. *Macromolecules,* **2001**. *34*, 8851-8857.

86. Jansen, J.C., Addink, R., Nijenhuis, K.t., and Mijs, W.J., Synthesis and characterization of novel side-chain liquid crystalline polycarbonates, 4a Synthesis of side-chain liquid crystalline polycarbonates with mesogenic groups having tails of different lengths. *Macromol. Chem. Phys,* **1999**. *200*, 1407-1420.

87. Zhu, Q., Meng, Y.Z., Tjong, S.C., Zhao, X.S., and Chen, Y.L., Thermally stable and high molecular weight poly(propylene carbonate)s from carbon dioxide and propylene oxide. *Polymer International,* **2002**. *51* (10), 1079-1085.

88. Taton, D., Le Borgne, A., Spassky, N., and Noel, C., Synthesis and thermal properties of side chain liquid crystalline poly(glycidylethers) with racemic and chiral backbone, *Macromol. Chem. Phys. ,* **1995**. *196*, 2941-2954.

89. Inoue, S., Matsumoto, K., and Yoshida, Y., Ternary copolymerization of carbon dioxide with epoxybutanes, *Makromol. Chem.,* **1980**. *181* (11), 2287-2292.

90. Inoue, S., Koinuma, H., Yokoo, Y., and Tsuruta, T., Stereochemistry of copolymerization of carbon dioxide with epoxycyclohexane, *Makromol. Chem.,* **1971**. *143* (1), 97-104.

91. Inoue, S., Hirano, T., and Tsuruta, T., Ternary copolymerization of carbon dioxide with optical isomers of 1,2-Epoxypropane and Phenylepoxyethane. *Polym J,* **1977**. *9*,101.

92. Rokicki, A. and Kuran, W., The application of Carbon dioxide as a direct material for polymer synthesis in polymerization and polycondensation reactions. *J. Macromol. Sci.-Rev. Macromol. Chem. Phys. .* Vol. C21. **1981**, Tokyo. 135-186.

93. Chisholm, M.H., Navarro-Llobet, D., and Zhou, Z., Poly(propylene carbonate). 1. More about Poly(propylene carbonate) Formed from the Copolymerization of Propylene Oxide and Carbon Dioxide Employing a Zinc Glutarate Catalyst *Macromolecules,* **2002**. *35* (17), 6494-6504.

94. Byrne, C.M., Allen, S.D., Lobkovsky, E.B., and Coates, G.W., Alternating Copolymerization of Limonene Oxide and Carbon Dioxide *J. Am. Chem. Soc.,* **2004**. *126*, 11404-11405.

95. Kim, J., Novak, B.M., and Waddon, A.J., Liquid Crystalline Properties of Polyguanidines. *Macromolecules,* **2004**. *37* (22), 8286-8292.

96. Lam, J.W.Y., Kong, X., Dong, Y., Cheuk, K.K.L., Xu, K., and Tang, B.Z., Synthesis and Properties of Liquid Crystalline Polyacetylenes with Different Spacer Lengths and Bridge Orientations, *Macromolecules,* **2000**. *33* (14), 5027-5040.

97. Hu, J.-S., Zhang, B.-Y., Guan, Y., and He, X.-Z., Side-chain cholesteric liquid-crystalline elastomers derived from smectic crosslinking units: Synthesis and phase behavior, *J Polym Sci Part A: Polym Chem*, **2004**. *42,* (20), 5262-5270.

98. Hsu, T.-J. and Tan, C.-S., Synthesis of Polycarbonate from Carbon Dioxide and Cyclohexene Oxide by Yttrium-Metal Coordination Catalyst. *Polymer,* **2001**. *42*, 5143-5150.

99. Wang, S.J., Du, L.C., Zhao, X.S., Meng, Y.Z., and Tjong, S.C., Synthesis and characterization of alternating copolymer from carbon dioxide and propylene oxide, *J Appl Polym Sci,* **2002**. *85* (11),2327-2334.

100. Liu, B., Zhao, X., Wang, X., and Wang, F., Copolymerization of carbon dioxide and propylene oxide with neodymium trichloroacetate-based coordination catalyst, *Polym Inter,* **2003**. *44* (6),1803-1808.

101. Zhi, J., Zhang, B., Zang, B., and Shi, G., Synthesis and properties of photochromic cholesteric liquid crystalline polysiloxane containing chiral mesogens and azobenzene photochromic groups. *J Appl. Polym Sci,* **2002**. *85* (10), 2155-2162.

102. Dubois, J.C., Decobert, G., and Barny, P., Liquid Crystalline Side Chain Polymers derived from Polyacrylate, Polymethyacrylate and Polyalphachloroacrylate. *Mol Cryst Liq Cryst* **1986**. *137*,349.

103. Sahin, Y.M., Serhatli, İ.E., and Menceloglu, Y.Z., Synthesis of a Side Chain Liquid Crystalline Polycarbonate with a Chiral Backbone *accepted in J Appl Polym Sci,* **2006, February**. *unpublished work, manuscript number: APP-2006-01-0019.R1*

104. Rule, J. *Unpublised Work, CO2 as a monomer for polycarbonate synthesis* polycarbonate synthesis on GlobalSpec 2002, September [cited; Available from:
http://polaris.scs.uiuc.edu/chem/gradprogram/chem435/Abstract%20Rule1.pdf

105. Darensbourg, D.J., Adams, M.J., Yarbrough, J.C., and Phelps, A.L., Synthesis and Structural Characterization of Double Metal Cyanides of Iron and Zinc: Catalyst Precursors for the Copolymerization of Carbon Dioxide and Epoxides *Inorg. Chem.,* **2003**. *42* (24), 7809-7818.

106. Collyer, A.A. *In Liquid Crystal Polymers: From   Structures to Applications* ed. A.A. Collyer. **1993**, Oxford: Elsevier.

107. Nakano, K., Nozaki, K., and Hiyama, T., Spectral Assignment of Poly[cyclohexene oxide-alt-carbon dioxide], *Macromolecules,* **2001**. *34* (18), 6325-6332.

108. Sato, H., Tanaka, Y., and Hatada, K., 13C NMR analysis of polystyrene by means of model compounds, *Makromol. Chem. Rapid Commun.,* **1982**. *3* (3), 181-185.

109. A. Zambelli, P. Locatelli, G. Bajo, and Bovey, F.A., Model Compounds and 13C NMR Observation of Stereosequences of Polypropylene *Macromolecules,* **1975**. *8* (5), 687-689.

110. Mang, S., Cooper, A.I., Colclough, M.E., Chauhan, N., and Holmes, A.B., Copolymerization of CO2 and 1,2-Cyclohexene Oxide Using a CO2-Soluble Chromium Porphyrin Catalyst, *Macromolecules,* **2000**. *33* (2), 303-308.

111. Kuran, W. and Listo, T., nitiation and propagation reactions in the copolymerization of epoxide with carbon dioxide by catalysts based on diethylzinc and polyhydric phenol. *Macromol Chem Phys,* **1994**. *195* (3), 977-984.

112. Nozaki, K., Nakano, K., and Hiyama, T., Optically Active Polycarbonates: Asymmetric Alternating Copolymerization of Cyclohexene Oxide and Carbon Dioxide, *J. Am. Chem. Soc.,* **1999**. *121* (47), 11008-11009.

113. Cheng, M., Darling, N.A., Lobkovsky, E.B., and Coates, G.W., Enantiomerically-Enriched Organic Reagents via Polymer Synthesis: Enantioselective Copolymerization of Cycloalkene Oxide and CO2 using Homogeneous, Zinc-based Catalysts *Chem. Comm.,* **2000**,2007-2008.

114. Nakano, K., Kosaka, N., Hiyama, T., and Nozaki, K., Metal-catalyzed Synthesis of Stereoregular Polyketones, Polyesters, and Polycarbonates. *Dalton,* **2003**, 4039-4050.

115. Antelmann, B., Chisholm, M.H., Iyer, S.S., Huffman, J.C., Navarro-Llobet, D., Pagel, M., Simonsick, W.J., and Zhong, W., Molecular Design of Single Site Catalyst Precursors for the Ring-Opening Polymerization of Cyclic Ethers and Esters. 2.1 Can Ring-Opening Polymerization of Propylene Oxide Occur by a Cis-Migratory Mechanism? *Macromolecules,* **2001**. *34* (10), 3159-3175.

116. Kasperczyk, J.E., Microstructure Analysis of Poly(lactic acid) Obtained by Lithium tert-Butoxide as Initiator, *Macromolecules,* **1995**. *28* (11), 3937-3939.

117. Lednor , P.W. and Rol, N.C., Copolymerization of propene oxide with carbon with carbon dioxide: aselective incorporation of propene oxide into the polycarbonate chains, determined by 100 MHz 13C n.m.r. spectroscopy, *J. Chem. Soc, Chem. Commun,,* **1985**, 598 - 599.

118. Beckman, E.J. and Green Chemical Processing Using CO2 *Ind. Eng. Chem. Res,* **2003**. *42* (8), 1598-1602.

119. Sanda, F., Kamatani, J., and Endo, T., Synthesis and Anionic Ring-Opening Polymerization Behavior of Amino Acid-Derived Cyclic Carbonates *Macromolecules,* **2001**. *34* (6), 1564-1569.

120. Moore, D.R., Cheng, M., Lobkovsky, E.B., and Coates, G.W., Mechanism of the Alternating Copolymerization of Epoxides and CO2 Using -Diiminate Zinc Catalysts: Evidence for a Bimetallic Epoxide Enchainment *J. Am. Chem. Soc.,* **2003**. *125* (39), 11911-11924.

121. Coates, G.W., Waymouth, R.M., and Enantioselective cyclopolymerization of 1,5-hexadiene catalyzed by chiral zirconocenes: a novel strategy for the synthesis of optically active polymers with chirality in the main chain, *J. Am. Chem. Soc.,* **1993**. *115* (1),91-98.

122. Lifson, S., Green, M.M., Andreola, C., and Peterson, N.C., Macromolecular stereochemistry: helical sense preference in optically active polyisocyanates. Amplification of a conformational equilibrium deuterium isotope effect *J. Am. Chem. Soc.,* **1989**. *111* (24), 8850-8858.

123. Ciardelli, F. *In Encyclopedia of Polymer Science*, ed. J.I. Kroschwitz. Vol. 10. **1987**, New York: John Willey and Sons. 463-493.

124. Dieter Arlt, B.B., Rolf Grosser, Walter Lange, New Chiral Polyamide Stationary Phases for Chromatographic Enantiomer Separation. *Angew. Chem. Int. Ed. Eng.,* **1991**. *30* (12), 1662-1664.

125. Moore, J.S. and Stupp, S.I., Materials chemistry of chiral macromolecules. 1. Synthesis and phase transitions *J. Am. Chem. Soc.,* **1992**. *114* (9), 3429-3441.

126. Wulff, G., Main-Chain Chirality and Optical Activity in Polymers Consisting of C-C Chains, *Angew. Chem. Int. Ed. Eng.,* **1989**. *28* (1), 21-37.

127. Chamberlain, B.M., Cheng, M., Moore, D.R., Ovitt, T.M., Lobkovsky, E.B., and Coates, G.W., Polymerization of Lactide with Zinc and Magnesium -Diiminate Complexes: Stereocontrol and Mechanism, *J. Am. Chem. Soc.,* **2001**. *123* (14), 3229-3238.

128. Rieth, L.R., Moore, D.R., Lobkovsky, E.B., and Coates, G.W., Single-Site -Diiminate Zinc Catalysts for the Ring-Opening Polymerization of -Butyrolactone and -Valerolactone to Poly(3-hydroxyalkanoates), *J. Am. Chem. Soc.,* **2002**. *124* (51), 15239-15248.

129. Cheng, M., Attygalle, A.B., Lobkovsky, E.B., and Coates, G.W., Single-Site Catalysts for Ring-Opening Polymerization: Synthesis of Heterotactic Poly(lactic acid) from rac-Lactide, *J. Am. Chem. Soc.,* **1999**. *121* (49), 11583-11584.

130. Jonza, J.M. and Porter, R.S., High-melting bisphenol-A polycarbonate from annealing of vapor induced crystals. *J Polym Sci Part B: Polym Phys,* **1986**. *24* (11), 2459-2472.

131. Guittard, F. and Geribaldi, S., Highly fuorinated molecular organised systems: strategy and concept. *J Fluorine Chem,* **2001**. *107*, 363-374.

132. Yakubov, A.A., Study of molecular structure and interactions in partially fluorinated liquid crystal by infrared spectroscopy. *J Molec Struc,* **2000**. *519,*205-209.